FIRAT UNIVERSITY
GRADUATE SCHOOL OF NATURAL AND APPLIED SCIENCES
TÜRKİYE

THE HYDROGEOLOGICAL INVESTIGATION OF KARST SPRINGS LOCATED AT THE NORTHEAST OF ERBIL (NORTHERN PART OF IRAQ)

Zana HUSSEIN OMAR OMAR

Master's Thesis

DEPARTMENT OF GEOLOGICAL ENGINEERING
Program of
Division of Hydrogeology

JULY 2022

FIRAT UNIVERSITY
GRADUATE SCHOOL OF NATURAL AND APPLIED SCIENCES
TÜRKİYE

Department of Geological Engineering

Master's Thesis

THE HYDROGEOLOGICAL INVESTIGATION OF KARST SPRINGS LOCATED AT THE NORTHEAST OF ERBIL (NORTHERN PART OF IRAQ)

Author
Zana HUSSEIN OMAR OMAR

Supervisor
Assist. Prof. Dr. Özlem ÖZTEKİN OKAN

Co-Supervisor
Assist. Prof. Dr. Rebwar Nasir DARA

JULY 2022
ELAZIG

FIRAT UNIVERSITY
GRADUATE SCHOOL OF NATURAL AND APPLIED SCIENCES
TÜRKİYE

Department of Geological Engineering

Master's Thesis

Title:	The Hydrogeological Investigation of Karst Springs Located at the Northeast of Erbil (Northern Part of Iraq)
Author:	Zana HUSSEIN OMAR OMAR
Submission Date:	31 May 2022
Defense Date:	01 July 2022

THESIS APPROVAL

This thesis, which was prepared according to the thesis writing rules of the Graduate School of Natural and Applied Sciences, Fırat University, was evaluated by the committee members who have signed the following signatures and was unanimously approved after the defense exam made open to the academic audience.

		Signature
Supervisor:	Assist. Prof. Dr. Özlem ÖZTEKİN OKAN Fırat University, Faculty of Engineering	Approved
Chair:	Assoc. Prof. Dr. Ayla AYAZ BOZDAĞ Konya Technical University, Faculty of Engineering	Approved
Member:	Assist. Prof. Dr. Esra YILDIRIM Fırat University, Faculty of Engineering	Approved

This thesis was approved by the Administrative Board of the Graduate School on

.... / .... / 20 ....

Signature

Prof. Dr. Kürşat Esat ALYAMAÇ
Director of the Graduate School

DECLARATION

I hereby declare that I wrote this Master's Thesis titled “The Hydrogeological Investigation of Karst Springs Located at the Northeast of Erbil (Northern Part of Iraq) ” in consistent with the thesis writing guide of the Graduate School of Natural and Applied Sciences, Firat University. I also declare that all information in it is correct, that I acted according to scientific ethics in producing and presenting the findings, cited all the references I used, express all institutions or organizations or persons who supported the thesis financially. I have never used the data and information I provide here in order to get a degree in any way.

01 July 2022

Zana HUSSEIN OMAR OMAR

PREFACE

First of all, I want to express my gratitude to GOD for His grace and for providing me with the strength to accomplish this study, and then I would like to thank my supervisor, Dr. Öğr. Üyesi ÖZLEM ÖZTEKİN OKAN, for his continuous encouragement and valuable assistance throughout the study; his deep interest in this investigation and his guidance enabled me to complete this research. In addition to my supervisor, I would like to thank my Co-Supervisor. Dr. Rebwar Nasir Dara for his continuous help and support during this study.

I'd also like to thank my Mother for her advice and talks, which helped me get through difficult times.

I'd like to thank Mr Abdulsamad Osman for their encouragement and assistance in the field study.

I would like to extend my thanks to Mrs (Bahsdar Pusho,Peshawa Barzan, Ahmed Wasman, Bakhtyar Ibrahim, Hawkar Ajeb, and Karwan Hassan) for their continuous help and support during this study. and also I would like to My thanks to my collages, Nashwan Jalal, Salman Kareen for their help during my thesis works.

Finally, I'd like to thank my friends for their encouragement and assistance in completing my thesis successfully.

Zana HUSSEIN OMAR OMAR

ELAZIG, 2022

TABLE OF CONTENTS

ABSTRACT

The Hydrogeological Investigation of Karst Springs Located at the Northeast of Erbil (Northern Part of Iraq)

Zana HUSSEIN OMAR OMAR

Master's Thesis

FIRAT UNIVERSITY
Graduate School of Natural and Applied Sciences

Department of Geological Engineering

July 2022, Page: xiii + 75

The aim of this study is to investigate the hydrogeology of the Haudian, Mergasur-1, Kani Shakir, Khardin karstic springs. The study area lying throughout the mountainous region of northern Iraq, is located in Diana – Mergasur Sub-Basin. The age of geological formations ranges from Lower Cretaceous to Pliocene. The discharge rates of the karstic springs were measured periodically (twice a month during one year) using the specific volume method and other suitable flow values such as a current meter, rectangular/v-notch. Groundwater levels were monthly measured during one year for two wells (Haudian-2 and Shivazyarat) in the study area using an electrical sounder, which started in January 2021.

The fractured-karstic limestones of Bekhme and Govanda formations are the aquifers for karstic springs. The investigated wells in the present study recharge from Bekhme and Shiranish Formation. According to the Jacob method calculation, no meaningful difference is determined in the average hydraulic conductivity ($1.03*10^{-6}$ m/s) of marly limestone belong to Shiranish Formation and average hydraulic conductivity ($1.15*10^{-6}$ m/s) of both marly limestones (belong to Shiranish Formation) and dolomitic limestones (belong to Bekhme Formation) in the study area.

Maillet formula is used to calculate the recession coefficient and water storage capacity above the discharge level of karstic springs in their real regimes. The storage capacity (V_0) of Haudian Spring above the discharge level in the real regime between 12.04.2021 and 16.10.2021 is calculated 461218 m^3. According to the Iraqi Standard data, the average amount of drinking and domestic usage per person is 392 L/day. Around 1500 local residents utilize Haudian spring for drinking and domestic purposes. If just this spring alone is used for drinking and domestic purposes by a population of 1500, the period of this spring, in the real regime, was calculated as 785 days. The recession coefficients (α) for Haudian Spring were calculated as $\alpha 1$= 0,01 day $^{-1}$ and $\alpha 2$= 0,0025 day $^{-1}$. The real regime period of the Kani Shakir spring was between 12.04.2021 and 16.10.2021, and the water storage capacity of the spring (V_0) was calculated as 13133 m^3, two flow regimes are determined for Kani Shakir springs in the real regime. The first recession coefficient = 0,01 day^{-1}, whereas the second recession coefficient = 0,005 day^{-1}. The real regime period of the Khardin spring is between 29.03.2021 and 16.10.2021, and the water storage capacity of the spring (V_0) is 44280 m^3. The real regime period of the Mergasur-1 spring was between 12.04.2021 and 16.10.2021. The water storage capacity of the spring (V_0) in the real regime was calculated as 50594 m^3. The calculated recession coefficient for Khardin and Mergasur-1 springs in the real regimes was 0.012 day^{-1}. In order to get better efficiency from the karstic springs in dry periods, it is necessary to protect the recharge areas, to license the wells to be drilled in the study area in a controlled manner and not to draw too much water from these wells.

Keywords: Karst Aquifer, Hydrogeology, Maillet Formula, Recession Coefficient, Haudian Spring

ÖZET

Erbil (Irak'ın Kuzeyi)'in Kuzeydoğusunda bulunan Karst Kaynaklarının Hidrojeoloji İncelemesi

Zana HUSSEIN OMAR OMAR

Yüksek Lisans Tezi

FIRAT ÜNİVERSİTESİ
Fen Bilimleri Enstitüsü

Jeoloji Mühendisliği Anabilim Dalı

Temmuz 2022, Sayfa: xiii + 75

Bu çalışmanın amacı, Haudian, Mergasur-1, Kani Shakir, Khardin karstik kaynaklarının hidrojeolojisinin incelenmesidir. Çalışma alanı, Kuzey Irak'ın dağlık bölgesinde, Çalışma alanı, Kuzey Irak'ın dağlık bölgesinde, Soran ilçesinden başlayıp Bradost antiklinaliyle Mergasur ilçesine kadar uzanan Diana – Mergasur Alt Havzası'nda yer almaktadır. Çalışma alanındaki birimlerin yaşı Alt Kretase'den Pliyosen'e kadar değişmektedir.

Karstik kaynakların debileri, belirli hacim yöntemi, muline, dikdörtgen savak gibi uygun debi ölçme yöntemleri ile periyodik olarak (bir yıl boyunca, ayda iki kez) ölçülmüştür. Çalışma alanındaki iki kuyuda (Haudian-2 ve Shivazyarat) bir yıl boyunca elektrikli su seviye ölçüm cihazı kullanılarak yeraltı suyu seviyeleri, Ocak 2021'den başlayarak aylık olarak ölçülmüştür.

Bekhme ve Govanda formasyonlarına ait kırıklı ve karstik kireçtaşları incelenen karstik kaynakların akiferleridir. Bu çalışmada incelenen kuyular ise Bekhme ve Shiranish Formasyonu'ndan beslenmektedir. Jacob yöntemi hesaplamasına göre Shiranish Formasyonu'na ait marnlı kireçtaşının ortalama hidrolik iletkenliği ($1.03*10^{-6}$ m/sn) ile Shiranish Formasyonu ile birlikte Bekhme Formasyonu'na ait dolomitik kireçtaşlarının birlikte ortalama hidrolik iletkenlikleri ($1.15*10^{-6}$ m/sn) arasında anlamlı bir fark bulunmamıştır.

Maillet formülü, İncelenen karstik kaynakların gerçek rejim dönemlerinde boşalım katsayıları ve boşalım kotu üzerindeki depolama güçleri Maillet Formülü ile hesaplanmıştır. Haudian Kaynağı'nın 12.04.2021 ile 16.10.2021 yılları arasındaki gerçek rejim döneminde, boşalım kotu üzerindeki üzerindeki depolama kapasitesi (V_0) 461218 m^3 olarak hesaplanmıştır. Irak Standart verilerine göre kişi başına içme ve evsel kullanım su miktarı 392 L/gün'dür. Haudian Kaynak suyunun, gerçek rejim döneminde, 1500 civarında nüfusa sahip Haudian köy halkı tarafından, içme ve evsel kullanım amacıyla 785 gün kullanılabileceği hesaplanmıştır. Haudian Kaynağı'nın gerçek rejimde boşalım katsayıları (α) $\alpha1 = 0,01$ $gün^{-1}$ ve $\alpha2 = 0,0025$ $gün^{-1}$ olarak hesaplanmıştır. Kani Shakir Kaynağı'nın gerçek rejim dönemi 12.04.2021-16.10.2021 tarihleri arasında olup, kaynağın bu dönemde su depolama kapasitesi (V_0) 13133 m^3 olarak hesaplanmıştır. Gerçek rejim döneminde, Kani Shakir Kaynağı'na ait boşalım katsayıları; $\alpha1 = 0,01$ $gün^{-1}$, ve $\alpha2 = 0,005$ $gün^{-1}$ olarak belirlenmiştir. Khardin Kaynağı'nın gerçek rejim dönemi 29.03.2021-16.10.2021 tarihleri arasında olup, kaynağın gerçek rejimde su depolama kapasitesi (V_0) 44280 m^3'tür. Mergasur-1 Kaynağı'nın gerçek rejim dönemi ise 12.04.2021 ile 16.10.2021 yılları arasında olup, kaynağın bu dönemdeki su depolama kapasitesi (V_0) 50594 m^3 olarak hesaplanmıştır. Khardin ve Mergasur-1 kaynaklarının gerçek rejim dönemlerinde hesaplanan boşalım katsayıları 0.012 $gün^{-1}$'dir. Kurak dönemlerde karstik kaynaklardan daha iyi verim alabilmek için beslenme alanlarının korunması, çalışma alanında açılacak kuyuların kontrollü bir şekilde ruhsatlandırılması ve bu kuyulardan çok fazla su çekilmemesi gerekmektedir.

Anahtar Kelimeler: Karstik akifer, Hidrojeoloji, Maillet Formülü, Boşalım Katsayısı, Haudian Kaynağı

LIST OF FIGURES

LIST OF TABLES

Page

LIST OF APPENDICES

Page

SYMBOLS

PET	: Potential evapotranspiration in mm
La	: Monthly correction constant function of latitude
j	: Monthly temperature parameter
J	: Annual heat index (°C)
t	: Mean monthly temperature (°C)
K	: Correction factor which is equal to (0.0311t + 0.24)
P	: Percentage of sunshine hours in each month to sunshine hours of one year.
t	: Mean monthly temperature (°C)
m	: Constant (1.31)
a	: Constant (0.33)
Rs	: The water surplus represents the summation of surface runoff
Re	: groundwater recharge
Ri	: soil moisture
AET	: Actual evapotranspiration
Rs	: Surface runoff
I	: Infiltration
T	: Transmissivity (m^2 /day)
K	: Hydraulic conductivity (m/day)
b	: Saturated thickness of the aquifer (m)
S	: represents storativity
V	: the amount of water obtained or lost
A	: surface area of the aquifer impacted by the recharge or discharge
h	: the average water level decline.
K	: Hydraulic conductivity (m/day)
V	: Groundwater velocity (m/day)
$\mathrm{dh/dl}$	: hydraulic gradient
Sy	: Specific yield
Wy	: Water spent size (m^3),
V	: Total volume (m^3)
b	: Saturated thickness
Sc	: Specific yield
Q	: Rate of discharge (m3/day)
H	: Saturated thickness (m)
HD	: Total depth of the well (m)
S	: Drawdown (m)
T	: Transmissivity (m2 /day)
Q	: Pumping rate (m3 /day)
Δs	: Difference of drawdown per log cycle t.
t/to	: Time of last record / initial time
q0	: discharge at the beginning of the recession (time to) (m3 /s)
e	: basis of natural logarithm
a	: recession coefficient (day-1)
t/to	: duration since the start of recession (day)
q	: discharge at time t (m3 /s)

ABBREVIATIONS

ZSZ : Zagros Suture Zone
IZ : Imbricate Zone
FHZ : Foothill Zone
HFZ : High Folded Zone
ZFTB : Zagros Fault Thrust Belt
MFB : Mesopotamian Foreland Basin
UTM : Universal Transverse
GIS : Geographic Information System
GPS : Global Positioning System
PET : Potential Evapotranispiration
ET : Evapotranispiration
G.W : ground water
M.A.S.L : Meter above sea level
G.W.L : Groundwater level

1. INTRODUCTION

The subject of the present study is to investigate the hydrogeology of karstic springs located at the northeast of Erbil, and investigate the hydrogeological parameters (hydraulic conductivity, transmissivity, storage coefficient) of karstic aquifers.

Karst springs are the primary source of water supply for parts of villages and urban areas in northern Iraq, but limited research is available on spring water management and sustainability. The largest available source of fresh water in the mountain lies in underground springs. To obtain fresh water in cases where surface waters are insufficient, groundwater use is also increasing considerably.

However, karst aquifers serve as a significant source of freshwater. 25% of the world's population relies on karst aquifers as their primary freshwater supply (Ford and Williams, 2007). Karst aquifers exhibit various unique properties that distinguish them from other aquifer types. Consequently, carbonate rocks and karst aquifers have more complicated hydrogeology than different main rock types (Bakalowicz, 2005).

Population growth and water scarcity are essential issues in Erbil and the surrounding regions. Due to a lack of freshwater, finding and operating additional water resources became mandatory. To ensure the sustainability of current groundwater resources, rational usage is required. Furthermore, the arid climatic situation impacted the amount of groundwater recharging in the study area, particularly from karst aquifers. Because precipitation is the primary recharging source for karst springs, rain that falls on the earth's surface infiltrates filters down and recharges groundwater. Karst springs frequently discharge large quantities of water, attracting the attention of water resource experts, particularly in arid and semi-arid regions experiencing water shortages.

Spring water from relatively water-rich karstic aquifers is used as the primary drinking source and supplies traditional gravity irrigation schemes in the mountains of northern Iraq (Stevanovic and Markovic, 2004).

The principal outflows within the Group of karst springs were thought to be draining in the karstic Bekhma aquifer. The systems of faults and fractures that border carbonate rock massifs in contact with non-carbonate rocks are typically used to locate the location of karst springs. Most karst springs belong to their suitable geologic geomorphologic setting. The karst in northern Iraq (Southwestern Zagros Mountains) was largely unknown to researchers, although carbonate rocks with varying karstification cover around 35% of that area (Stevanovic and Markovic, 2004).

Climate change and land development may have a negative effect on spring source replenishment and jeopardize their dependability as a source of water. Typically, an aquifer's karstification conditions are uncertain, and information about the internal structure may only be obtained via the spring hydrograph shape resulting from rainfall (Atkinson, 1977).

The importance of hydrogeological studies, which will help ensure water resource efficiency and drinking-use quality sustainability, is increasing. Natural springs provide water for all purposes, including drinking water, domestic, irrigation, and other purposes (orchard, livestock).

Therefore, great care was given to groundwater exploitation in the study area. The main problem in the study area is the lack of scientific data about the discharges of the springs in the recent years. The discharges of the springs have been only measured between 2001 and 2003. The discharges of the karst springs and the groundwater levels in two wells that had been drilled in limestones were measured twice a month for one year (during 2021). The reasons for the changes in the flow rates of the karst springs and the reasons for the increase and/or decrease in the groundwater levels in the wells were investigated within the scope of the present study.

In the present study, karst springs were investigated to get more insight into this complex karst system's hydrogeologic, hydraulic, and hydrodynamic behaviour. Four springs (Haudian, Kani Shaker, Khardin, and Mergasur-1 springs) were studied in terms of hydrogeology during one year beginning from the January, 2021 to December, 2021.

Generally, all springs are within the Bradost Anticline Mountain, except the Khardin spring, located in the Piran Anticline.The aims of this study are (i) to explain and evaluate regular flow measurements made in the field and calculate the volume of water aquifers stored in the real regime for 2021, (ii) to determine the changes in discharges of the karst springs, compare by using the previous data of springs in previous years and interpret the reasons for the changes, (iii) to investigate some hydrogeological properties (such as permeability and transmitivity) of the aquifers in the study area related to the pumping well tests.

1.1. Overview of the previous studies

Many studies have been carried out in the research area, including sedimentological and stratigraphic features of geological units outcrop in study area and its surrounding. However, according to earlier research, very limited geological (including hydrology and hydrogeology) studies are carried out in the study area.

Stevanovic and Markovic (2004) and Stevanovic and Iurkiewicz (2004) have studied the climate, hydrology, geomorphology, geology, and hydrogeology of Northern Iraq. They have investigated the hydrogeology and regional geology of the three northern governorates as part of a comprehensive FAO program (Sulaimani, Erbil, and Dohuk). This may be regarded as the first comprehensive regional hydrogeological research performed to date. The researchers have classified lithologies and types of aquifers and springs discharges and have drawn a general hydrogeology map of Northern Iraq.

Hamed (2013) has studied hydrogeology, hydrochemistry, and groundwater flow modelling of the Shaqlawa-Hiran Basin in Northern Iraq. The current hydrogeological investigations have revealed three distinct aquifers: the Karst-Fissure aquifer (Aqra-Bekhme and Shiranish formations), the Fracture aquifer (Pilaspi formation), the Complex inter-granular aquifer (upper and Lower Fars formations and Quaternary deposit), and an aquiclude unit (Gercus and Kolosh formations)

Tobia and Kafy (2016) have studied heavy mineral contents in sediments collected from the Balakyan River. They mentioned that the heavy minerals are mainly represented by pyroxene, amphibole, epidote, serpentine, apatite, tourmaline, zircon, and opaque minerals (chromian spinel, magnetite, hematite, goethite, and ilmenite).

Balaki and Omar (2019) have studied the structural evolution of the Bradost, Pers Berat and Maqloub-Bardarash anticline in Zagros fold-thrust belt NE Iraq. He suggests that The present study suggests that the duplex structures within both the Berat and Bradost structures, rather than the imbricate thrust system, are principally responsible for accommodating the possible uplift of the studied formations.

Ali et al. (2009) have studied the mechanism and its influence on karstic springs flow of sarchinar spring, a case example, sulaimaniyah, NE Iraq, the researchers have mentioned that The regime of this spring is determined by several factors, the principals are: arid climate and unstable recharge (six months without rainfall), well karstified and fractured aquifer system, and recharge by seepage from the nearby Chaq Chaq valley.

Mustafa et al. (2015) have studied the karst springs of the Makook karst system in Northern Iraq. They aimed to learn more about the complicated karst system's hydrogeologic, hydraulic, and hydrodynamic activity and the geochemistry of Sr-isotopes, rare earth elements REE, and trace elements. The researchers have mentioned that REE concentrations in karst waters are controlled by flow, dissolved organic carbon, and redox reactions.

1.2. Location of the study area

The study area lies in the mountainous region, between latitudes 36º39′15″N-39º77′00″N and longitudes 44º24′0″E- 44º54′0″E (Figure 1.1). The study area is located within Diana – Mergasur Sub-Basin: The Diana – Mergasur Sub-basin coverage area is about 625 km², which starts from Soran district and extends with Bradost anticline to Mergasur district. The study area is characterized by rugged topography, deep canyons, and narrow valleys with well-defined mountainous topography (Sissakian and Al-Jiburi, 2014). The Balakyan River originates in the study area and flows towards the southeast, and intersects the Sidekan River. The study area is located within the climate of the mountainous region, which is wet in winter and dry in summer, influenced by the Mediterranean climatological system.

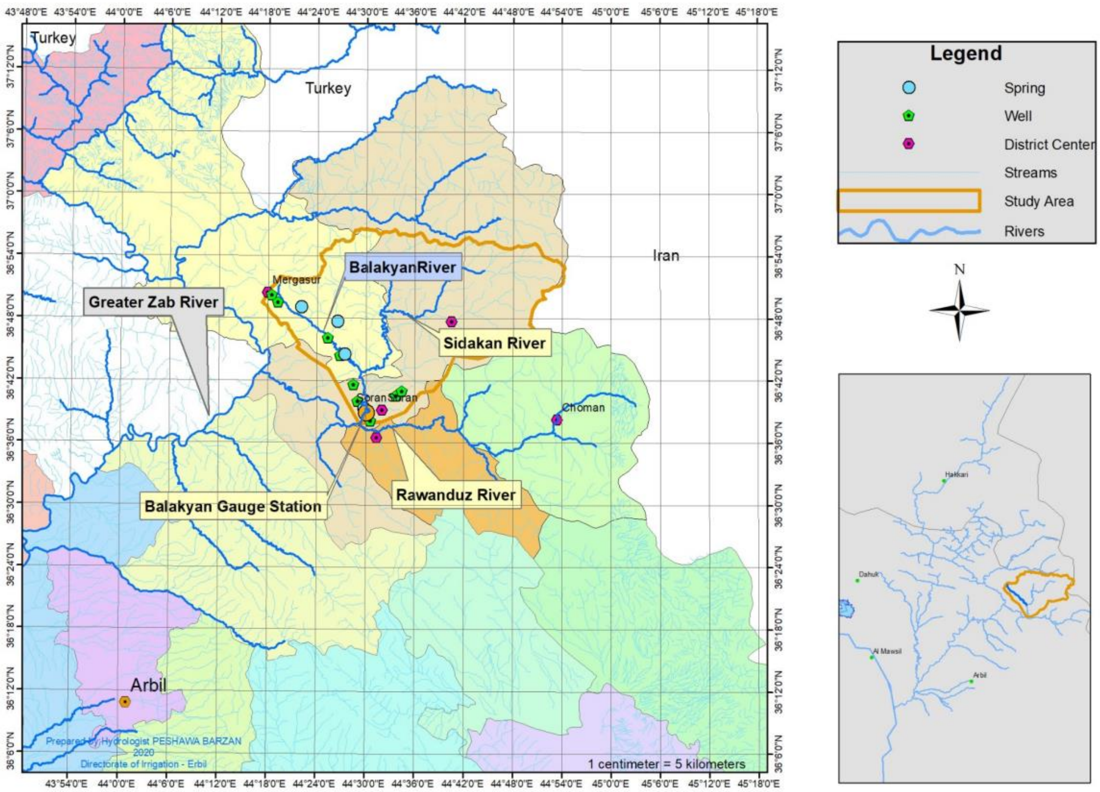

Figure 1.1. Location map of the study area

2. GEOLOGICAL SETTING

In the study area, a variety of geological formations are visible. The age of these formations ranges from Lower Cretaceous to Pliocene.

2.1. Stratigraphy of the study area

From oldest to youngest, the Lower Cretaceous Qamchuqa, Upper Cretaceous Bekhme, Late Campanian-Maastrichtian Shiranish, Campanian-Maastrichtian Tanjero, and Paleocene-Pliocene Red Bed Series formations are outcropped in the study area (Figure 2.1).

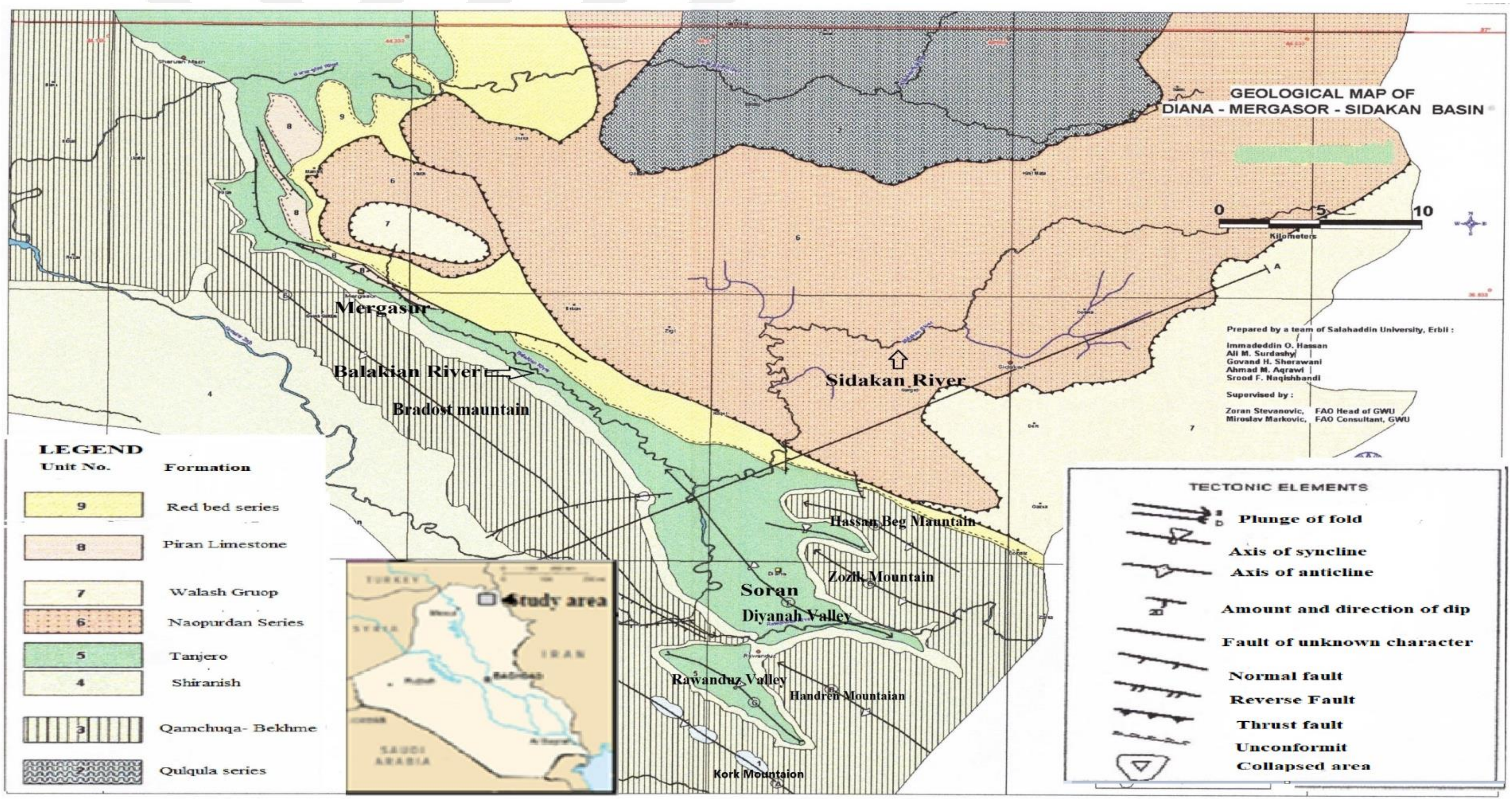

Figure 2.1. Geological map of the study area (after Stevanovic and Markovic, 2003)

Following is a concise description of these formations:

i. Qamchuqa Formation (Lower Cretaceous)

The Qamchuqa Formation is one of the most widely distributed formations in Iraq. This formation contains the Bradost anticline's core, evident on the northern limb. Qamchuqa Formation is constituted mainly of alternating massive to very hard coarse crystalline dolomites and argillaceous limestone and is usually dark grey. The thickness ranges from 300 to 1000 m.

ii. Bekhme Formation (Upper Cretaceous)

Wetzel defined The Bekhme Formation in 1950 from the Bekhme Gorge of the Greater Zab in the high folded zone. The formation consists of well bedded limestones, and dolostones with locally bituminous, coralline and recrystallized, very hard, light grey (Figure 2.2). The thickness ranges from 75 to 315 m. This deposit also contains chert nodules, iron concretions, and carbonate veins (Sissakian, 2013). This formation comprises the cores of many anticlines in the south and southwest parts of the high folded zone, and it often lies at the top of the Qamchuqa formation.

Figure 2.2. Limestones of Bekhme Formation in Haudian village (36.69974N,44.47149 E)

The Bekhme Formation unconformably overlies the Qamchuqa Formation with a basal conglomerate. The formation is typically deposited in a reef-fore reef situation (Jassim and Goff, 2006). The Bekhme Formation's upper contact is conformable to the Shiranish Formation above it (Buday, 1980). Chert nodules are discovered close to the contact.

iii. Shiranish Formation (Upper Cretaceous (Late Campanian-Maastrichtian))

This formation represents the lower part of an Upper Cretaceous ((Late Campanian-Maastrichtian) regional transgressive-regressive depositional sequence that flooded nearly all of Iraq (Dunnington, 1958). The formation includes white, yellowish-white, greyish whit greyish-white marly limestone, and chalky limestones followed (upwards) by thinly bedded or papery marl, blue and grey, with some marly limestone beds (Figure 2.3). The thickness ranges from 400 to 1000 m (Sissakian, 2013).

Figure 2.3. Limestones of Shiranish Formation near Balakian village (36.66108N,44.48944 E)

Henson (1940) described the Shiranish Formation for the first time in the town of Shiranish Islam, northeast of Zakho in the High Folded Zone in Northern Iraq. The Shiranish Formation was deposited in a deep marine environment (Jan et al., 2012). Tectonically, the basin of the Shiranish Formation merged with that of the above Tanjero Formation in a single basin which is known as the initial Zagros Foreland Basin (Karim and Surdashy, 2005, Karim et al., 2008). Petrographic, facies, and textural investigations indicate that the Shiranish Formation was formed in a deep basinal, pelagic, often reducing–euxic environment (Abdula, 2018).

iv. Tanjero Formation (Upper Cretaceous (Campanian-Maastrichtian))

Tanjero Formation is an Upper Cretaceous (Campanian-Maastrichtian) unit that outcrops in the Imbricated and High folded zones in northeastern Iraq. The formation exists in the Balambo-Tanjero area of NE Iraq. The lithology formation involves alternating dark green and yellowish-green shale layers, claystone, sandstone, and siltstone, some conglomerates in the upper portion and marly limestones in the bottom. The thickness ranges from 400 to 1000 m (Sissakian, 2013) (Figure 2.4).

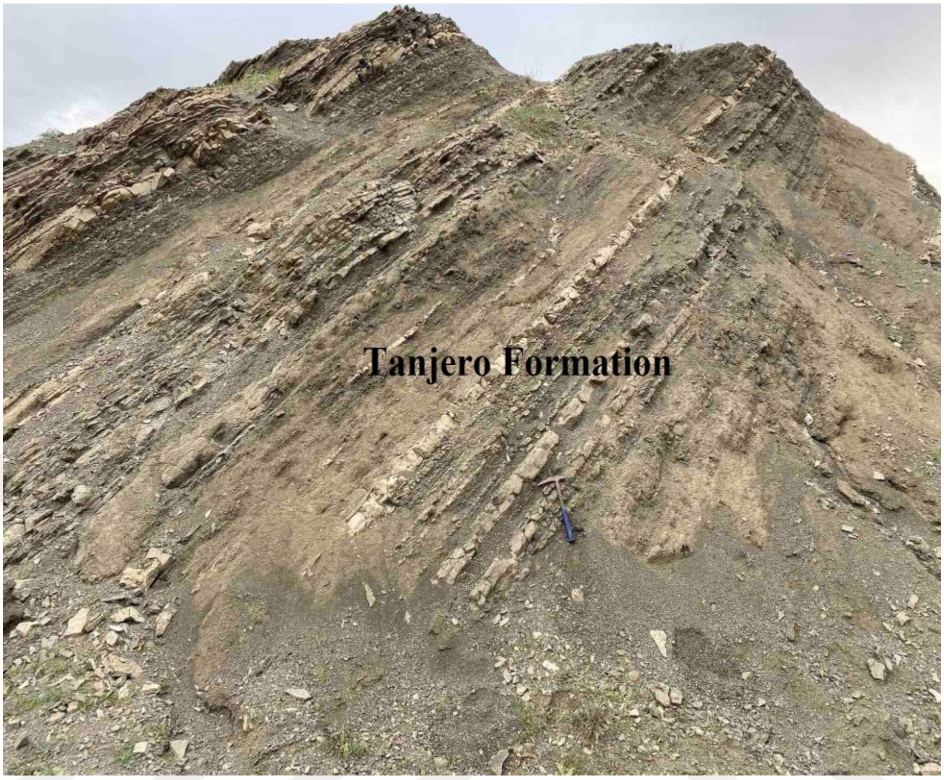

Figure 2.4. Outcrops of Tanjero Formation near Ashkawtwan village on the road (36.75766N,44,44059 E)

The Tanjero Formation (Upper Cretaceous) basin is integrated (tectonically) with the Shiranish Formation beneath it (Karim and Surdashy, 2005).

v. Red Bed Series (Paleocene-Pliocene)

The Red Bed Series was introduced by Bolton (1958). He divided the series into the lower Suwais Red Beds, the middle Govanda limestone, and the upper Merga Red Beds (Bolton, 1958). The Suwais Red Beds group lithology comprises conglomerates, red shales, red sandstones, and red mudstones. In addition, grey shales with sandstones and lenticular limestones (Surgala Red and Grey Layers), grey shales, sometimes marly with intercalations of thin greywacke beds, and impure extremely lenticular limestone make up the Surgala Red and Grey Beds (Razga Grey Beds). The thickness varies between 500 to 1200 m (Sissakian, 2013).

The Govanda Limestone (Middle Miocene) comprises massive grey limestone beds. The thickness is around 150 m (Sissakian, 2013).

Merga Red Beds (Upper Miocene –Pliocene) consist of a massive boulder conglomerate, in the upper part, red, calcareous, silty shales and pebbly sandstones in the lower layer. Igneous and metamorphic rocks compose the conglomerate's pebbles, and the thickness is about 500 m (Sissakian, 2013) (Figure 2.5 a and b).

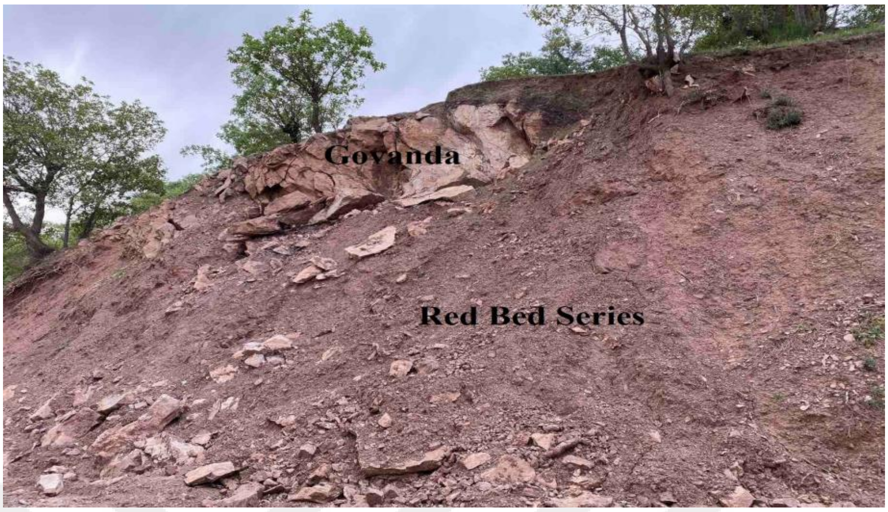

(a)

(b)

Figure 2.5. Outcrops of (a) Red bed series and (b) Limestone of Gowanda Formation in study area (36.81975N, 44.36622 E)

2.2. Tectonic

The Arabian Plate, as a part of young, active Zagros orogeny, has a complex tectonic history, which comprises a passive and active margin (Jassim and Goff, 2006). Zagros mountain orogeny process recognized as a collisional belt with ~2000 km length, started in SE of Turkey to Northern of Iraq and then East – Iraq and depression direction to Strait of Hormuz and Oman mountains in SE (Mouthereau et al., 2012). Based on morpho-tectonic features The Zagros Fold Thrust Belt (ZFTB) in Northern Iraq can be subdivided into four tectonic zone (Fouad, 2010, Buday and

Jassim, 1987). The subdivisions from hinterland (NE) to foreland (SW) are; (1) the Zagros Suture Zone (ZSZ), (2) Imbricate Zone (IZ), (3) High Folded Zone (HFZ), and (4) Foothill Zone (FHZ) or Low Folded Zone (LFZ) (Figure 2.6).

The significant thrusts segregate these tectonic zones into approximately parallel regions. According to tectonic division and subdivision, the study area, which includes Soran district and extended with Bradost anticline to Mergasur district location, exists within the Imbricate Zone (IZ) (Balaki and Omar, 2019). Which is part of the unstable shelf tectonic zone. This zone was the most strongly subsiding part of the Arabian Plate since the opening of the southern Neo-Tethys in the Late Jurassic. Since the entrance of the southern Neo-Tethys in the Late Jurassic, this zone has been the most strongly subsiding portion of the Arabian Plate (Buday, 1980).

Bradost anticline is the primary structure that appears in the study area and is elongated from Soran to Mergasur district. The Bradost anticline is a relatively long (55 kilometres) and broad (6 to 9.5 kilometres) asymmetrical anticline with double plunging; the southeastern plunge of the Bradost anticline intersects with the Korek and Handrin anticlines, while the northwest plunge intersects with the Shirin anticline near the southeast of the Barzan area in Rukuchk river (Balaki and Omar, 2019).

The Bradost anticline shield comprises a thick carbonate sequence containing limestone and dolomitic limestone. The Qamchuqa Formation is responsible for the lowest portion of these carbonates, while the Bekhme Formation is responsible for the upper part (Balaki and Omar, 2019). Bradost anticlines are distinguished by several significant faults of various scales and types distributed throughout the anticline.

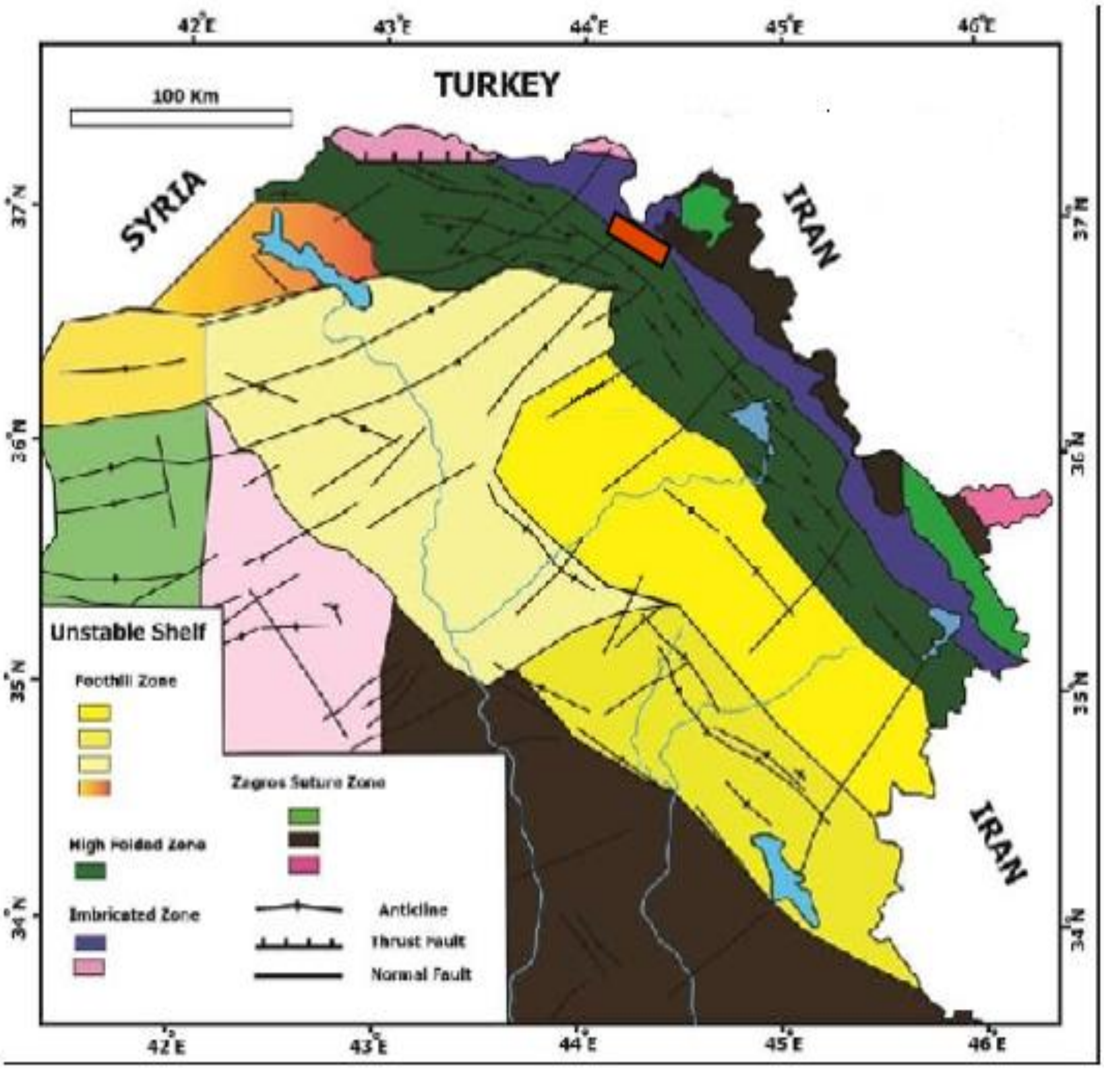

Figure 2.6. Tectonic zones of North part of Iraq (Modified from Buday and Jassim, 1987)

3. MATERIAL AND METHOD

This thesis was carried out in three stages including pre-field works (literature research), fieldwork and office studies.

3.1. Pre field works

Literature studies were initiated before the field studies and continued at every steps of the thesis. At the beginning of the study, all available data from different sources including topographic and geological maps with suitable scales for the area and satellite images were collected. Systemization and analyses of all available documentation in the basin's hydrology, geomorphology, geology, and hydrogeology were made. The meteorological data (precipitation and temperature) were collected from the General Directorate of Agriculture Erbil. Documentation of 10 drilled wells (lithological columns of drilled wells), and pumping tests were supplied from the Erbil’s Groundwater Directorate. Data of groundwater level measurement for the Haudian-1 well between the years 2000 and 2014 were taken from the Erbil's Groundwater Directorate. The coordinates and locations of the wells were determined by the GPS (UTM) System. The coordinates of the investigated wells are given on Table 3.1.

Table 3.1. Locations of the investigated wells

Well no.	Well Name	(UTM) X	(UTM) Y	Elevation (m)	Pumping test results
1	Kampi zankoy Soran	458611	4055979	*	+
2	Saruchawa 8	460684	4059438	765	+
3	Sarychawa 9	460789	4058901	715	+
4	Prozhay Gashtyari Hasti	458374	4053948	*	+
5	Mzgawti Majidawa	453795	4058325	655	+
6	Majidawa 4	453643	4058304	655	+
7	Shawrawa	453070	4060789	725	+
8	Shevazyarat	453070	4060440	701	+
9	Haudian 1	453080	4061017	698.5	-
10	Haudian 2	452988.5	4061133	717.5	-
11	Mazni-Garaki gulan	452095	4063570	789	+
12	Khardin	442467	4073711	792	+

(*: not determined; +: pumping test results are available; -: pumping test results are not available)

3.2. Fieldworks

The coordinates of the karstic springs were determined by GPS (UTM) in the field (Table 3.2; Figure 3.1).

Table 3.2. Locations of the springs

Spring No.	Spring Name	Latitude	Longitude	Elevation (m)
1	Haudian	453022.5	4061645	682.5
2	Kani Shakir	449928.48	4067316.25	655
3	Khardin	443506.91	4075079.64	1058
4	Mergasur-1	438105.84	4077220.53	1150.8

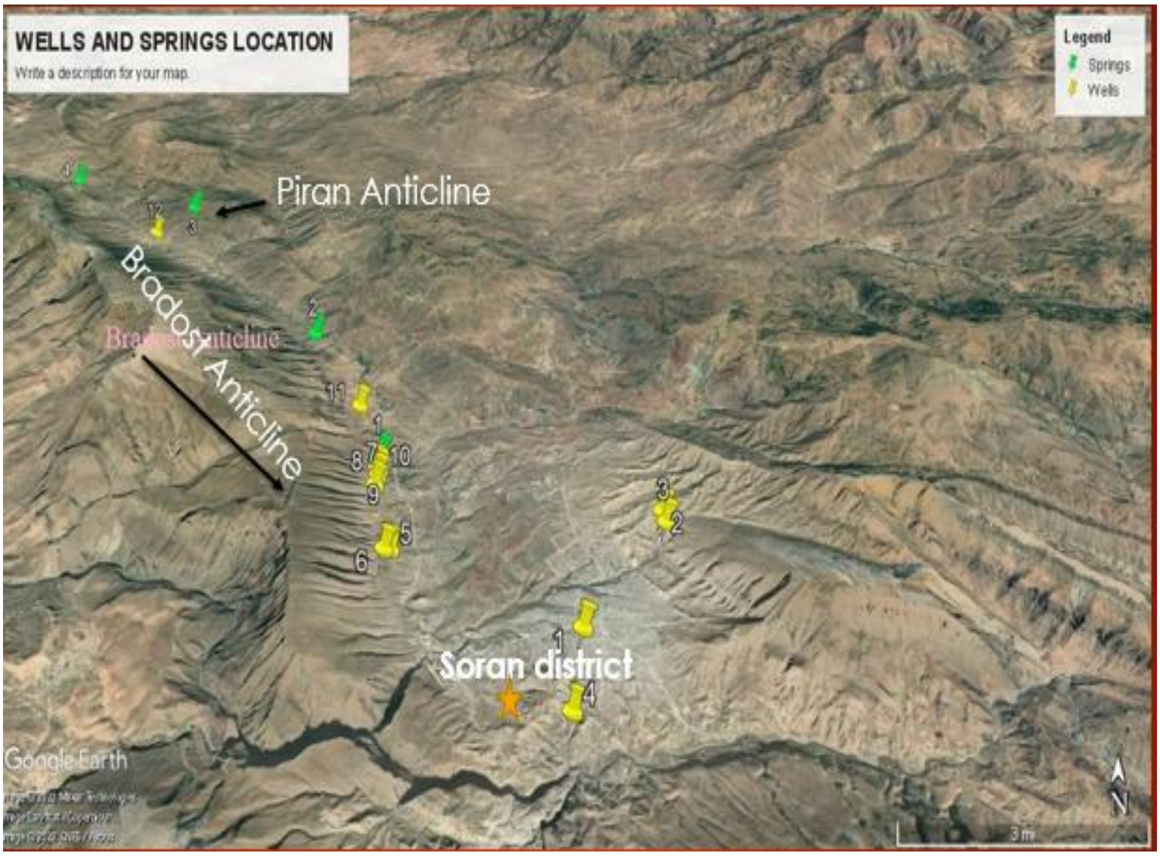

Figure 3.1. Locations of the investigated karstic springs and wells

The groundwater levels (G.W fluctuation) of Haudian-2 and Shivazyarat wells were monthly measured during one year that is started from January 2021. The groundwater levels were measured by using an electrical sounder (Figure 3.2a).

The discharges of the four springs, including Haudian, Kani Shakir, Khardin,and Mergasur-1 springs, were measured periodically (twice a month for a year) by using the specific volume method and by using Akim Hydrometry brand muline meter. The discharge rates of the springs related to the previous studies were measured by muline meter, and rectangular/v-notch weirs (Figure 3.2 b, c, d).

(a) (b)

(c) (d)

Figure 3.2. Measurement of a) groundwater level in the wells by using a sounder, discharge rates of the springs b) by specific volume method, and c, d) by using of current meter

3.3. Office work

The office work consisted of representing fieldwork. The analytic and mapping tools and programs utilized in this research are the following:

Microsoft Office 2016 (Word and Excel) have been used for writing, calculating equations, and creating tables and charts. Google Earth Pro was used to expose the location of wells and springs. ArcGIS (2011) was used to construct location maps and create a moisture balance chart. Aqtesolve software (2011) was used for calculating the hydrogeological parameters by using the data of pumping tests. Maillet equation was used to calculate and interpret the flow rates of the karstic springs in the real regimes.

4. RESULT AND DISCUSSION

4.1. Hydrology

The study area is located in a mountainous region. The climate of this Zone is primarily semi-arid, with the Mediterranean climate having a strong influence on all areas. Summers are dry and hot, while winters are cold with moderate rain (Stevanovic and Markovic, 2004). Anticyclones and subtropical high-pressure belts moving from west, southwest, north, and northeast influence Erbil in the summer.

During the winter season, which lasts from December to the Spring Equinox on March 21, about 80% of precipitation falls. During the winter, Mediterranean cyclones take over, moving east to northeast through the Erbil and the entire region. Arabian Sea cyclones pass northward, passing over the gulf, carrying large quantities of moisture and precipitation. Extremely cold polar air masses also affect the region. With the aid of polar jet streams, these air masses descend to the gulf and then veer northward, carrying moisture, leading to a massive increase in precipitation. The winter and spring seasons carry all of the precipitation. The rainy season typically lasts from October to the end of May (Stevanovic and Markovic, 2004).

Soran and Mergasur gauge stations' meteorological data were used to determine the climatic condition of the study area. They are located on latitude 36°68862´N, longitude 44° 5406´E, and elevation 728m and latitude 36°9986´N, longitude 44° 1797´E, and elevation 1113m, respectively.

Precipitation

Precipitation is the most critical parameter in the water balance and aquifer recharge. The study area is part of a region influenced by the Mediterranean climatological system, so precipitation occurs during the winter and spring seasons.

Internal water supplies in northern Iraq, both surface and groundwater resources, are obtained from precipitation (rainfall and snow). A large portion of the precipitation falls as rain or drizzle. Snow may additionally fall on highlands, and hail is generic during thunderstorms. The topographical features of northern Iraq significantly impact the rainfall regime. Rainfall amounts increase as one moves from the southwest to the northeast. The lack of precipitation during the summer is the main characteristic of the rainfall period (Stevanovic and Markovic, 2003).

The highest average monthly precipitation in the Soran district occurs in December is 114.42 mm, and the lowest average monthly precipitation occurs in August is 1.60 mm (Appendix 1; Table 4.1; Figure 4.1).

Table 4.1. Average monthly precipitation of the Soran district (related to the meteorological data of Soran gauge station between 2001 and 2021 years)

Months	Precepitation (mm)	Months	Precepitation (mm)
Jan.	105.25	**Jul.**	2.30
Feb.	110.77	**Aug.**	1.60
Mar.	114.42	**Sep.**	10.34
Apr.	90.90	**Oct.**	52.62
May.	30.91	**Nov.**	74.85
Jun	1.42	**Dec.**	107.95
		Average	**58.61**
		Total	**703.32**

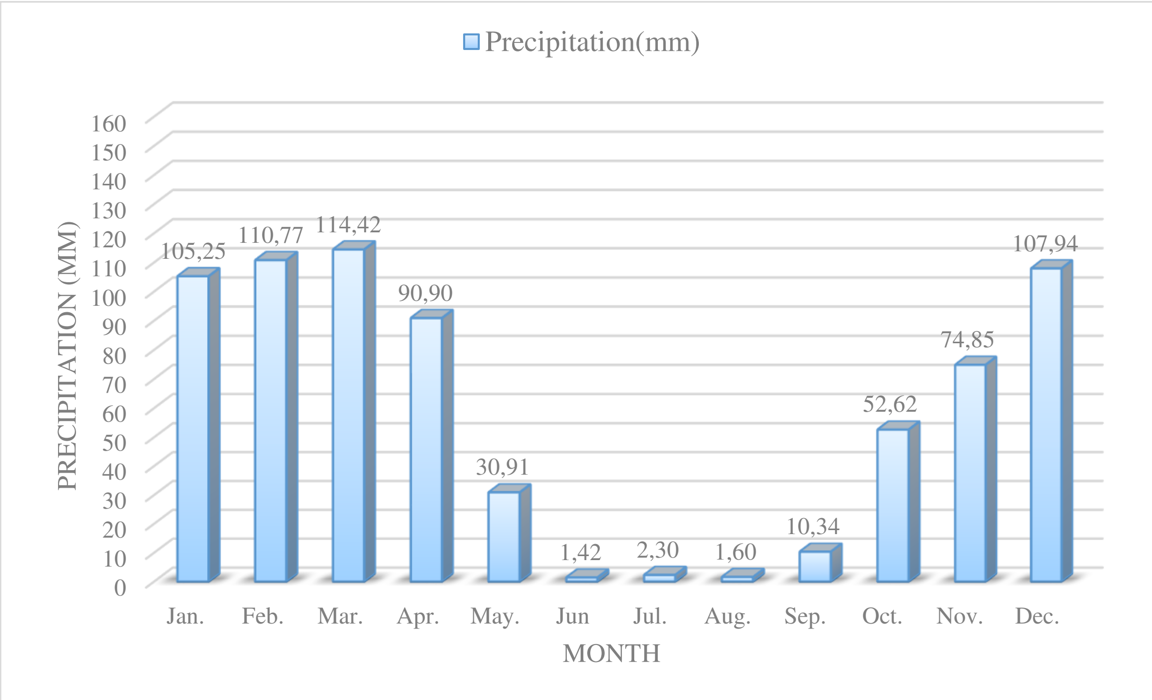

Figure 4.1. monthly precipitation of Soran district (related to the meteorological data of Soran gauge station between 2001 and 2021 years)

While the highest average monthly precipitation in Mergasur occurs in January is 336.10 mm, and the lowest average monthly precipitation occurs in July and August is 0.0 mm (Appendix 2; Table 4.2; Figure 4.2).

Table 4.2. Average monthly precipitation of the Mergasur district (related to the meteorological data of Mergasur gauge station between 2001 and 2021 years)

Months	Precipitation(mm)	Months	Precipitation(mm)
Jan.	336.10	**Jul.**	0.00
Feb.	203.67	**Aug.**	0.00
Mar.	247.64	**Sep.**	13.37
Apr.	143.91	**Oct.**	72.20
May.	45.90	**Nov.**	155.62
Jun	0.50	**Dec.**	279.15
		Average	124.84

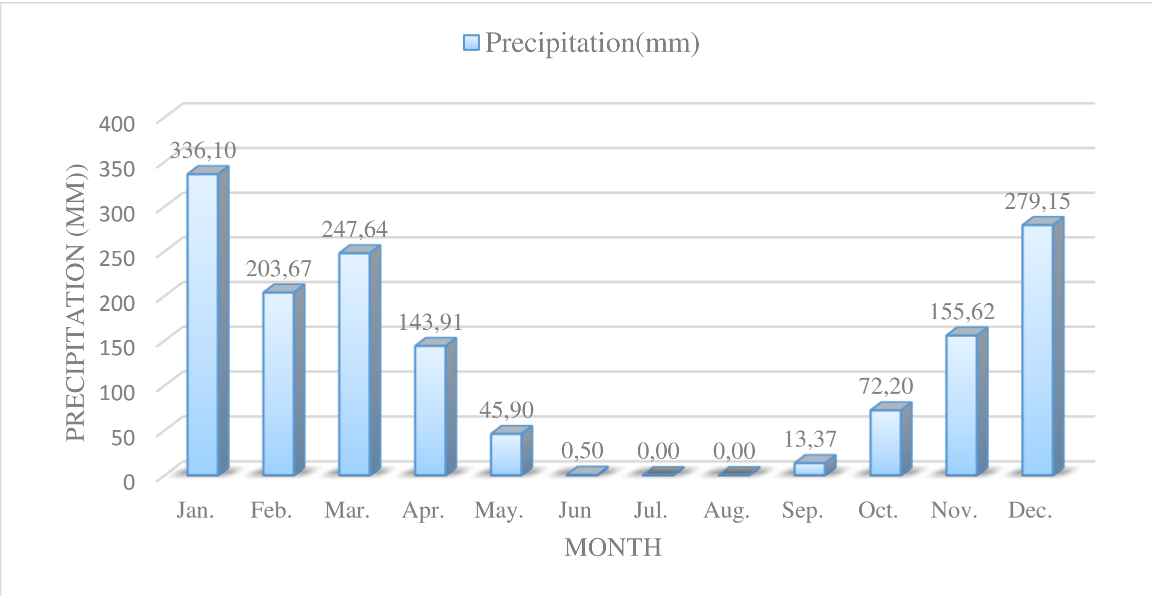

Figure 4.2. Average monthly precipitation of Mergasor district (related to the meteorological data of Mergasur gauge station between 2001 and 2021 years)

Temperature

Temperature has a significant impact on both evaporation and evapotranspiration. There is a significant relationship between plant growth and temperature, where plants react to specified temperature restrictions through which their activities can be done (Thornthwaite, 1948).

The highest average monthly temperature in the Soran district measured in July and August was 31.86°C, and the lowest average monthly temperature measured in January was 4.84°C (Appendix 3; Table 4.3; Figure 4.3).

Table 4.3. The average monthly temperature of the Soran district (related to the meteorological data of Soran gauge station between 2002 and 2021 years)

Months	Temperature T°C	Months	Temperature T°C
Jan.	4.84	**Jul.**	31.86
Feb.	7.09	**Aug.**	31.86
Mar.	11.65	**Sep.**	27.05
Apr.	16.27	**Oct.**	20.41
May.	21.94	**Nov.**	12.36
Jun	28.28	**Dec.**	6.67
		Average	**18.35**

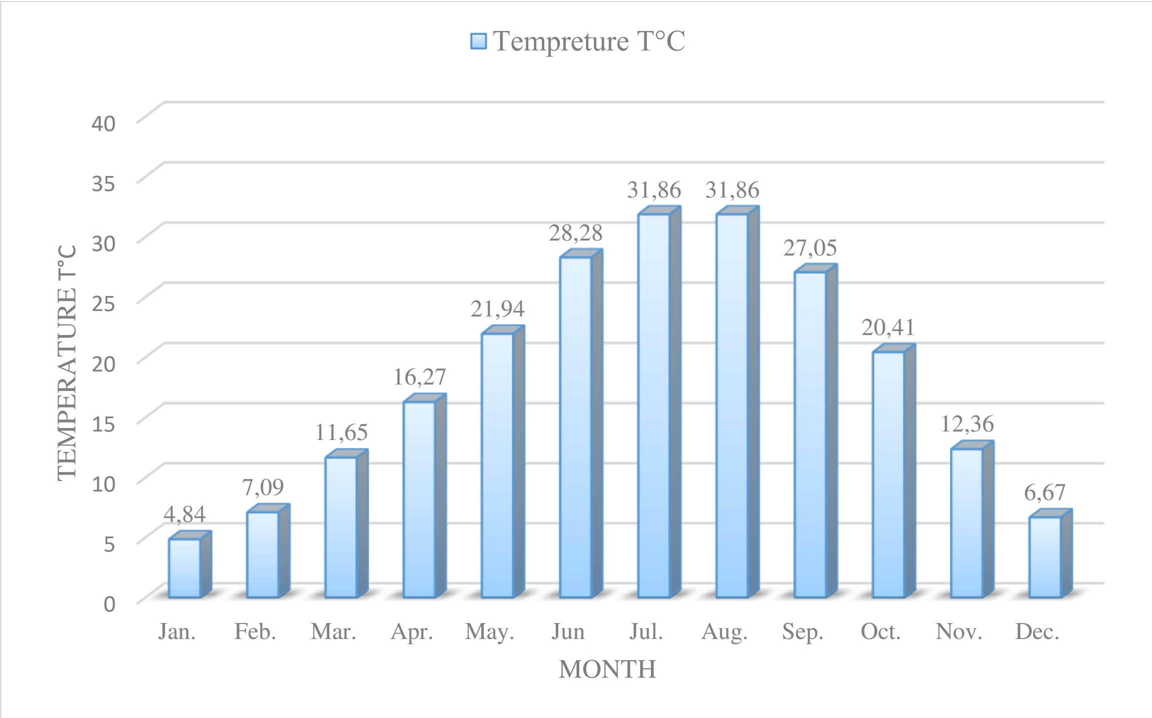

Figure 4.3. The average monthly temperature of Soran district (related to the meteorological data of Soran gauge station between 2001 and 2021 years)

The highest average monthly temperature in the Mergasur district measured in July was 30.15°C, and the lowest average monthly temperature measured in January was 2.49°C (Appendix 4; Table 4.4; Figure 4.4).

Table 4.4. Average monthly temperature of the Mergasur district (related to the meteorological data of Mergasur gauge station between 2011 and 2021 years)

Months	Temperature T°C	Months	Temperature T°C
Jan.	2.49	**Jul.**	30.15
Feb.	5.30	**Aug.**	27.37
Mar.	9.26	**Sep.**	22.22
Apr.	13.12	**Oct.**	17.23
May.	17.78	**Nov.**	11.37
Jun	24.61	**Dec.**	5.76
		Average	**15.55**

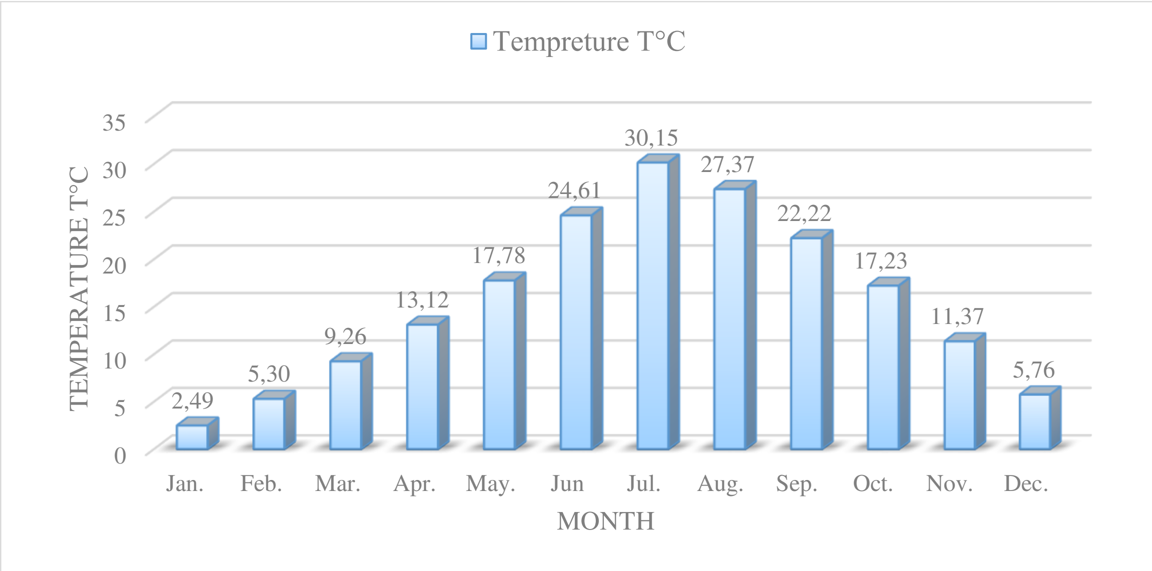

Figure 4.4. Average monthly temperature of Mergasoor district (related to the meteorological data of Mergasur gauge station between 2011 and 2021 years)

Evapotranspiration (ET)

It is the release of water from soil and vegetation into the atmosphere. Evaporation is the transformation of solid or liquid precipitation that reaches the earth's surface into water vapour and the subsequent return of that water to the atmosphere. Plants lose moisture via transpiration. Often, it is difficult to distinguish between transpiration from plants and evaporation from a water surface; As a result, they are integrated into a single term known as evapotranspiration, or ET (Weight and Sonderegger, 2001). Actual evapotranspiration is the quantity of water released into the atmosphere as a result of these two processes. Actual evapotranspiration is a water output based on available moisture, temperature, and humidity.

Potential evapotranspiration (PET) is the maximum quantity of water that would be evacuated from the surface by evapotranspiration if there was adequate water in the soil to satisfy the demand (Dara et al., 2021).

Depending on the climatic data available for the study area, potential evapotranspiration can be estimated using Thornthwaite Method

Thornthwaite method

Thornthwaite method presented an empirical approach for calculating potential evapotranspiration using data on mean temperature (Thornthwaite, 1944). The technique assumes that air temperature is connected with the combined effects of net radiation and other evapotranspiration controls. Several researchers have used this method (Hassan, 1998, Chnaray, 2003, Hamed, 2013). The equation has the following form:

$$PET = La\,16\frac{(10t)^{a}}{J} \quad (4.1)$$

$$J = \sum_{1}^{12} j \quad (2.2)$$

$$a = (679 \times 15^{-4})j^{3} - (771 \times 10^{-7})j^{2} + (179 \times 10^{-4})J + 0.492 \quad (4.2)$$

Where:

PET - Potential evapotranspiration (mm)

La - Monthly correction constant function of latitude

j - Monthly temperature parameter

J - Annual heat index (°C)

t - Mean monthly temperature (°C)

Water Surplus and Water Deficit

Water surplus means that precipitation exceeds potential evapotranspiration during a given period, while water deficit means that potential evapotranspiration exceeds precipitation.

$$WS = P - PE;\ P > PE \quad (4.3)$$

$$WD = PE - P;\ P < PE \quad (4.4)$$

Where:

WS - Water Surplus

WD - Water Deficit

P - Rainfall

PE - Potential evapotranspiration

During the water surplus period, the actual evapotranspiration approaches its potential value, while in the water deficit period, the actual evapotranspiration (AET) is equal to rainfall (Hassan, 1998).

$$P > PE\ then\ PE = AET \quad (4.5)$$

$$P < PE\ then\ P = AET \quad (4.6)$$

The water surplus represents the summation of surface runoff (Rs), groundwater recharge (Re), and soil moisture (Ri). The water table in the study area is deep. Thus, the soil moisture is consumed either by evaporation from the soil or by the plant. The general equation for water balance is:

$$P = Rs + I + AET \quad (4.7)$$

$$Rs + I = WS \quad (4.8)$$

$$WS = P - AET \quad (4.9)$$

where:

AET - Actual evapotranspiration

Rs - Surface runoff

I – Infiltration

Potential evapotranspiration and actual evapotranspiration values were calculated by the Thornthwaite method for the period (2002-2021) for Soran district.

The Thornthwaite (1948) method was used to determine the potential evapotranspiration, surface runoff in the study area. Average monthly precipitation data have been collected from Soran and Mergasur meteorology stations for 20 years between 2002 and 2021, average monthly temperature data have been collected at the Soran meteorology station for 20 years between 2002 and 2021, and from the Mergasur meteorology station for 10 years between 2011 and 2021.

According to the Thornthwaite's moisture balance sheet, the annual average precipitation was calculated (between 2002 and 2021) 703.32 mm, and corrected potential evapotranspiration was calculated 1113.78 mm in Soran district. Therefore, the surface runoff was calculated 54.65% of the precipitation in Soran district (Table 4.5).

Table 4.5. Moisture balance of Soran district between the years 2002 and 2021 according to Thornthwaite method (related to the meteorological data of Soran gauge station)

Months	Jan.	Feb.	Mar.	Apr.	May.	Jun	Jul.	Aug.	Sep.	Oct.	Nov.	Dec.	Total
Mean temperature CO	4.84	7.09	11.65	16.27	21.94	28.28	31.86	31.86	27.05	20.41	12.36	6.67	
Tempreture index (i)=(t/5)1.514	0.95	1.69	3.59	5.96	9.38	13.78	16.50	16.50	12.88	8.41	3.93	1.54	95.11
Potential Evapotranspiration Etp mm	3.92	8.68	24.39	48.87	91.03	154.35	197.78	197.78	140.71	78.32	27.59	7.64	
Latitude Adjustment Coefficient	0.87	0.85	1.03	1.10	1.21	1.22	1.24	1.16	1.03	0.97	0.86	0.84	
Corrected Evapotranspiration Etpc-mm	3.41	7.37	25.12	53.75	110.14	188.30	245.24	229.42	144.93	75.97	23.72	6.41	1113.78
Precipitation (mm)	105.25	110.77	114.42	90.90	30.91	1.42	2.30	1.60	10.34	52.62	74.85	107.94	703.32
Soil water storage capacity -mm	100.00	100.00	100.00	100.00	20.77	0.00	0.00	0.00	0.00	0.00	51.13	100.00	
Acual evapotranspiration Etr (mm)	3.41	7.37	25.12	53.75	110.14	22.19	2.30	1.60	10.34	52.62	23.72	6.41	318.97
Water surplus (mm)	101.84	103.40	89.30	37.15	0.00	0.00	0.00	0.00	0.00	0.00	0.00	52.66	384.35
Water deficit (mm)	0.00	0.00	0.00	0.00	0.00	166.11	242.94	227.82	134.59	23.35	0.00	0.00	794.81

The graph used to determine evapotranspiration and surface runoff for the Soran district is given in Figure 4.5. Surface runoff was determined from the beginning of November to the end of April, and followed by a water shortage from the middle of June to the middle of October related to decreasing precipitation and increasing evaporation.

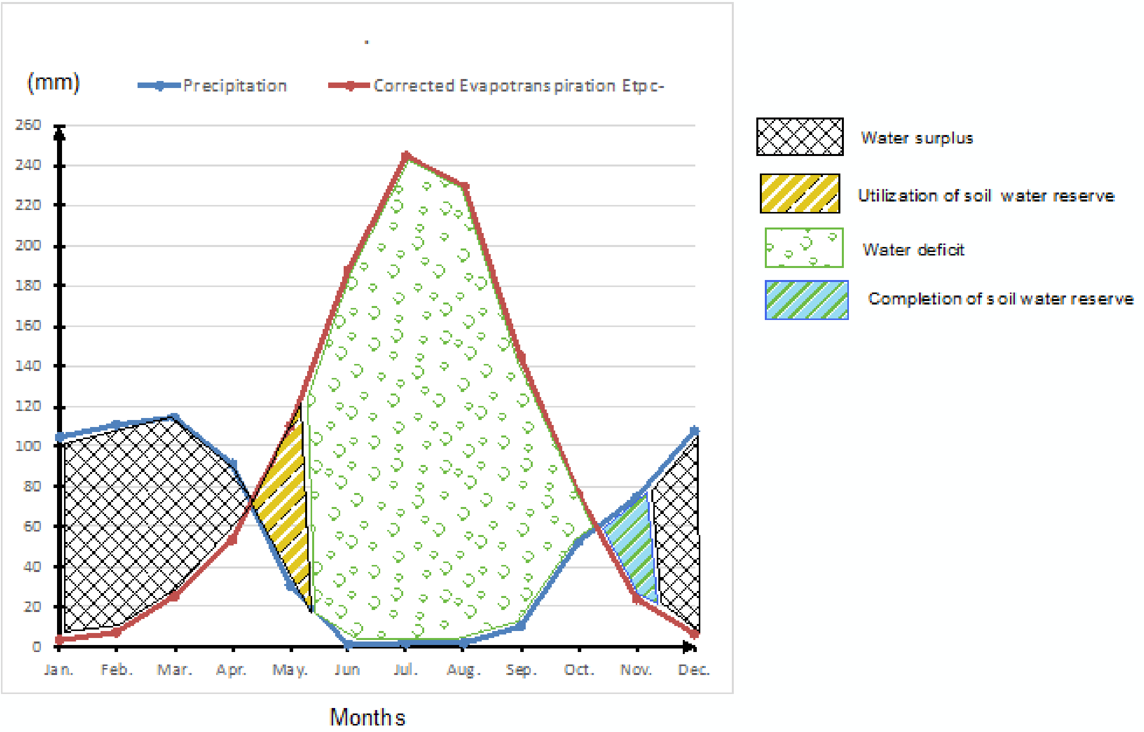

Figure 4.5. Graph of monthly changes of precipitation and Etp for the Soran district according to the Thornthwaite method (related to the meteorological data of Soran gauge station between 2002 and 2021 years)

According to the Thornthwaite's moisture balance sheet (between 2011 and 2021 years) for Mergasur district, the annual average precipitation and corrected potential evapotranspiration were calculated 1486.06 mm, and 878.12 mm, respectively. The surface runoff was 77.52% of the precipitation in Mergasur district (Table 4.6).

Table 4.6. Moisture balance of Mergasur district between the years 2011 and 2021 according to Thornthwaite method (related to the meteorological data of Mergasur gauge station)

Months	Jan.	Feb.	Mar.	Apr.	May.	Jun	Jul.	Aug.	Sep.	Oct.	Nov.	Dec.	Total
Mean temperature °C	2.49	5.3	9.26	13.12	17.78	24.61	30.15	27.37	22.22	17.23	11.37	5.76	
Tempreture index (i)=(t/5)1.514	0.34	1.09	2.54	4.3	6.82	11.16	15.18	13.11	9.56	6.5	3.46	1.23	75.29
Potential Evapotranspiration Etp mm	2.46	8.84	22.69	40.9	68.36	118.41	166.88	141.71	99.63	64.82	32.11	10.17	
Latitude Adjustment Coefficient	0.87	0.85	1.03	1.1	1.21	1.22	1.24	1.16	1.03	0.97	0.86	0.84	
Corrected Evapotranspiration Etpc-mm	2.14	7.51	23.37	44.99	82.71	144.46	206.93	164.38	102.61	62.87	27.61	8.54	878.12
Precipitation (mm)	336.1	203.67	247.64	143.91	45.9	0.5	0	0	13.37	72.2	155.62	279.15	1498.06
Soil water storage capacity -mm	100	100	100	100	63.19	0	0	0	0	9.33	100	100	
Acual evapotranspiration Etr (mm)	2.14	7.51	23.37	44.99	82.71	63.69	0	0	13.37	62.87	27.61	8.54	336.8
Water surplus (mm)	333.96	196.16	224.27	98.92	0	0	0	0	0	0	37.34	270.61	1161.26
Water deficit (mm)	0	0	0	0	0	80.77	206.93	164.38	89.24	0	0	0	541.32

The graph used to determine evapotranspiration and surface runoff for the Mergasur district is given in Figure 4.6. Surface runoff was determined from the beginning of November to the end of April, followed by a water shortage beginning from the middle of June to the middle of October related to decreasing precipitation and increasing evaporation.

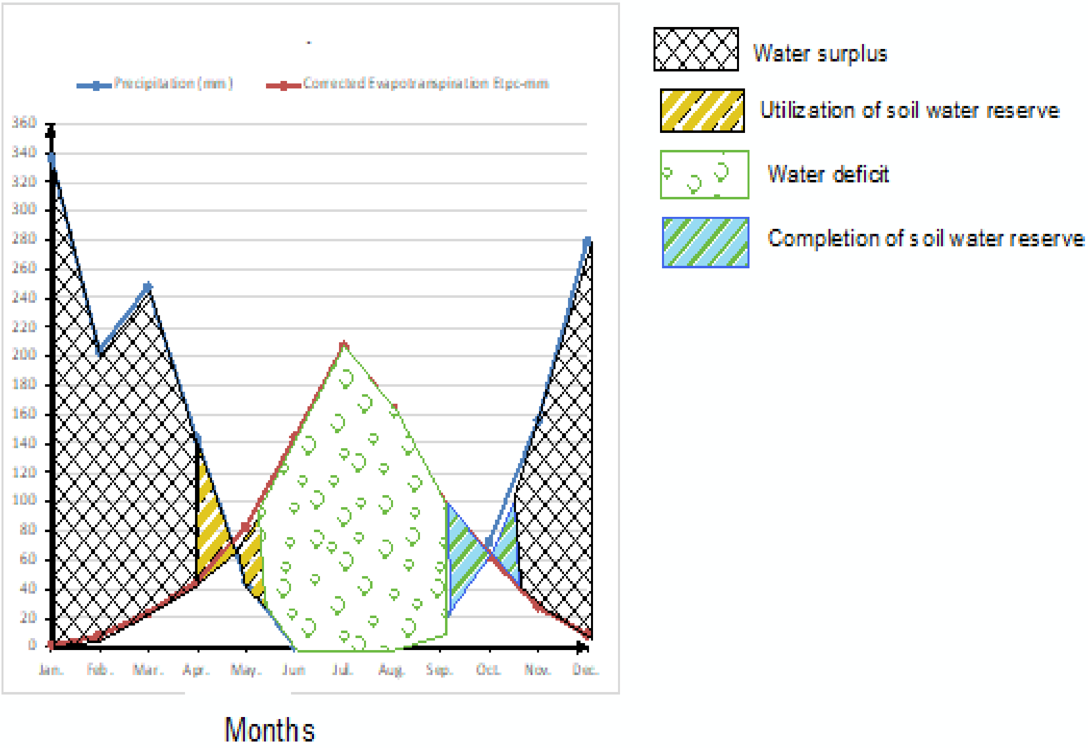

Figure 4.6. Graph of monthly changes of precipitation and Etp for the Mergasur district according to the Thornthwaite method (related to the meteorological data of Mergasur gauge station between 2011 and 2021 years)

4.2. Hydrogeology

The primary aquifer in the study area is the karstic aquifer (Stevanovic and Markovic, 2004). The spring water from relatively water-rich karstic aquifers is the primary source for drinking and irrigation purposes. Furthermore, the study area is tapped by numerous supply wells to the surrounding communities and villages. The study area which lies in the imbricated zone affected by several tectonic activities, leading to a series of anticlines, synclines, and faults. The source of recharge water within the study area is mainly from direct precipitation and snowmelt at the highest elevated areas of the zone.

The structural setting and lithology of rocks influence the hydrogeological conditions. Intensive uplifting and folding of geological formations resulted from a few Alpine Orogenic phases. The formation of numerous large anticlines and synclines with axis mainly oriented NW-

SE parallel to the primary structural setting with weathering most of the core of anticlines and orientation of drainage patterns to the regional fault system. Typically, a karst aquifer is produced in bedded limestone with a fractured structure. The most significant examples of karstic–fissured aquifers are the limestones of the Qamchuqa, Bekhme, and Shiranish formations (Stevanovic and Markovic, 2004). Therefore, these formations are the aquifers for karstic springs in the study area.

Karstification

Numerous soluble rocks, including dolomite, evaporates, and limestone were deposited groundwater during the Tertiary geological history of Northern Iraq. These rocks facilitated the development of surface and subsurface karstic morphology and severe karstification. The folding and uplift of carbonate rocks has continued until today, allowing surface waters to infiltrate into the underground. Numerous cracks, joints, and fault surfaces reinforced this and increased the karstification's basis.

The limestones of the Bekhme and Qamchuqa formations reacted more strongly to karstification processes than other Cretaceous rocks (Figure 4.7) (Stevanovic and Markovic, 2004).

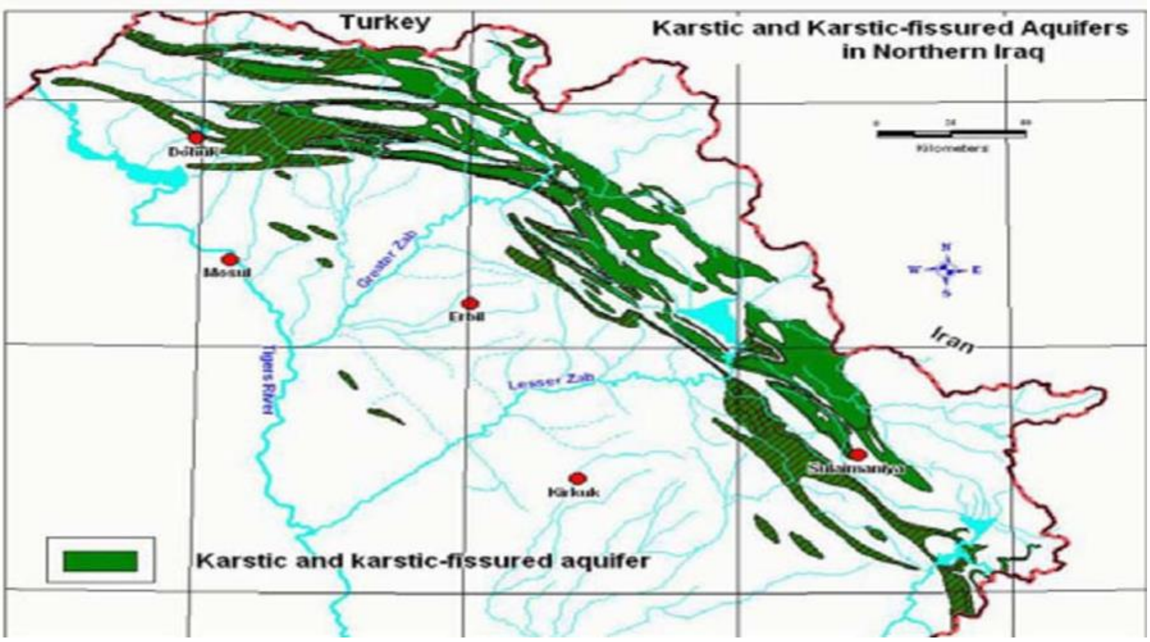

Figure 4.7. Distribution of calcareous rocks and karstic aquifers in northern Iraq (Stevanovic and Markovic, 2004)

There are many karstic caves occurred in the limestones of Bekhme and Qamchuga formations (Figure 4.8).

Figure 4.8. Karstic cave close to Haudian village.

4.2.1. The formation of karstic springs

Haudian Spring is located in Haudian village, at 682.5 m elevation (Figure 4.9). Haudian Spring, which is one of the important water resources for Haudian village, is used for drinking and irrigation purposes.

Figure 4.9. Shiranish and Bekhme Formations's outcrops around Haudian village

The aquifer of the Haudian, Kani Shaker and Mergasur-1 karstic springs in the study area is thick bedded limestones belonging to the Bekhme formation. These limestones are folded depending on the compression regime in the area and are generally presented at the bottom of Shiranish and Tanjero formations (Figure 4.10).

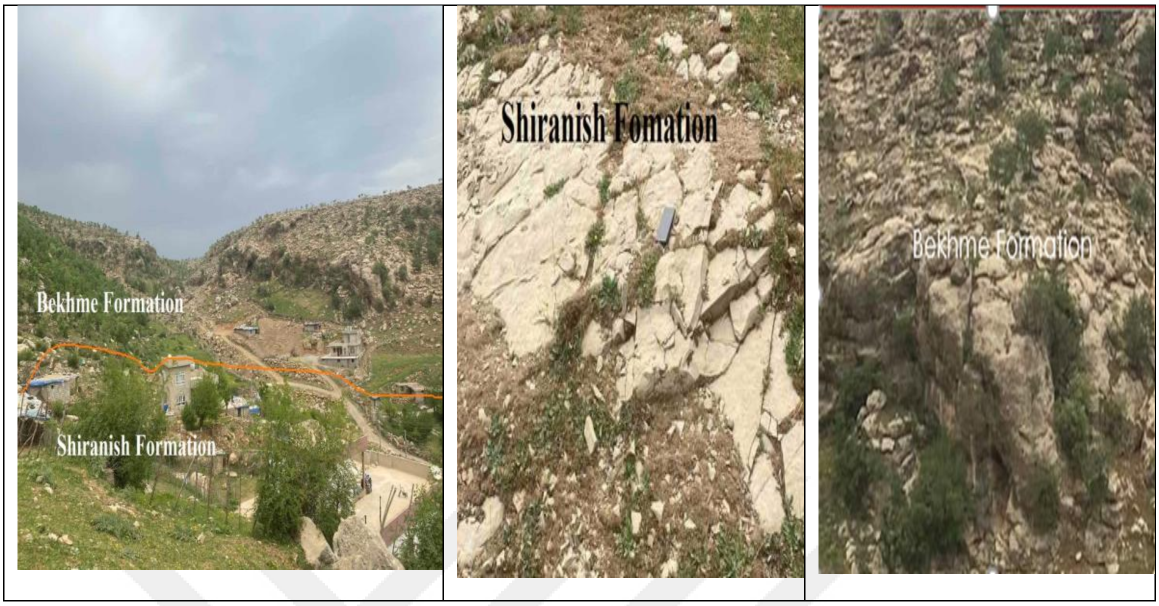

Figure 4.10. The discharge and catchment point of Haudian Spring (449928.48 N, 4067316.25E)

The Haudian Spring is discharged from the contact between Shiranish and Bekhme Formations (Figure 4.11). The limestones of the Bekme formation have gained fractured structure due to the tectonism in the region. Large karstic cavities and even caves have developed within the limestones depending on the karstification, and their secondary porosity and permeability have increased. For this reason, Bekhme limestones are good aquifers for the karstic springs in the study area. As the depth increases, the fractures and fissures decrease and disappear or are filled with clays. Limestones without fractures/fissures, as well as with clay-filled fractures, can act as an impermeable layer for the groundwater saturated zone in their own body. Furthermore, the thin beddings of marl and marly limestone of Shiranish Formation are impermaable layers of karstic aquifer.

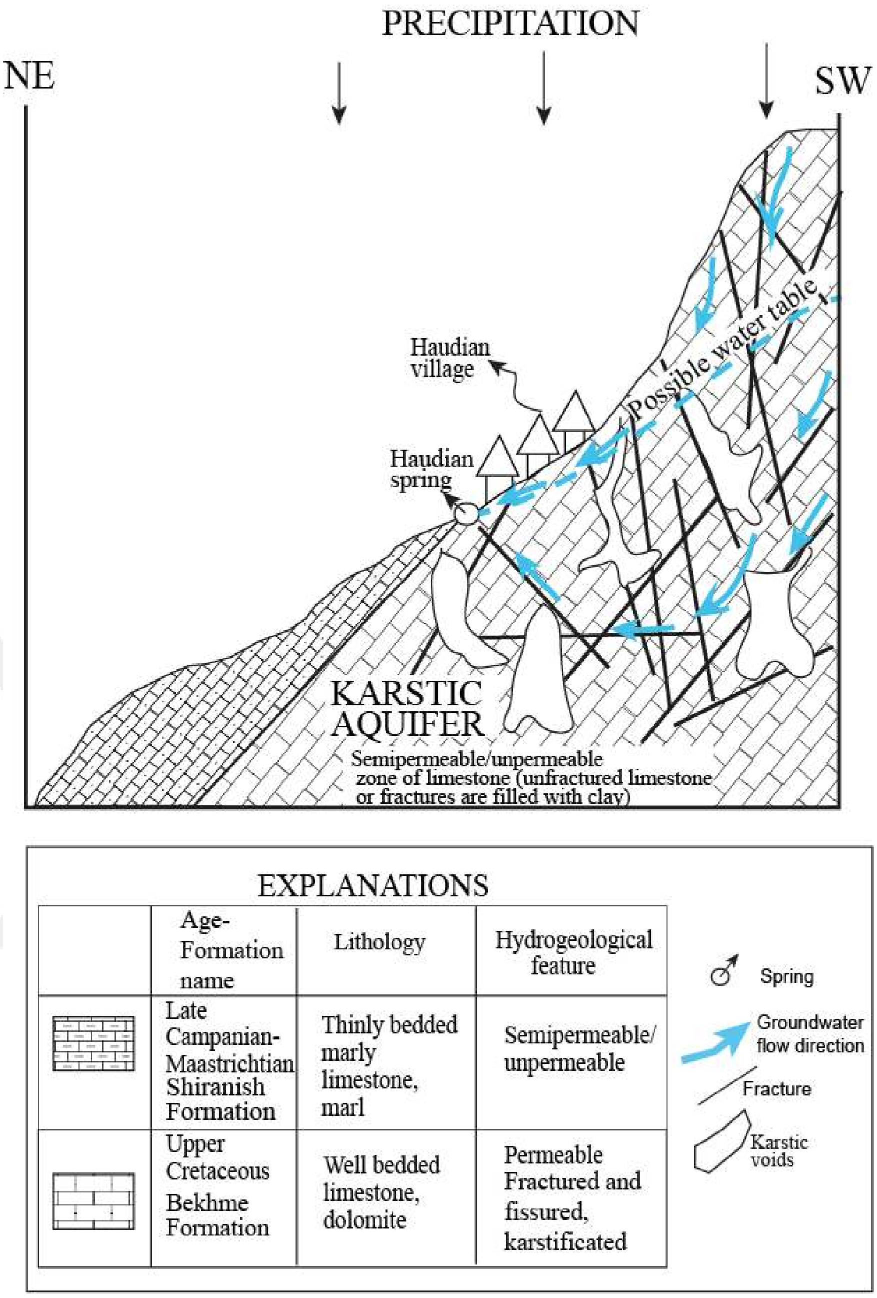

Figure 4.11. Conceptual hydrogeological model for Haudian spring

The livestock barns and septic tanks are present on the recharge area of the Haudian Spring. In addition, the garbage of the village was emptied into the stream water passing through the village settlement area. These pollutants are great risks for the Haudian spring. Because, highly fractured, and karstic limestone aquifers are affected by surface pollutants very quickly and in a short time. In order to maintain the groundwater quality of Haudian spring, domestic waste must be discharged into an appropriate sewage system. In addition, impermeable levels must be provided at the base of animal manure storage areas (Figure 4.12).

Figure 4.12. Views from the livestock barns and garbage area presented on the recharge area of the Haudian spring.

Kani Shakir Spring is located in Sardaw village, at 683 m elevation. In summer Kani Shakir Spring is used for irrigation purposes. The Kani Shakir Spring outlets at the contact between Shiranish Formation and Bekhme Formation (Figure 4.13).

Figure 4.13. The discharge and catchment point of Kani Shakir Spring (449928.48N, 4067316.25E)

Mergasur1 Spring is located Mergasur District, at elevation 1150.8m. The spring is used for drinking and irrigation purposes. The Mergasur-1 Spring outlets at the contact between Tanjero Formation and Bekhme Formation (Figure 4.14).

Figure 4.14. Views of Mergasur 1 Spring (438105.84N, 4077220.53E)

Khardin Spring is located in Piran mountain, near Khardin Village, at elevation 1058m. Khardin Spring is used for drinking and irrigation purposes (Figure 4.15).

(a)

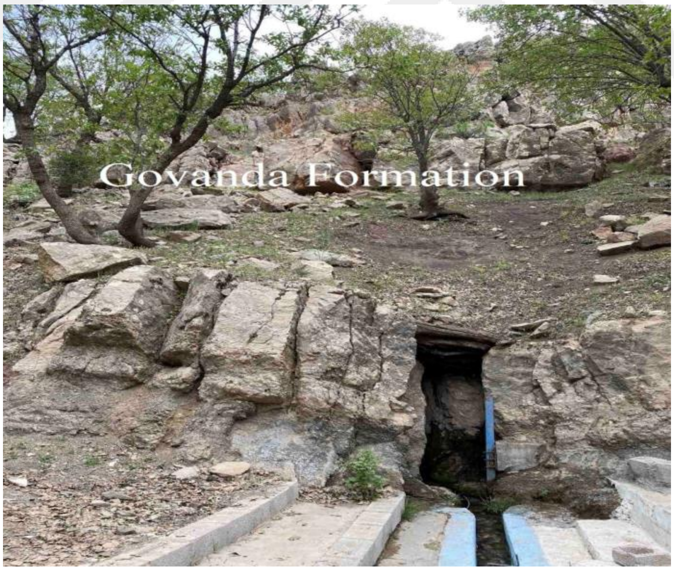

(b)

Figure 4.15. (a) View of Khardin Spring 443506.91N, 4075079.64 E, (b) outcrop of limestone of Govanda Formation around Khardin spring

Khardin Spring is fed from cracked, fractured and kartificated limestones of Govanda. The crack systems developed within Govanda limestones due to tectonism in the region, have given the unit secondary porosity and permeability. These fractures and cracks are quite dense and interconnected at the upper levels and provide aquifer media for the groundwaters. Vertical fractures have developed in the limestones and are filled with secondary calcite. The thickness of limestones in the study area ranges from 50 m to 75 m. The shales and mudstones at the bottom of the Govanda Formation are the impermeable layers of karstic aquifer. Furthermore, the fractures and fissures could filled with clay in the depths and they also act as the impermeable zone for the karstic-fractured aquifer (Figure 4.16).

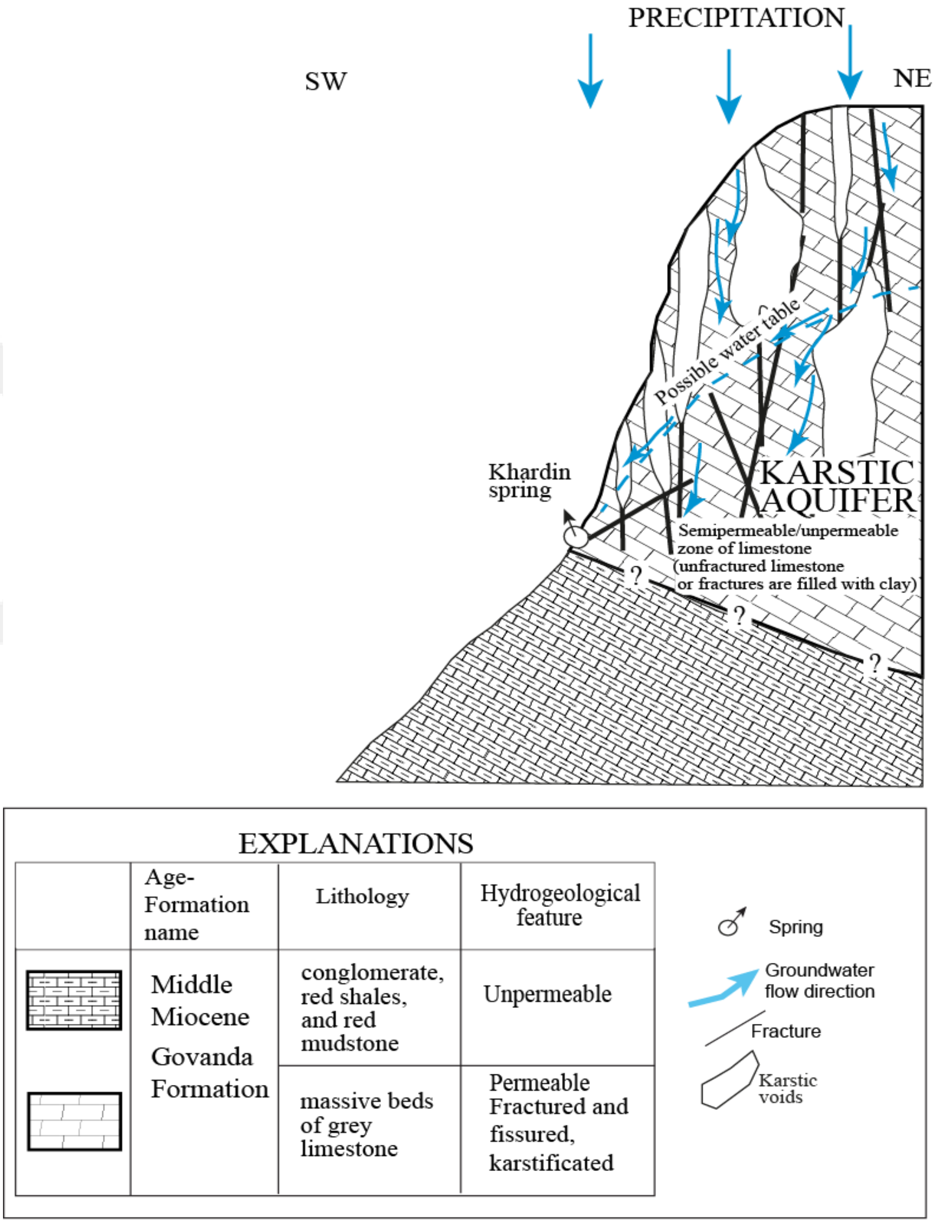

Figure 4.16. Conceptual hydrogeological model for Khardin spring

4.2.2. Hydrogeological parameters of the aquifers

The primary critical method to assess the aquifer parameters is pumping test. Pumping tests were carried out in the studied area to estimate saturated thickness and obtain the aquifers' hydrogeologic parameters. Conducting and analyzing aquifer tests, which is a pricey procedure, is one of the most effective means of evaluating these qualities. Alternatively, when observation wells are not available, the physical parameters of the aquifer might be calculated using a single well test (Van der Schaaf, 2004). Thus, during the recent decade, several attempts have been made to develop a system for estimating aquifer characteristics (hydraulic conductivity, transmissibility, storage coefficient, specific yield) from the analysis of single-well test data (Choi, 2007, Chnaray, 2003, Hassan, 1998, Hamed, 2013, Shwani, 2008).

Numerous properties of pumped wells are critical for comprehending aquifers. The first property is the static water level, which refers to the water level in a well while no water is being extracted. The static water level indicates the location of the water table in a water-table aquifer; in an artesian aquifer, it indicates the level of the potentiometric surface. The water level in a well while pumping is underway is known as the pumping water level. The difference between the water table or potentiometric surface and the pumping level is known as well drawdown. The volume of water released from a well in a certain period, e.g., m^3 /day, whether by pumping or free flow, is referred to as well yield. The optimal well produces a high well yield while requiring little drawdown. The yield per unit of drawdown is referred to as the well's specific capacity.

There are about 30 accessible wells in the research area, which were drilled/dug for water supply. The data of the pumping test of 10 wells were taken to assess aquifer characteristics, the wells in the studied area penetrate the Bekhme and Shiranish formations, according to the lithological profiles of wells, the wells' depth drilled in these formations ranges between 130 to 250 m (Appendix 5 and Table 4.7).

Table 4.7. Details about the 10 selected wells in study area

No	Well Name	Static w.l (m)	Dynamic w.l (m)	Depth (m)	Producing Formation	Shiranish F. (m)	Bekhme F. (m)
1	Kampi zankoy Soran	114	130	240	Shiranish+Bekhme	0-110	110-240
2	Saruchawa 8	82	99	229	Shiranish	0-229	
3	Sarychawa 9	45	55	107	hiranish	0-107	
4	Prozhay Gashtyari Hasti	94	110	205	Shiranish+Bekhme	0-172	172-205
5	Mzgawti Majidawa	96	112	200	Shiranish	0-200	
6	Majidawa 4	101	118	235	Shiranish+Bekhme	0-56	56-200
7	Shawrawa	56		250	Shiranish	0-160	160-250
8	Shevazyarat	34	50	157	Shiranish+Bekhme	0-43	43-157
9	Mazni-Garaki gulan	81	95	181	Shiranish+Bekhme	0-170	170-181
10	Khardin	43.7	157	255	Shiranish+Bekhme	0-85	85-255

Cooper – Jacob's approximation straight line method (1946) was used to determine the hydraulic conductivity, transmissivity and storage coefficient of aquifers in the study area.

Jacob Straight Line Method

Jacob method was applied for analysis of well-pumping test data (Jacob, 1947) noticed that values of transmissivity could be obtained by noting that the t/to =10 (one logarithmic cycle), then log t/to = 1. Therefore, if Δs is the drawdown difference per log cycle of t, the equation below can be used for transmissivity determination (Mays, 2005).

$$T = 0.183\frac{Q}{\Delta s} \tag{4.10}$$

Where: T - Transmissivity (m^2/day)

Q - Pumps constant rate discharge from the well (m^3/day)

Δs - Difference of drawdown per log cycle t.

t/to - Time of last record / initial time

The results of the Jacob straight-line method for the 10 wells have been given in Figure 4.17 a-j.

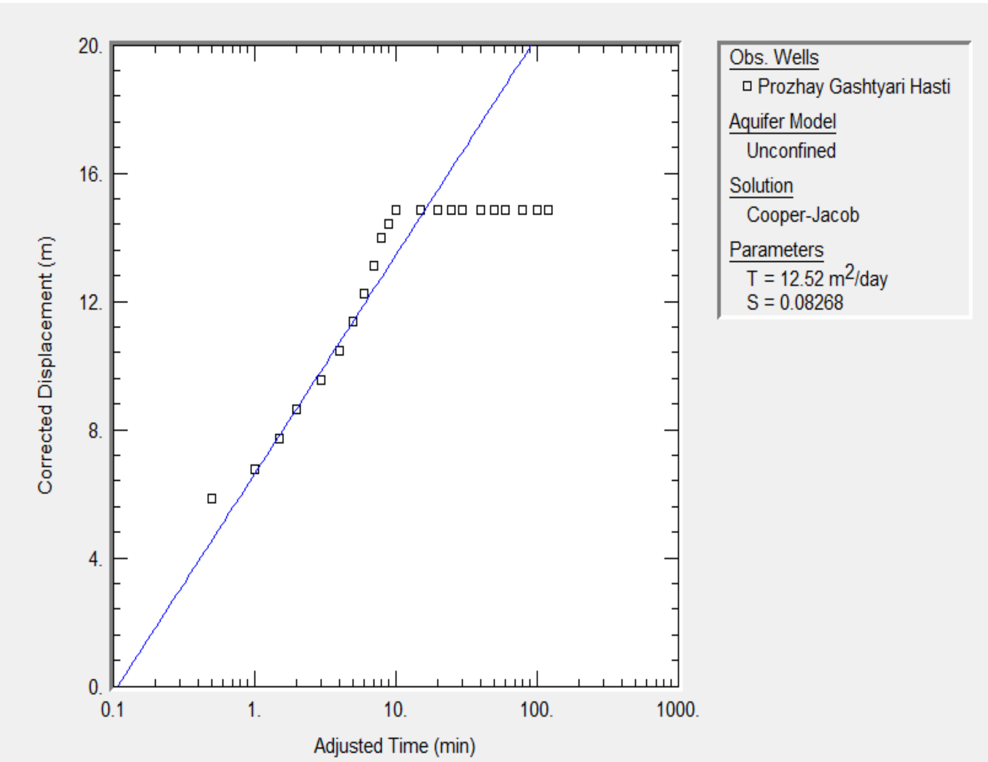

(a)

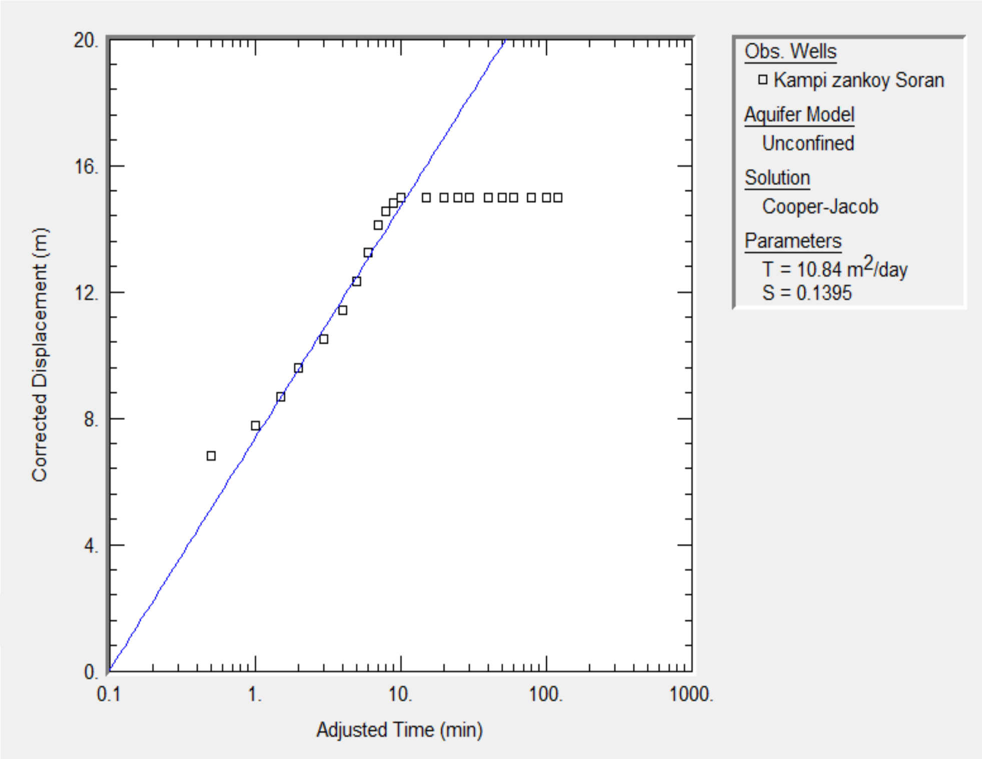
20.
16.
12.
8.
4.
0.
Corrected Displacement (m)
0.1
1.
10.
100.
1000.
Adjusted Time (min)
Obs. Wells
Kampi zankoy Soran
Aquifer Model
Unconfined
Solution
Cooper-Jacob
Parameters
T = 10.84 m2/day
S = 0.1395

(b)

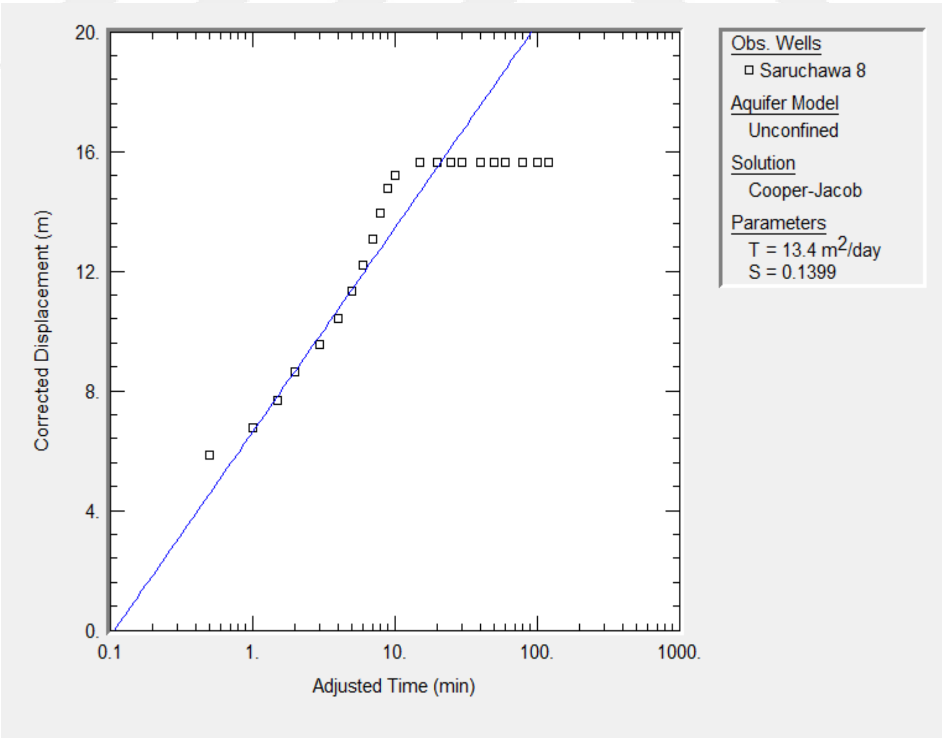
20.
16.
12.
8.
4.
0.
Corrected Displacement (m)
0.1
1.
10.
100.
1000.
Adjusted Time (min)
Obs. Wells
Saruchawa 8
Aquifer Model
Unconfined
Solution
Cooper-Jacob
Parameters
T = 13.4 m2/day
S = 0.1399

(c)

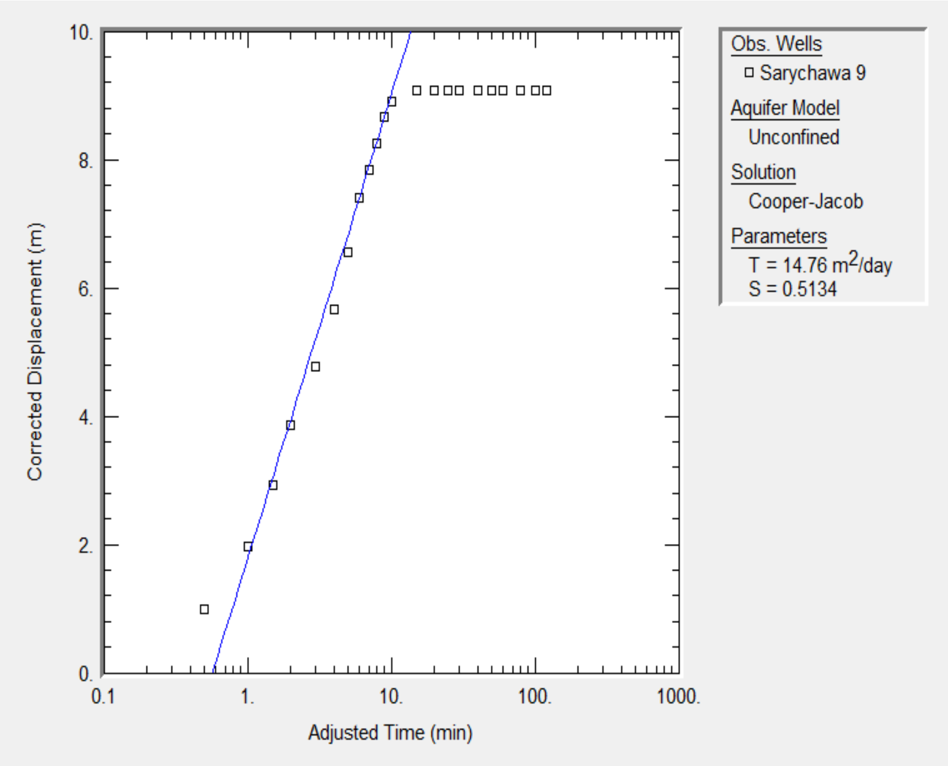
Obs. Wells
Sarychawa 9
Aquifer Model
Unconfined
Solution
Cooper-Jacob
Parameters
T = 14.76 m2/day
S = 0.5134
Corrected Displacement (m)
Adjusted Time (min)
10.
8.
6.
4.
2.
0.
0.1
1.
10.
100.
1000.

(d)

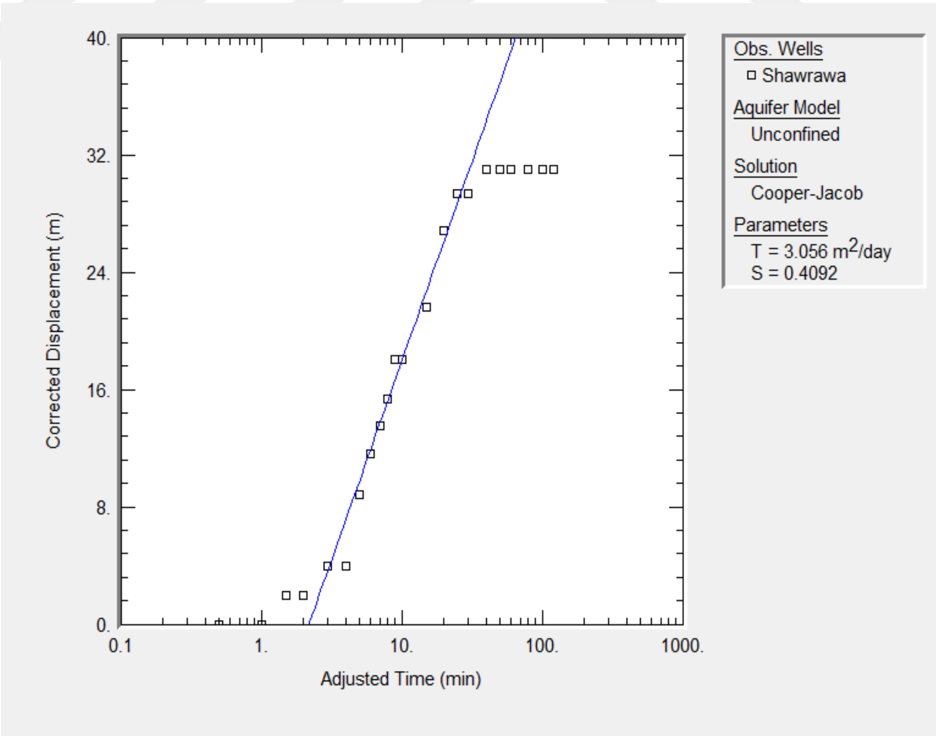
Obs. Wells
Shawrawa
Aquifer Model
Unconfined
Solution
Cooper-Jacob
Parameters
T = 3.056 m2/day
S = 0.4092
Corrected Displacement (m)
Adjusted Time (min)
40.
32.
24.
16.
8.
0.
0.1
1.
10.
100.
1000.

(e)

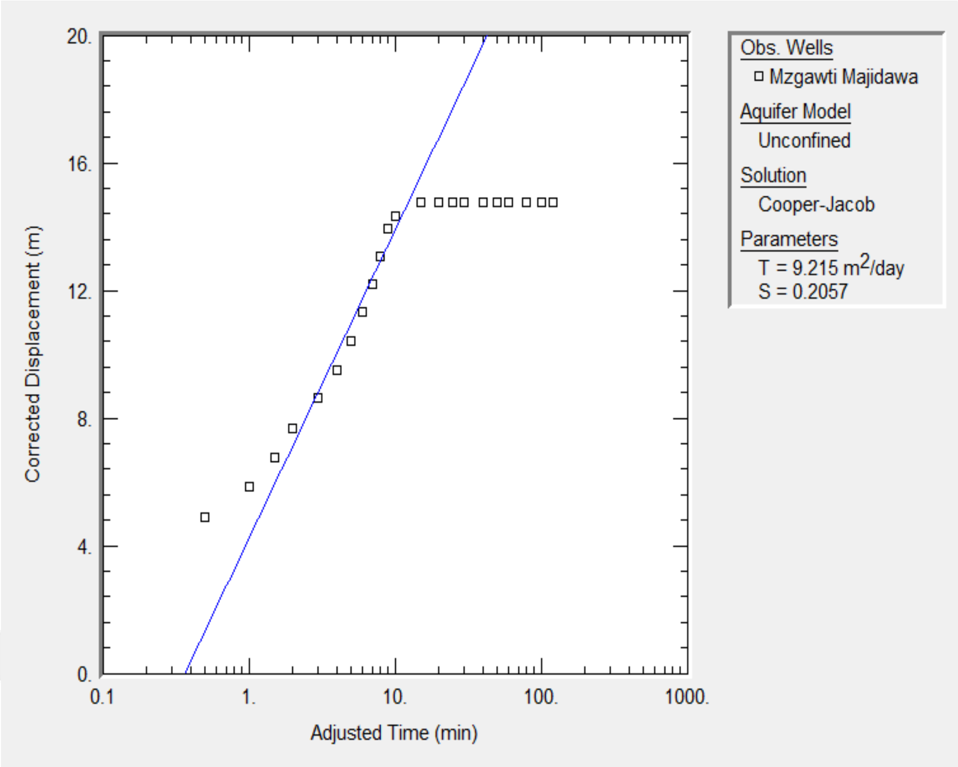
Obs. Wells
Mzgawti Majidawa
Aquifer Model
Unconfined
Solution
Cooper-Jacob
Parameters
T = 9.215 m2/day
S = 0.2057
Corrected Displacement (m)
Adjusted Time (min)
0.
4.
8.
12.
16.
20.
0.1
1.
10.
100.
1000.

(f)

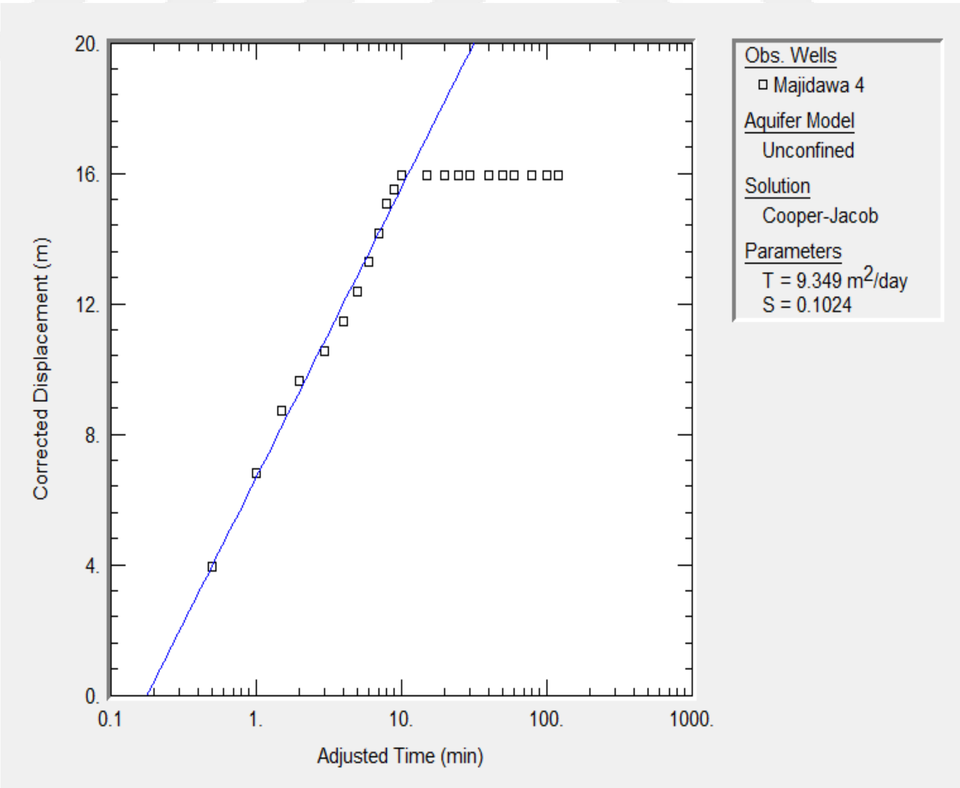
Obs. Wells
Majidawa 4
Aquifer Model
Unconfined
Solution
Cooper-Jacob
Parameters
T = 9.349 m2/day
S = 0.1024
Corrected Displacement (m)
Adjusted Time (min)
0.
4.
8.
12.
16.
20.
0.1
1.
10.
100.
1000.

(g)

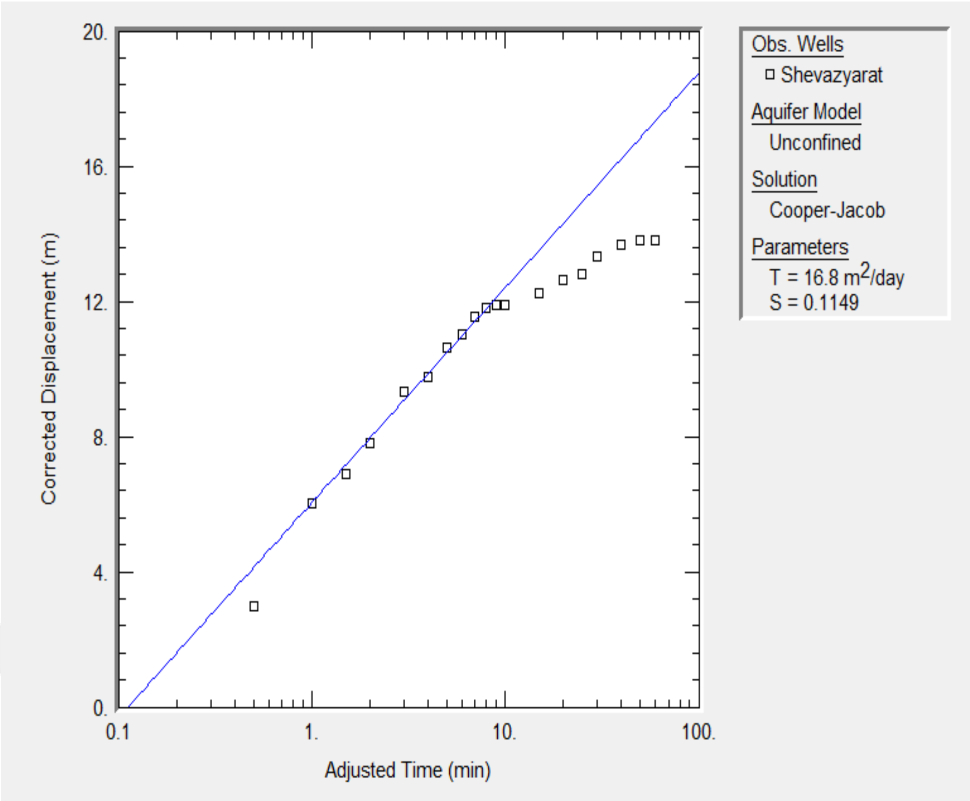

Obs. Wells
Shevazyarat
Aquifer Model
Unconfined
Solution
Cooper-Jacob
Parameters
T = 16.8 m2/day
S = 0.1149
Corrected Displacement (m)
Adjusted Time (min)
20.
16.
12.
8.
4.
0.
0.1
1.
10.
100.

(h)

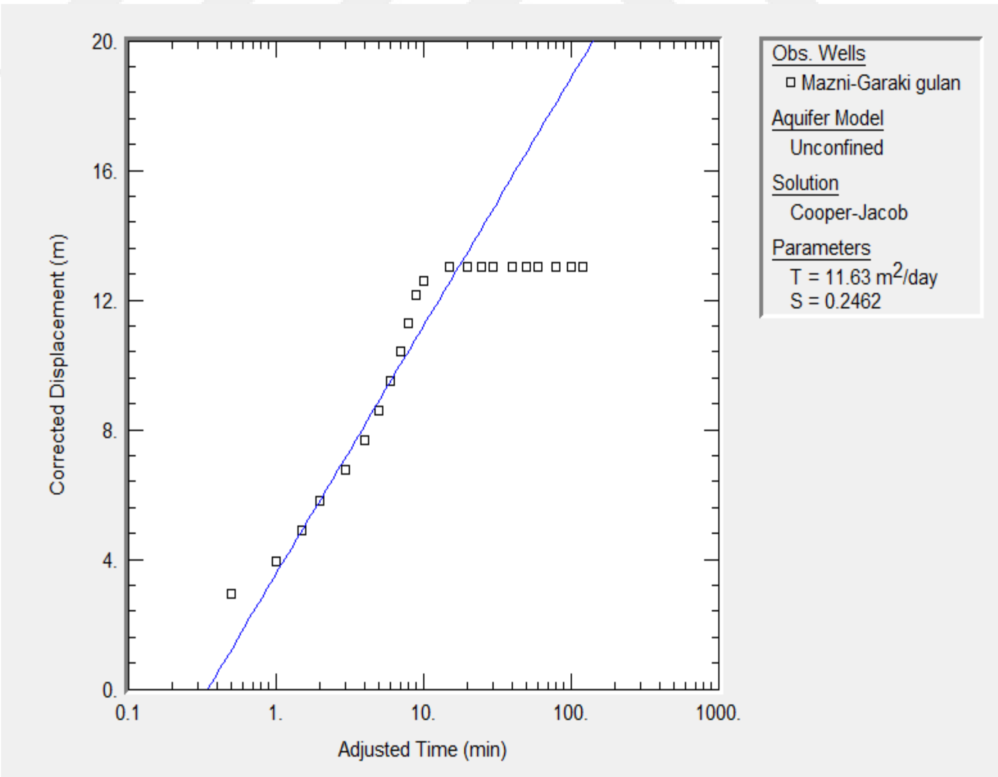

Obs. Wells
Mazni-Garaki gulan
Aquifer Model
Unconfined
Solution
Cooper-Jacob
Parameters
T = 11.63 m2/day
S = 0.2462
Corrected Displacement (m)
Adjusted Time (min)
20.
16.
12.
8.
4.
0.
0.1
1.
10.
100.
1000.

(i)

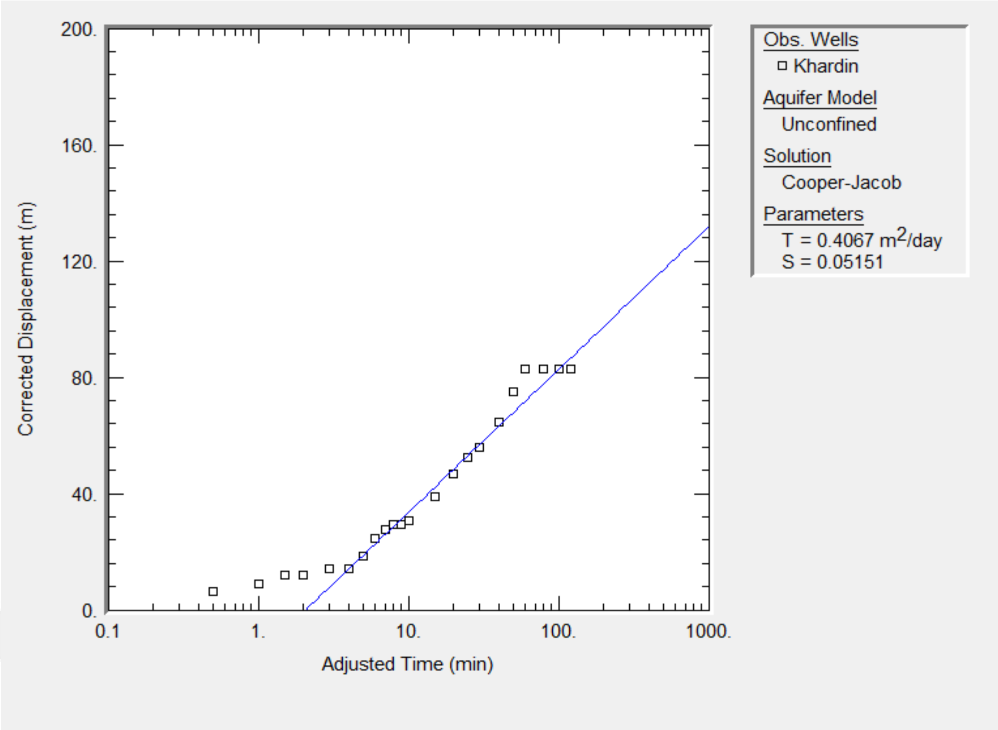

(j)

Figure 4.17. Drawdawn (Δ) and logarithmic time (log t) graph of (a) Kampi zankoy Soran (b) Saruchawa 8, (c) Saruchawa 9, (d) Prozhay Gashtyari Hasti ,(e) Mzgawti Majidawa, (f) Majidawa 4, (g) Shawrawa , (h) Shivazyarat, (i) Mazni- Garaki Gulan, (j) Khardin wells

Analysis of well tests

The parameters comprise the Transmissivity (T), Hydraulic conductivity (K), Specific yield (Sy) and storage coefficient (S).

i. Transmissivity

The capacity of an aquifer to transmit groundwater over its entire saturated thickness is referred to as transmissivity (Mays, 2005). The rate at which groundwater can flow through a unit-width aquifer section under a unit hydraulic gradient is referred to as transmissivity. The levels of drawdown over time pumped can be used to assess transmissivity in a pumping test. As a result, high transmissivity values are correlated with permeable or thick aquifers. Low transmissivity, on the other hand, is associated with thin aquifers or those with low permeability (Kruseman et al., 1970). Aquifers with high transmissivity are able to transmit large quantities of water to wells with a little drawdown of the water table or potentiometric surface. It follows, then, that confining units display low values of transmissivity.

The equation for calculating transmissivity is as follows:

$$T = K \, x \, b \tag{4.11}$$

where:

T = Transmissivity (m^2 /day)

K = Hydraulic conductivity (m/day)

b = Saturated thickness of the aquifer (m)

The transmissivity value determined in selected wells drilled in Bekhme and Shiranish formations are given in Table 4.8.

Table 4.8. Transmissivity and storage coefficient of marly limestones of Shiranish Formation and dolomitic limestones of Bekhme Formation according to Jacob Method using Aqtestolve Program.

Well Name	Discharge Q (m^3/day)	Transmissivity(m^2 /day)	Storage coefficient
Kampi zankoy Soran	434.16	10.84	0.139
Saruchawa 8	498.96	13.4	0.1399
Sarychawa 9	583.2	14.76	0.5134
Prozhay Gashtyari Hasti	466.56	12.52	0.082
Mzgawti Majidawa	486	9.215	0.2057
Majidawa 4	453.6	9.349	0.1024
Shawrawa	453.6	3.056	0.409
Shevazyarat	583.2	16.8	0.1149
Mazni-Garaki gulan	486	8.043	0.5612
Khardin	129.6	0.4067	0.05151

ii. Storage coefficient

A given storativity value represents the volume of water that is either expelled from or taken into aquifer storage in response to a change in the saturated thickness level. Storativity is a dimensionless ratio that can be expressed mathematically by the equation

$$S = (V / A)/h \tag{4.12}$$

where

S, represents storativity,

V, is the amount of water obtained or lost,

A, is the surface area of the aquifer impacted by the recharge or discharge,

h, represents the average water level decline.

Storativity is known as the volume of water released or stored by an aquifer per unit surface area of the aquifer per unit change in the component of head normal to that surface. A change in the storage volume inside an aquifer is represented by water recharge and discharge.

The storage coefficient value determined in selected wells drilled in Bekhme and Shiranish formations are given in Table 4.8.

iii. Hydraulic conductivity

Hydraulic conductivity is a term that refers to a soil's or rock's capacity to transport a fluid. It is determined by a range of physical properties, including porosity, particle size, and other variables (Deming, 2002). The hydraulic conductivity of an aquifer is a measure of its capacity to carry water. A high hydraulic conductivity number indicates that an aquifer is capable of efficiently conveying water, while a low value indicates inefficient transmission. The hydraulic conductivity represents as

$$k = \frac{\mathrm{V}}{\mathrm{dh/dlvV}} \tag{4.13}$$

$$K = T / b \tag{4.14}$$

Where: K - Hydraulic conductivity (m/day)

T = Transmissivity (m^2 /day)

b = Saturated thickness of the aquifer (m)

V - Groundwater velocity (m/day)

dh/dl - hydraulic gradient

Table 4.9 shows the calculated hydraulic conductivity value according to Jacob Method.

Table 4.9. Calculated hydraulic conductivity of marly limestones of Shiranish Formation and dolomitic limestones of Bekhme Formation according to Jacob Method.

Well No.	Well Name	Transmissivity (m^2 /day)	Transmissivity (m^2 /s)	Saturated thickness (m)	Hydraulic conductivity (m/day)	Hydraulic conductivity (m/s)
1	Kampi zankoy Soran	10.84	$1.25*10^{-4}$	126	0.086	$9.95*10^{-7}$
2	Saruchawa 8	13.4	$1.55*10^{-4}$	105	0.128	$1.47*10^{-6}$
3	Sarychawa 9	14.76	$1.70*10^{-4}$	54	0.273	$3.16*10^{-6}$
4	Prozhay Gashtyari Hasti	12.52	$1.44*10^{-4}$	111	0.113	$1.3*10^{-6}$
5	Mzgawti Majidawa	9.215	$1.06*10^{-4}$	104	0.089	$1.02*10^{-6}$
6	Majidawa 4	9.349	$1.08*10^{-4}$	134	0.070	$8.07*10^{-7}$
7	Shawrawa	3.056	$3.53*10^{-5}$	194	0.016	$1.82*10^{-7}$
8	Shevazyarat	16.8	$1.94*10^{-4}$	114	0.147	$1.7*10^{-6}$
9	Mazni-Garaki gulan	8.043	$9.30*10^{-5}$	100	0.080	$9.30*10^{-7}$
10	Khardin	0.4067	$4.70*10^{-6}$	211.3	0.002	$2.22*10^{-8}$

Generally, the results of 10 single well tests carried out mainly in Shiranish aquifer, and Shiranish and Bekhme aquifers. The average hydraulic conductivity ($1.03*10^{-6}$ m/sn) of marly limestone belong to Shiranish Formation and average hydraulic conductivity ($1.15*10^{-6}$ m/sn) of both marly limestones (belong to Shiranish Formation) and dolomitic limestones (belong to Bekhme Formation) are similar in study area (Table 4.10).

Table 4.10. Average hydraulic conductivity and transmissivity of marly limestones of Shiranish Formation, and marly limestones of Shiranish and dolomitic limestones of Bekhme Formation

Aquifer parameters	Shiranish Formation	Shiranish and Bekhme formations
Hydraulic conductivity (m/s)	$1.03*10^{-6}$	$1.15*10^{-6}$
Transmissivity (m^2 /s)	$4.663*10^{-4}$	$4.70*10^{-4}$

4.2.3. Groundwater Fluctuation

Groundwater fluctuation is caused by a variety of factors, but the recharge and discharge processes are the most important. The seasonal and annual fluctuation of the groundwater is the mirror image of recharge and discharge processes (Hassan, 1998). Many factors influence fluctuation, including rainfall intensity, rainfall quantity, the ability of soil and rock beds to absorb water, groundwater depth above sea level, topography, evapotranspiration, and water well discharge (Wilson, 1990).

In rainy and snowy months, the recharge quantity is greater than the discharge quantity in the wells, resulting in increased groundwater levels, whereas, in dry months (summer season), the discharge quantity is greater than the recharge quantity (recharge may be absent), leading to reduced groundwater levels.

The data of measured groundwater levels from the surface for two wells were given in Table 4.11. The maximum and minimum decreases of groundwater level were occurred in October and January for both wells, respectively.

Table 4.11. Groundwater level measurements in Haudian 2 and Shivazyarat wells (from 27/01/2021 to 22/12/2021)

Haudian 2 Well		Shivazyarat Well	
Date	Depth of static groundwater level from the surface (m)	Date	Depth of static groundwater level from the surface (m)
27/01/2021	22.10	27/01/2021	35.90
25/02/2021	22.50	25/02/2021	37.50
28/03/2021	22.80	28/03/2021	45.80
26/04/2021	29.10	26/04/2021	46.20
31/05/2021	38.95	31/05/2021	49.75
29/06/2021	47.70	29/06/2021	56.30
24/07/2021	53.75	24/07/2021	70.50
28/08/2021	59.00	28/08/2021	75.60
25/09/2021	62.10	25/09/2021	77.90
16/10/2021	65.70	16/10/2021	81.00
03/11/2021	63.20	03/11/2021	78.80
22/12/2021	60.30	22/12/2021	75.50

Figure 4.18 and Figure 4.19 show the relationship between groundwater fluctuation and precipitation for Haudian 2 and Shivazyarat wells. During 2021 the groundwater level in two wells significantly fluctuated. The major source of karstic springs and wells is the precipitation. Therefore, the changes in precipitation is the primary factor occurring groundwater fluctuations in aquifers in study area (Figure 4.18 and Figure 4.19).

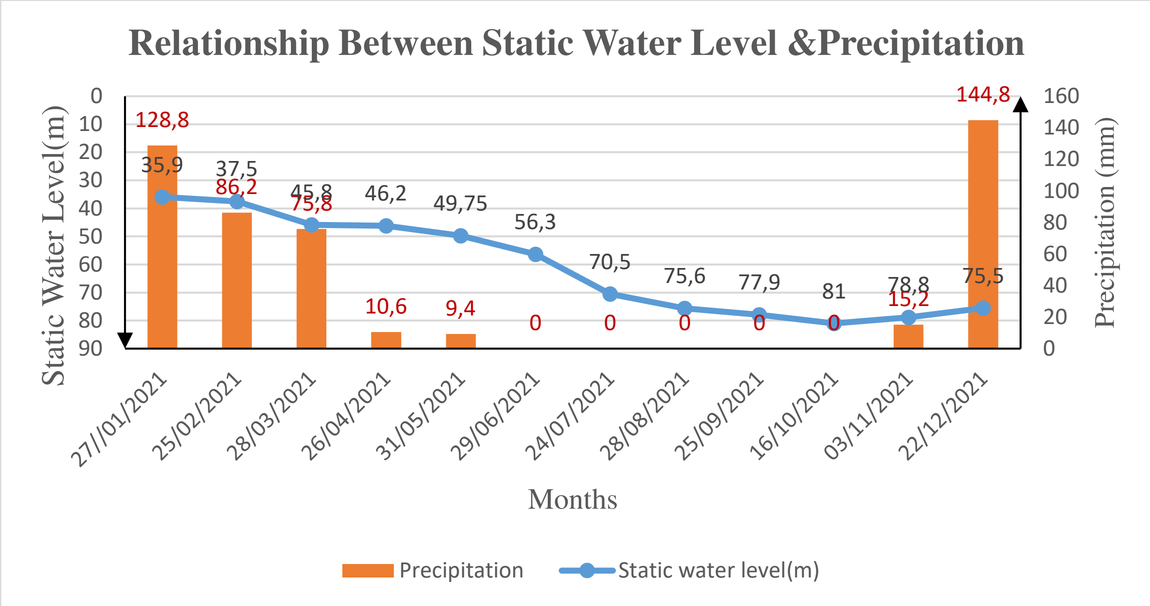

Figure 4.18. Groundwater fluctuation in Haudian 2 well from 27/01/2021 to 22/12/2021

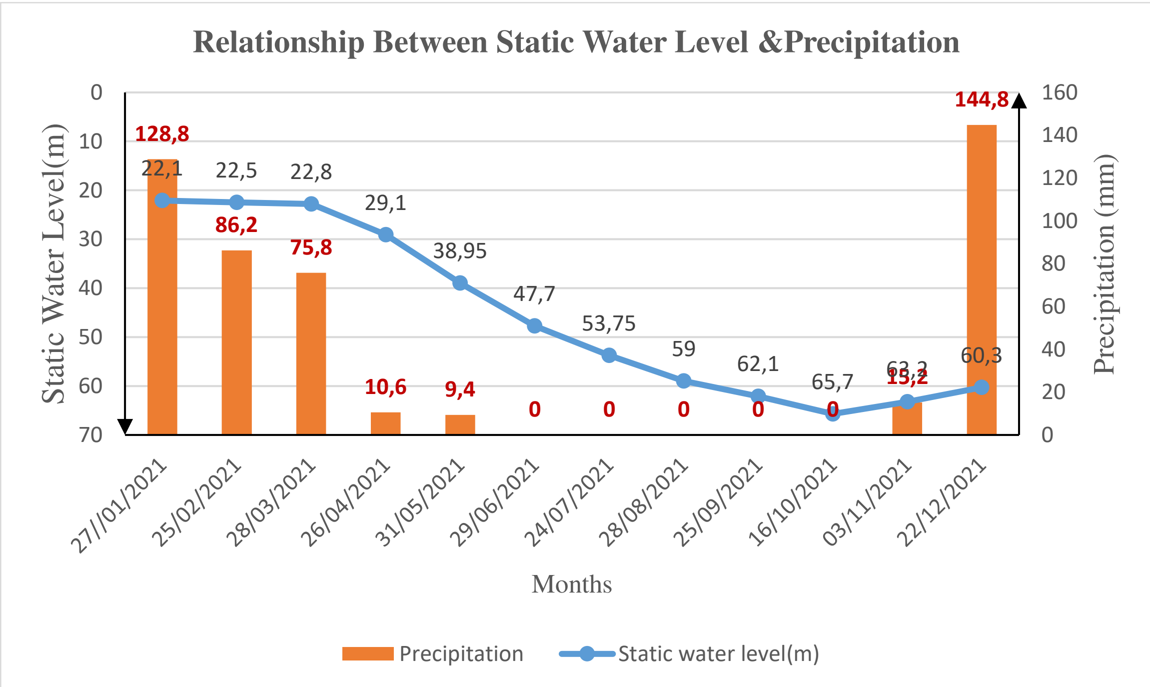

Figure 4.19. Groundwater fluctuation in Shivazyarat well from 27/01/2021 to 22/12/2021

The maximum and minimum depths of groundwater level from the surface in Haudian 1 well for each years beginning from 2000 to 2014 years have been given in Table 4.12 according to data collected from the Groundwater Directorate of Erbil (Appendix 6).

Table 4.12. The relationship between precipitation and groundwater levels measured in Haudian 1 well from 2000 to 2014 (*=minimum groundwater depth from the surface, **: maximum groundwater depth from the surface for each year)

Date	Depth of Groundwater Level from the surface (m)	Precipitation
03/09/2000	32.63*	
26/10/2000	34.18**	
05/04/2001	30.35*	
06/11/2001	38.9**	496.2
07/05/2002	22.00*	
12/11/2002	41.20**	830
04/02/2003	27.70*	
26/08/2003	45.02**	801.8
16/03/2004	22.05*	
04/11/2004	42.08**	802.2
26/04/2005	26.24*	
29/11/2005	37.50**	570.1
25/4/2006	25.65*	
26/9/2006	32.74**	976.6
24/4/2007	27.50*	
25/12/2007	35.50**	511.8
01/08/2008	35.54*	
30/12/2008	43.43**	449.2
28/4/2009	42.83*	
17/11/2009	46.82**	603.2
27/04/2010	42.69*	
21/12/2010	45.90**	433.5
25/01/2011	55.95*	
25/1/2011	55.95**	612.6
5/5/2012	83.30*	
7/8/2012	80.00**	625.2
19/6/2013	79.00*	
22/10/2013	80.72**	669.6
29/1/2014	80.10*	
22/5/2014	79.00**	708.6

The groundwater level in Haudian 1 well has been increased related to the increasing in the amount of precipitation, whereas has been decreased by the decreasing in precipitation until 2007. Furthermore, a steady decrease in groundwater level has been determined in Haudian 1 well beginning from 2007 until 2014. Drilling of wells next to this well, decreasing in the amount of precipitation, and growth of population could be the sourcesfor decreasing in groundwater level in Haudian 1 well (Figure 4.20).

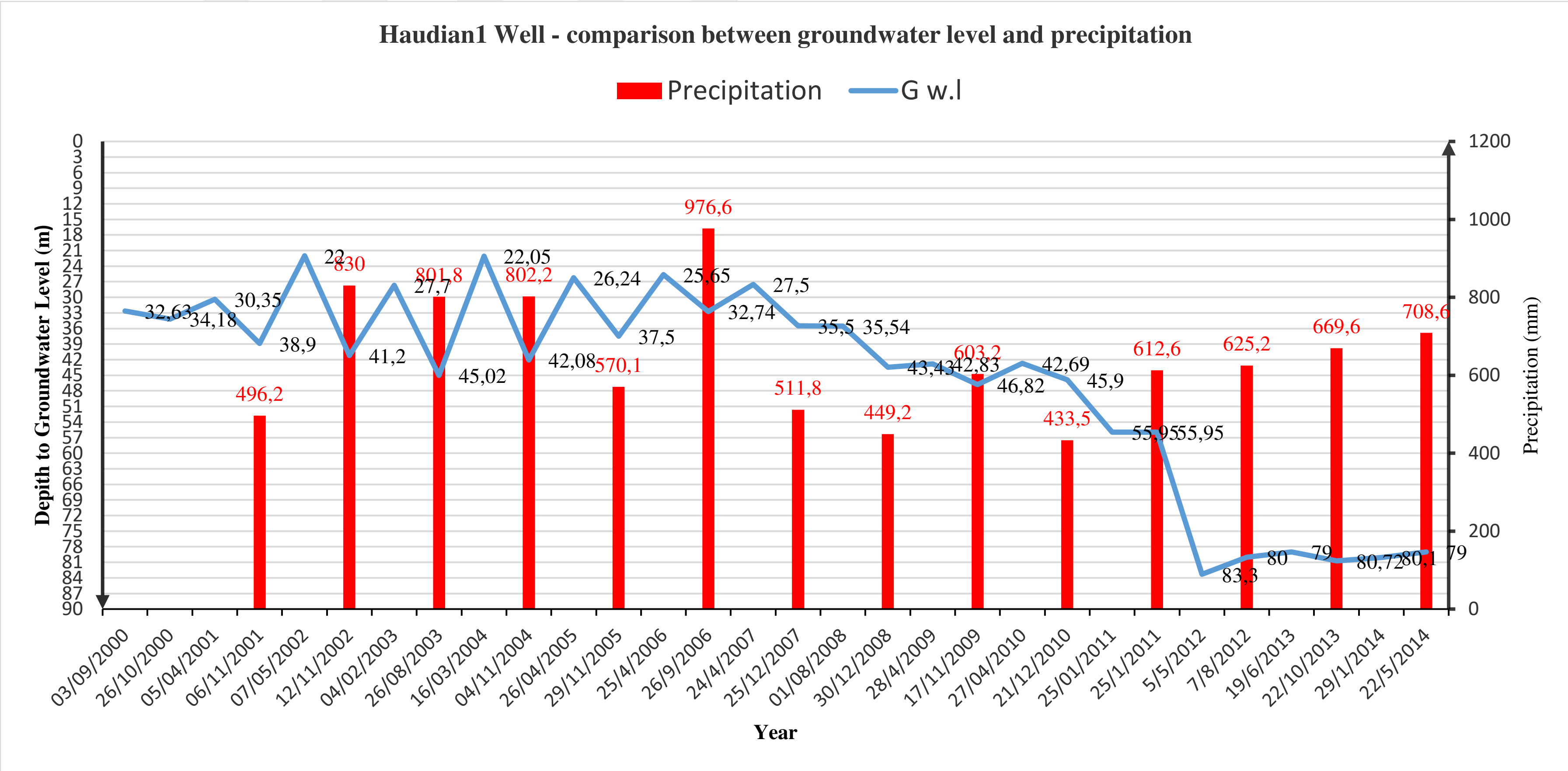

Figure 4.20. Groundwater fluctuation for each year for Haudian 1 well from 2000 to 2014 (the data of precipitation was taken from the General Directorate of Agriculture of Erbil and groundwater depths were taken from General Directorate of Erbil Groundwater)

Maillet equation

The basic calculation of the discharge graph of springs during the real regime period is calculated with the Maillet formula (1905).

$$Q = q0 * e - \alpha(t - to) \quad (4.15)$$

In the above equation;

q_0: discharge at the beginning of the recession (time to) (m^3 /s)

e: basis of natural logarithm

α: recession coefficient (day^{-1})

t-t_0: duration since the start of recession (day)

q: discharge at time t (m^3 /s)

With this formula, the real regime is determined from the flow rate change graph of the springs.

Recession curves include knowledge of the storage characteristics of many media types, including porous, fractured, cracked, and karst lithology. Analysis recession curve gives a function that quantifies the temporal discharge degradation and represents the drained volume within specific time limits (Amit et al., 2002). The curve that displays the fluctuation in its discharge over time is known as the spring hydrograph. The recession curve is the section of the hydrograph which enlarges from the peak of a discharge to the bottom of the next rising. The recession coefficient (α) is calculated from the recession curve with the following equation;

$$\alpha = \log q_0 - \log q / (t - t_o) * 0.4343 \quad (4.16)$$

The formula used to calculate the water storage capacity above the discharge level is given below.

$$V_0 = (q_0 / \alpha) * 86400 \quad (4.17)$$

4.2.4. The discharge and precipitation relationship of Haudian spring

Flow measurement was made twice a month from 07/01/ 2020 to 22/ 12/ 2021. Discharge - precipitation graph of Haudian spring and discharge in the real regime is shown in Figure 4.21.

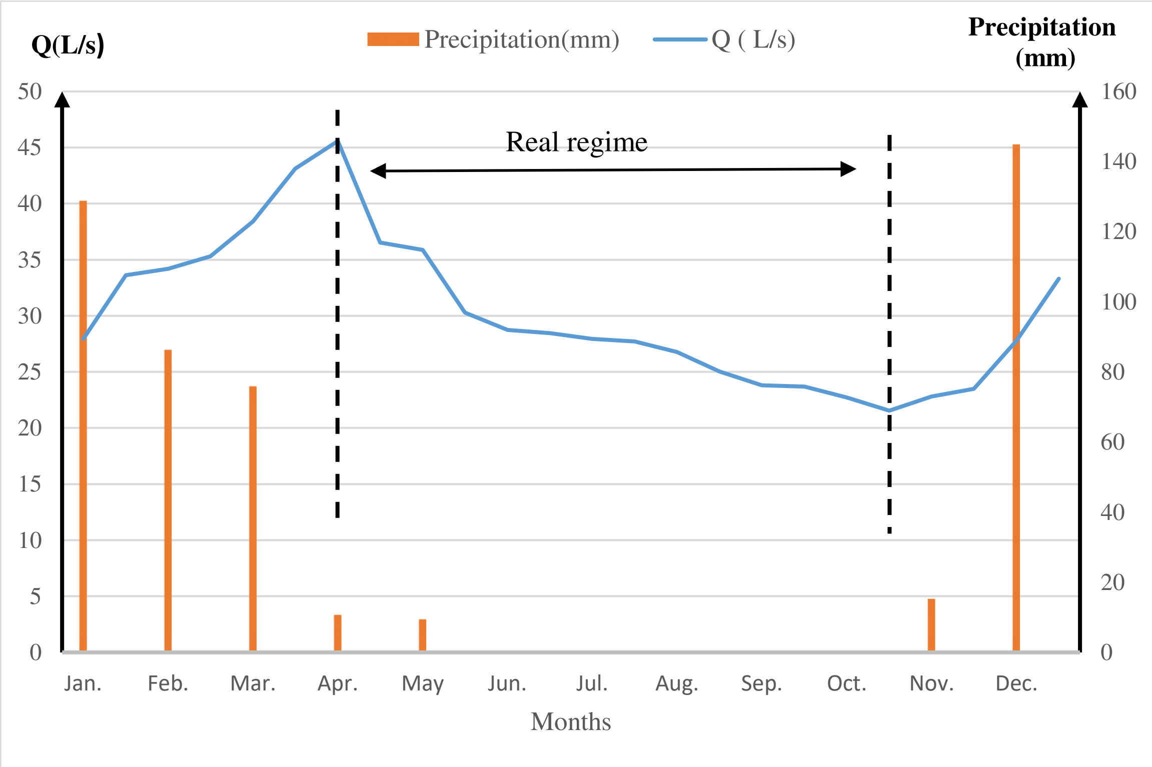

Figure 4.21. Discharge-precipitation graph of Haudian spring

According to the discharge curve in the real regime of the Haudian spring (Figure 4.22), the highest discharge (q_o) at the initial recession period was 45.573 l/s, while the lowest discharge (q) at the end of the dry period was 21.547 l/s.

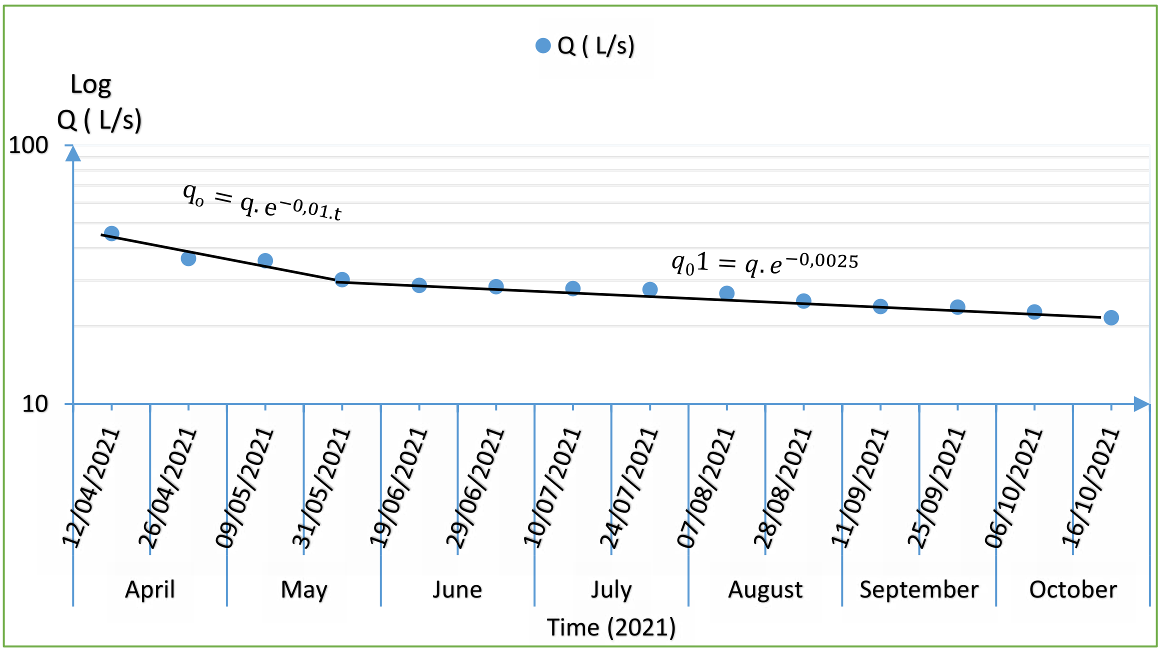

Figure 4.22. Discharge curve for recession period of the Haudian spring (2021)

The real regime period of the Haudian spring is between 12.04.2021 and 16.10.2021, and the water storage capacity above the discharge level in the recession period of Haudian spring for 2021 to 2022 was determined using the following Maillet (1905) formula: $V_0 = (q_0 / \alpha) * 86400$. The water storage capacity of Haudian spring (V_0) was calculated as 461218 m^3.

Based on the Iraq standard, the average amount of domestic water for daily consumption per person is 392 L/day (UN, 2013; Al-Furaiji et al., 2016). Around 1500 local residents utilize Haudian spring for drinking and domestic purposes. If just this spring alone is used for drinking and domestic purposes by a population of 1500, the period of this spring, in the real regime, was calculated as 785 days.

4.2.5. The discharge and precipitation relationship of Kani Shakir spring

Discharge - precipitation graph of Kani Shakir spring and discharge in the real regime is shown in Figure 4.23.

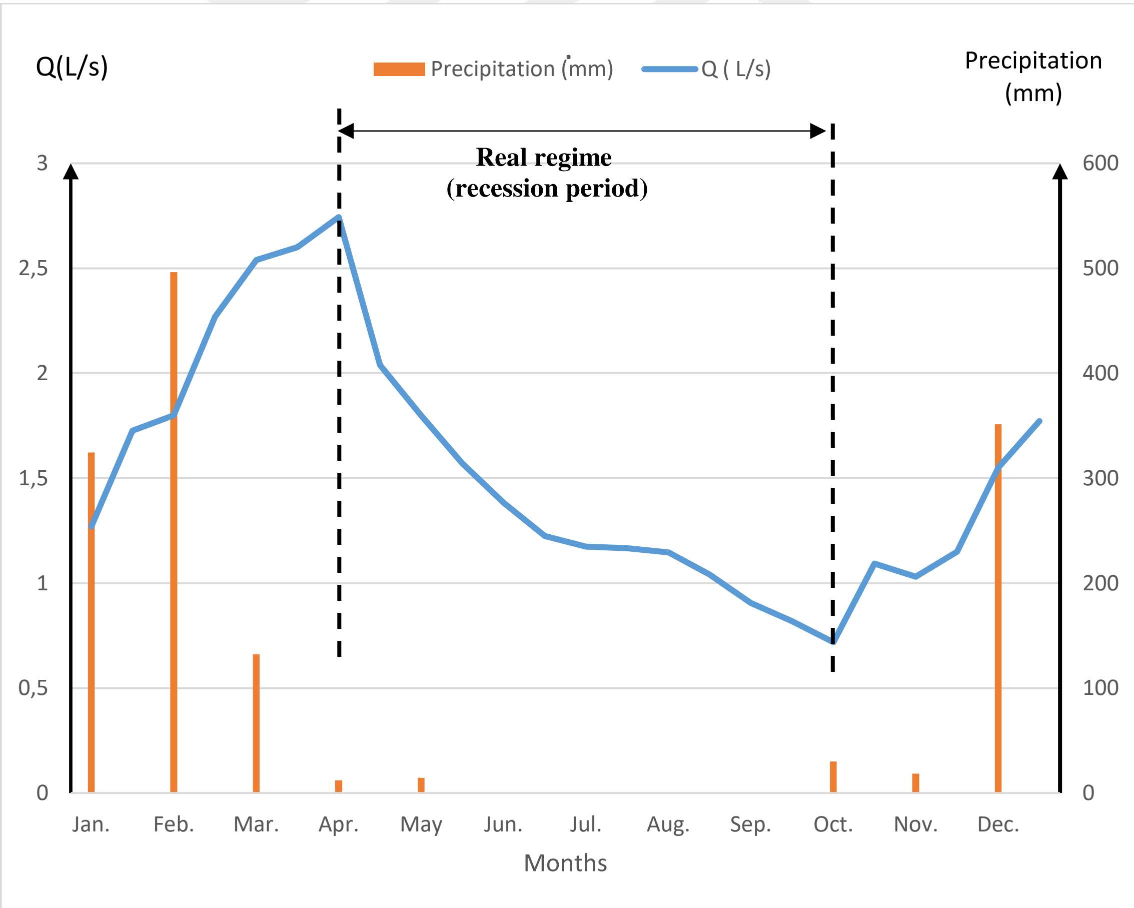

Figure 4.23. Discharge-precipitation graph of Kani Shakir spring

According to the discharge curve in the real regime of the Kani Shakir spring, the highest discharge (q_o) at the starting of the recession was 2.744 l/s, while the lowest (q) of discharge value was 0.718 l/s (Figure 4.24).

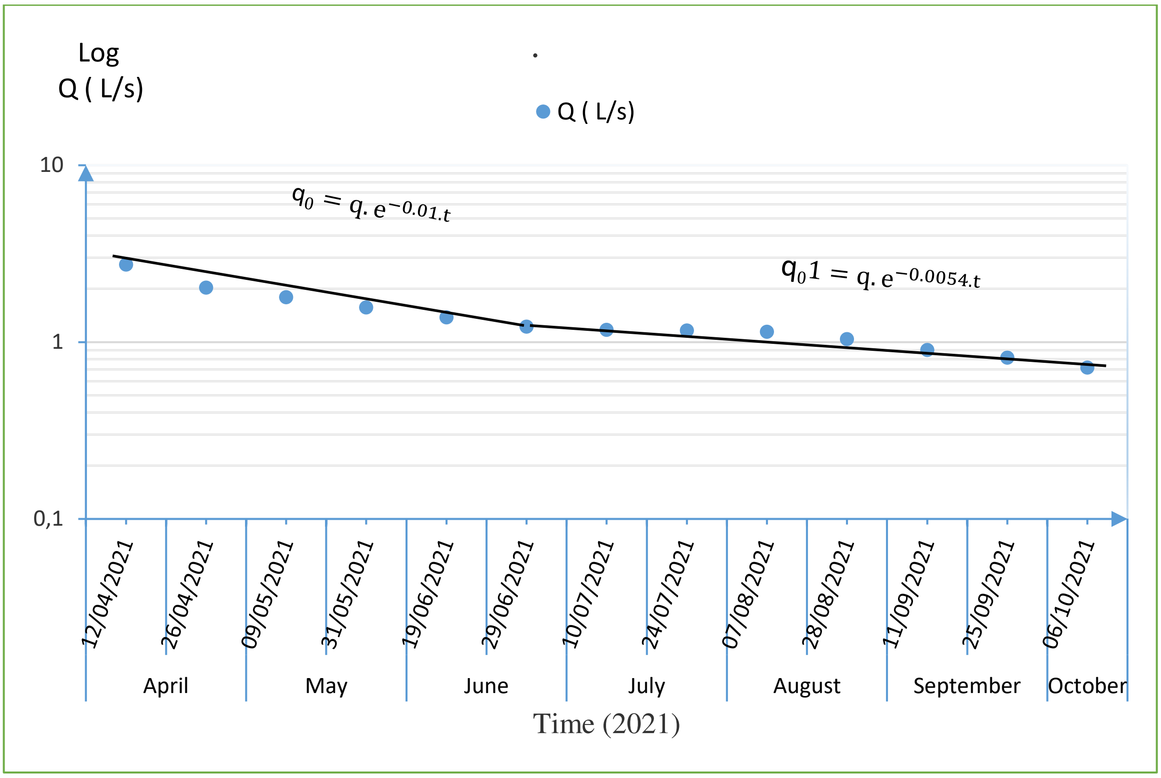

Figure 4.24. Discharge curve for recession period of the Kani Shakir spring (2021)

The real regime period of the Kani Shakir spring was between 12.04.2021 and 16.10.2021, and the water storage capacity of the spring (V_0) was calculated as 13133 m^3.

4.2.6. The discharge and precipitation relationship of Khardin spring

Discharge -precipitation graph of Khardin spring and discharge in the real regime is shown in Figure 4.25.

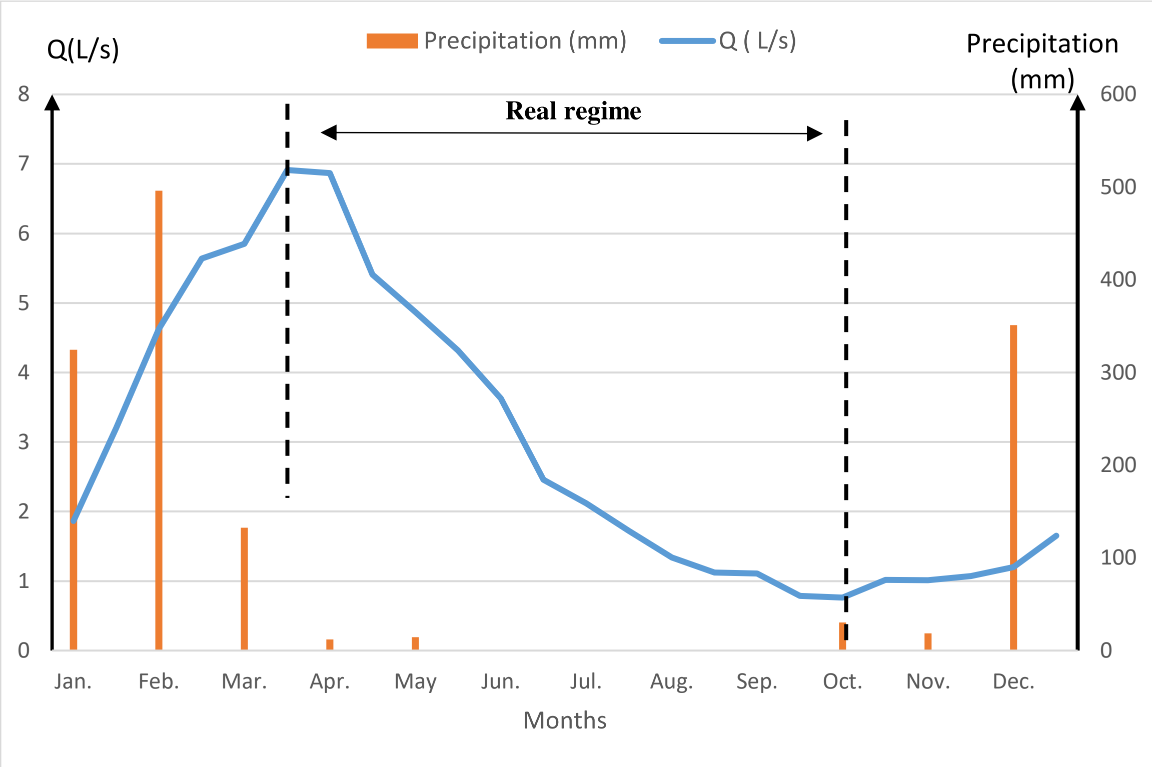

Figure 4.25. Discharge-precipitation graph of Khardin spring

According to the discharge curve in the real regime of the Khardin spring, the highest discharge (q_0) at the beginning of the recession was 6.912 l/s, while the lowest discharge (q) at the end of the dry period was 0.761 l/s (Figure 4.26).

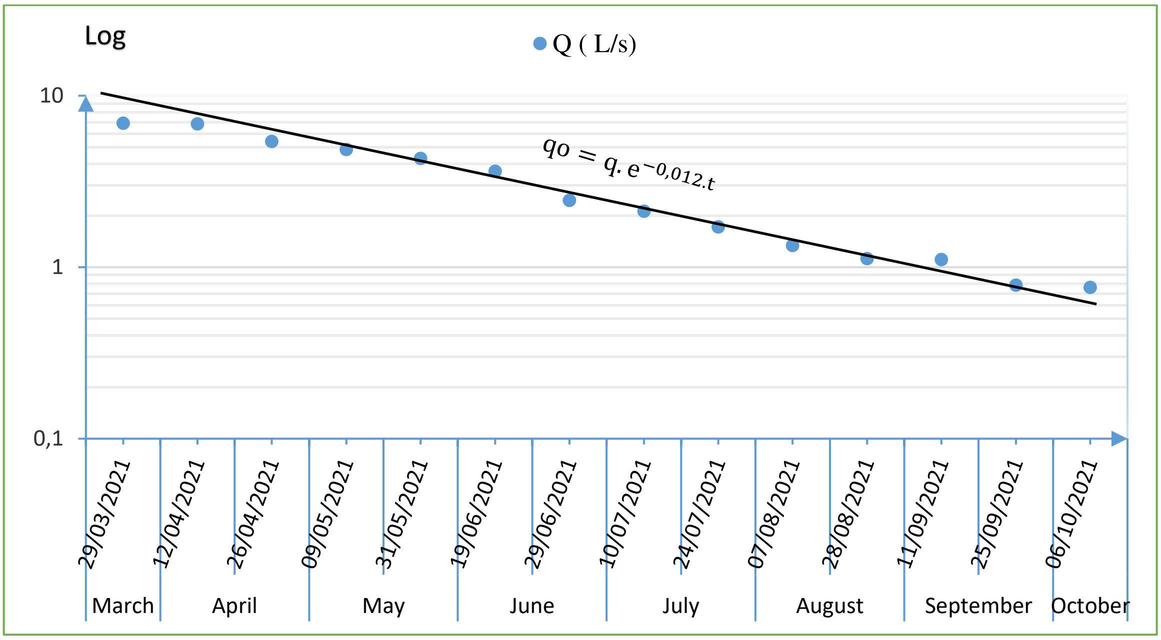

Figure 4.26. Discharge curve for recession period of the Khardin spring (2021)

The real regime period of the Khardin spring is between 29.03.2021 and 16.10.2021, and the water storage capacity of the spring (V_0) is 44280 m^3.

4.2.7. The discharge and precipitation relationship of Mergasur-1 spring

Discharge - precipitation graph of Mergasur-1 spring and discharge in the real regime is shown in Figure 4.27.

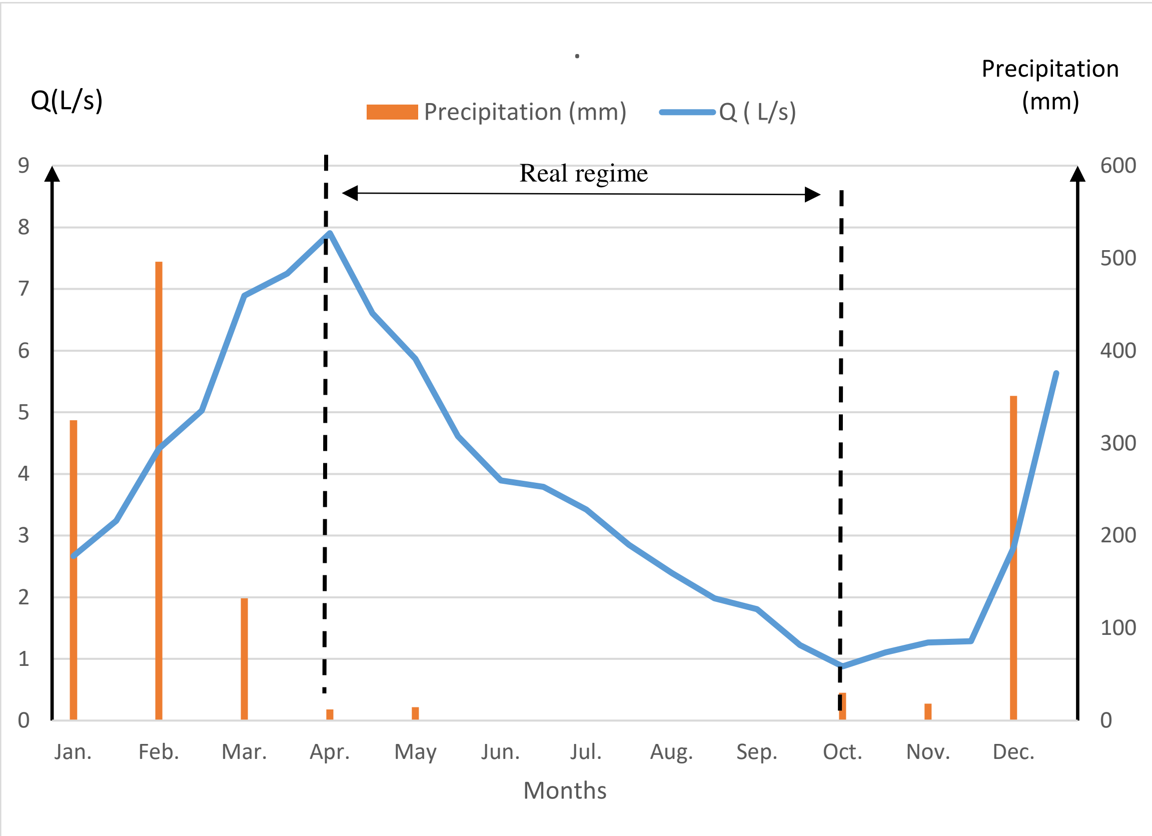

Figure 4.27. Discharge-precipitation graph of Mergasur-1 spring

According to the discharge curve in the real regime of the Mergasur-1 spring, the highest discharge (q_0) from the initial of the recession was 7.905 l/s, while the lowest value of discharge (q) at the end of the dry period was 0.879 l/s (Figure 4.28).

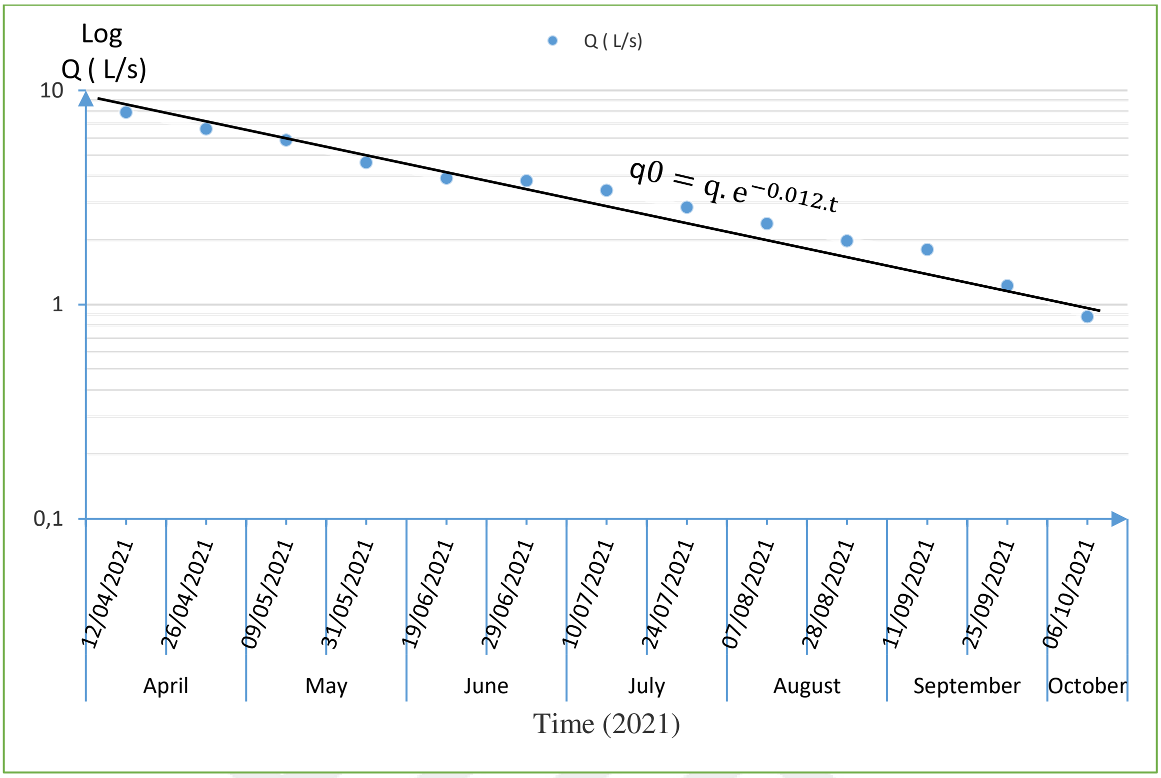

Figure 4.28. Discharge curve fr recession period of the Mergasur1 spring (2021)

The real regime period of the Mergasur-1 spring was between 12.04.2021 and 16.10.2021, and the water storage capacity of the spring (V_0) was calculated as 50594 m^3.

The flow regimes for Haudian, Khardin, Mergasur-1 and Kani Shakir springs in their real regimes, were given in Table 4.13.

Calculated recession coefficient, in the real regime, for Haudian spring were $\alpha1$= 0,01 day^{-1} and $\alpha2$= 0,0025 day^{-1} (Table 4.13). The $\alpha1$ recession coefficient indicates turbulent flow in wide fissures and channels for 49 days, whereas the $\alpha2$ recession coefficient shows laminar flow throw narrow fissures, fractures, and pores for 138 days in the karstic media (Canik, 1998; Öztekin et al., 2018).

Two flow regimes are determined for Kani Shakir springs in the real regime. The first recession coefficient (= 0,01 day^{-1}) shows the turbulent flow during 78 days, whereas the second recession coefficient (= 0,005 day^{-1}) indicates the laminar flow during 99 days in the real regime of the Kani Shakir spring (Table 4.13).

The calculated recession coefficient for Khardin and Mergasur-1 springs in the real regimes reflect turbulent flow through channels in karstic aquifer (Table 4.13).

Table 4.13. Calculate the recession coefficient of the springs

Spring Name	Time range (day)	α (recession coefficient)	Regime
Haudian spring	12/04/2021-31/05/2021 - (49 day)	α1= 0,0083	Turbulent flow
	31/05/2021-16/10/2021 - (138 day)	α2= 0,0025	Laminar flow
Kani Shakir spring	12/04/2021-29/06/2021 - (78 day)	α1: 0,01	Turbulent
	29/06/2021-06/10/2021- (99 day)	α2: 0,0054	Laminar
Khardin spring	29/03/2021-06/10/2021 - (191day)	α: 0,012	Turbulent
Mergasor spring	12/04/2021-06/10/2021 - (177 day)	α: 0,012	Turbulent

Changes in the discharge rates of investigated karstic springs during the years

The monthly average discharge rates of the investigated springs in previous years beginning from September, 2001 to July, 2003 and the current discharge rates measured in the present study have been evaluated together to determine the differences between the discharge rates of karstic springs during the years.

During previous years, the monthly maximum and minimum average discharge rates for Haudian Spring was determined 72.87 L/s in April, 2002, and 28.16 L/s in October, 2002, respectively (Table 4.14). Furthermore, the monthly maximum and minimum average discharge rates were measured in April, 2021 (41.05 L/s) and October, 2021 (22.14 L/s), respectively (Table 4.14 and Figure 4.29).

Table 4.14. Monthly average discharge rates of Haudian spring and precipitation data taken from Soran meteorology station (-: not measured)

Date	Monthly average discharge rates (from September, 2001 to July, 2003)	Monthly average discharge during (from January, 2021 to December, 2021)	Precipitation (mm) (from September, 2001 to July, 2003)	Precipitation (mm) (from January, 2021 to December, 2021)
Sep	28.61	-	7.4	-
Oct	42.21	-	8.2	-
Nov	38.21	-	73.4	-
Dec	52.01	-	166	-
Jan	65.87	30.78	179.1	127.1
Feb	67.74	34.75	47.9	81.1
Mar	65.66	40.77	116.6	70.6
Apr	72.87	41.05	169.6	7.8
May	63.57	33.08	21.6	15.2
Jun	49.24	28.60	0.4	0
Jul	37.82	27.82	0	0
Aug	32.13	25.89	0	0
Sep	29.18	23.75	0	0
Oct	28.16	22.14	47.6	24.5
Nov	30.07	23.14	54.2	13.5
Dec	36.42	30.53	189.4	145.6
Jan	42.15	-	113	-
Feb	42.9	-	176.6	-
Jun	50.75	-	3.7	-
Jul	36.6	-	0	-

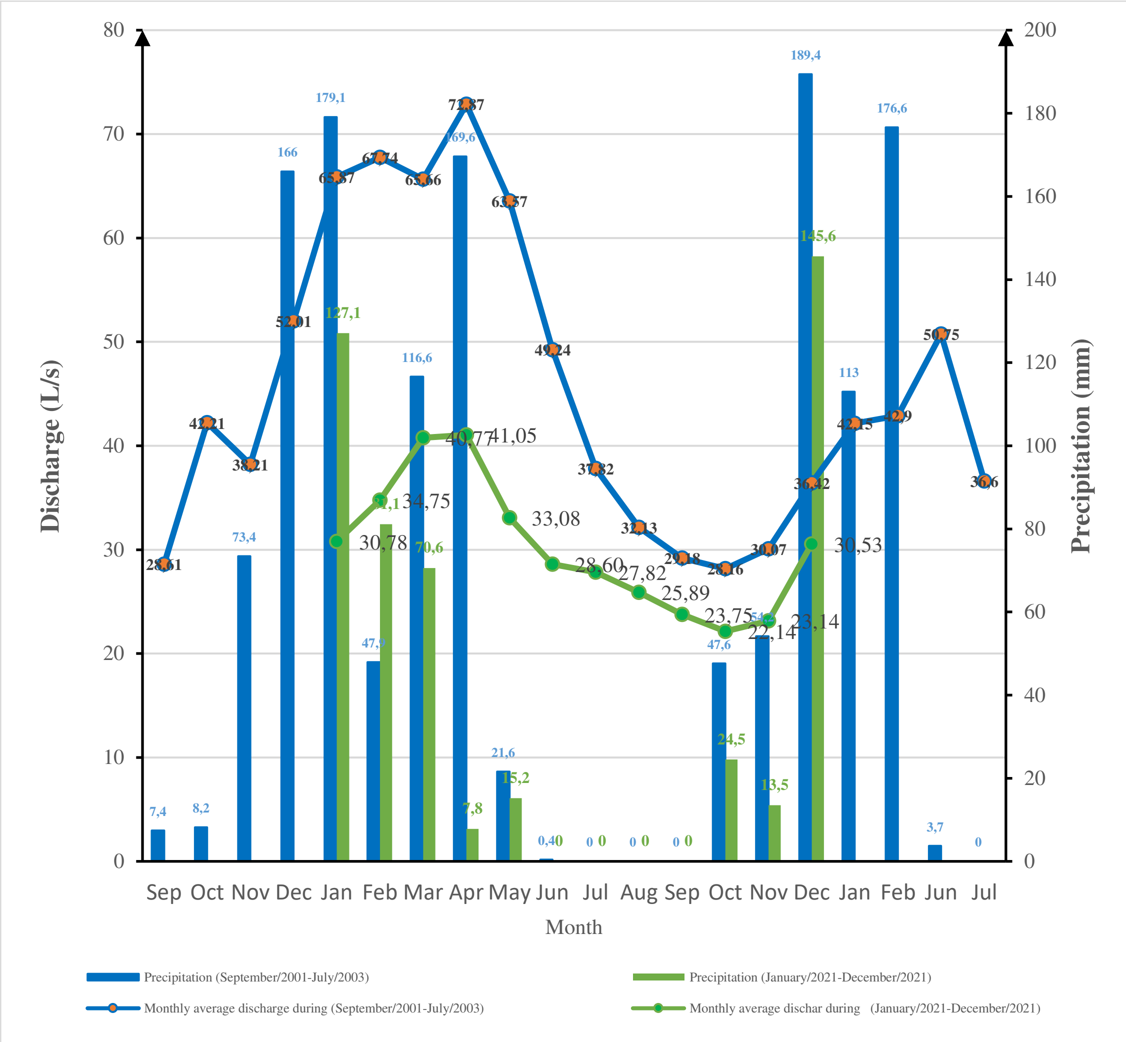

Figure 4.29. Average monthly discharge rates of Haudian spring between 2001 and 2003, and during 2021

During previous years, the monthly maximum and minimum average discharge rates for Kani Shakir Spring was determined 2.63 L/s in February, 2003, and 0.76 L/s in October, 2001, respectively (Table 4.15). Furthermore, the monthly maximum and minimum average discharge rates were measured in March, 2021 (2.57 L/s) and September, 2021 (0.86 L/s), respectively (Table 4.15 and Figure 4.30).

Table 4.15. Monthly average discharge rates of Kani Shakir spring and precipitation data taken from Mergasur meteorology station (-: not measured)

Date	Monthly average discharge rates (from September, 2001 to July, 2003)	Monthly average discharge during (from January, 2021 to December, 2021)	Precipitation (mm) (from September, 2001 to July, 2003)	Precipitation (mm) (from January, 2021 to December, 2021)
Sep	0.83	-	1.5	-
Oct	0.76	-	15.5	-
Nov	0.84	-	107.4	-
Dec	0.84	-	299.8	-
Jan	0.87	1.50	301.5	381
Feb	1.18	2.03	176.9	137
Mar	1.58	2.57	230.7	149.5
Apr	2.26	2.39	204.7	15.5
May	2.01	1.68	21.6	9
Jun	1.38	1.30	0	0
Jul	1.25	1.17	0	0
Aug	1.21	1.09	0	0
Sep	1.14	0.86	0	0
Oct	1.20	0.91	34.7	40.5
Nov	1.16	1.09	118	15
Dec	1.39	1.66	175.3	336.5
Jan	2.19	-	175.7	-
Feb	2.63	-	308.2	-
Jun	1.41	-	28.1	-
Jul	1.65	-	4.4	-

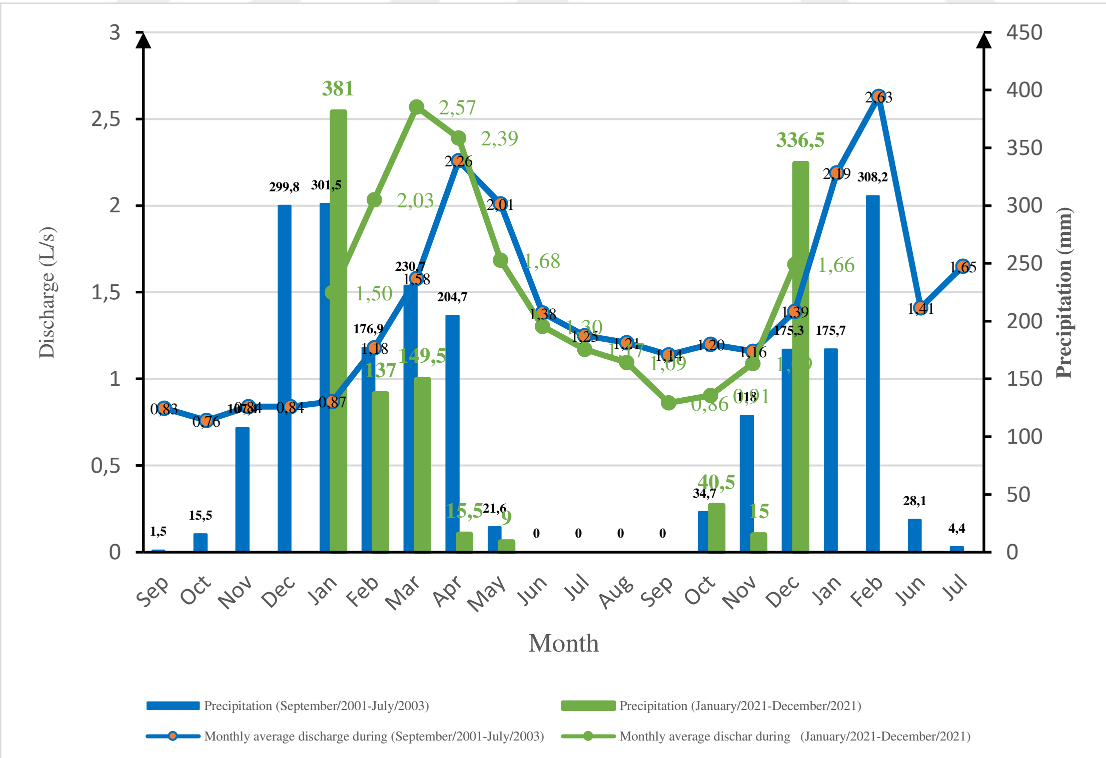

Figure 4.30. Average monthly discharge rates of Kani Shakir spring between 2001 and 2003, and during 2021

The monthly average discharge rates of Khardin spring were given on Table 4.16.

Table 4.16. Monthly average discharge rates of Khardin spring and precipitation data taken from Mergasur meteorology station (-: not measured)

Date	Monthly average discharge rates (from September, 2001 to July, 2003)	Monthly average discharge during (from January, 2021 to December, 2021)	Precipitation (mm) (from September, 2001 to July, 2003)	Precipitation (mm) (from January, 2021 to December, 2021)
Sep	1.75	-	1.5	-
Oct	1.36	-	15.5	-
Nov	1.31	-	107.4	-
Dec	2.62	-	299.8	-
Jan	5.12	2.53	301.5	381
Feb	10.78	5.13	176.9	137
Mar	16.35	6.38	230.7	149.5
Apr	21.52	6.14	204.7	15.5
May	20.00	4.59	21.6	9
Jun	11.55	3.04	0	0
Jul	7.30	1.92	0	0
Aug	4.87	1.23	0	0
Sep	2.93	0.95	0	0
Oct	1.87	0.89	34.7	40.5
Nov	1.18	1.04	118	15
Dec	1.08	1.43	175.3	336.5
Jan	2.60	-	175.7	-
Feb	8.01	-	308.2	-
Jun	6.85	-	28.1	-
Jul	11.66	-	4.4	-

During previous years, the monthly maximum and minimum average discharge rates for Khardin Spring was determined 21.52 L/s in April, 2002, and 1.08 L/s in December, 2002, respectively (Table 4.15). Furthermore, the monthly maximum and minimum average discharge rates were measured in March, 2021 (6.38 L/s) and October, 2021 (0.89 L/s), respectively (Figure 4.31).

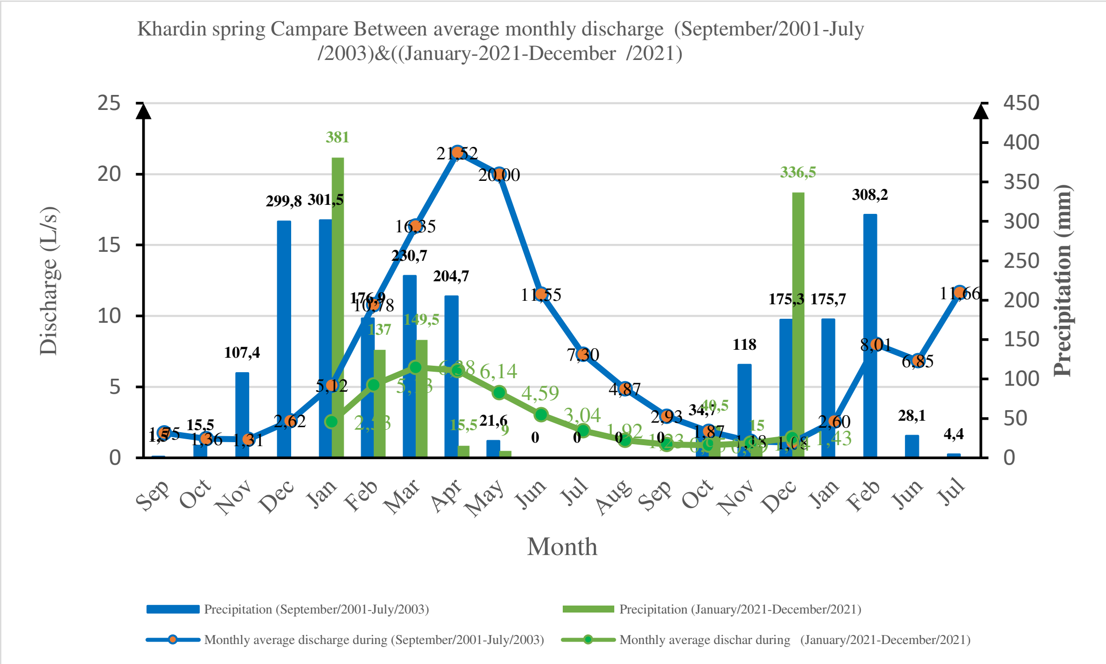

Figure 4.31. Average monthly discharge rates of Khardin spring between 2001 and 2003, and during 2021

The monthly average discharge rates of Mergasur-1 spring were given on Table 4.17.

Table 4.17. Monthly average discharge rates of Mergasur-1 spring and precipitation data taken from Mergasur meteorology station (-: not measured)

Date	Monthly average discharge rates (from September, 2001 to July, 2003)	Monthly average discharge during (from January, 2021 to December, 2021)	Precipitation (mm) (from September, 2001 to July, 2003)	Precipitation (mm) (from January, 2021 to December, 2021)
Sep	1.89	-	1.5	-
Oct	1.19	-	15.5	-
Nov	0.70	-	107.4	-
Dec	2.15	-	299.8	-
Jan	3.88	2.96	301.5	381
Feb	10.13	4.72	176.9	137
Mar	17.26	7.07	230.7	149.5
Apr	20.52	7.26	204.7	15.5
May	12.48	5.24	21.6	9
Jun	1.55	3.84	0	0
Jul	1.57	3.13	0	0
Aug	1.28	2.19	0	0
Sep	1.15	1.52	0	0
Oct	1.00	0.99	34.7	40.5
Nov	2.06	1.28	118	15
Dec	3.23	4.22	175.3	336.5
Jan	4.87	-	175.7	-
Feb	0.38	-	308.2	-
Jun	6.13	-	28.1	-
Jul	1.65	-	4.4	-

During previous years, the monthly maximum and minimum average discharge rates for Mergasur-1 Spring was determined 20.52 L/s in April, 2002, and 0.38 L/s in February, 2003, respectively (Table 4.17). Furthermore, the monthly maximum and minimum average discharge rates were measured in April, 2021 (7.26 L/s) and October, 2021 (0.99 L/s), respectively (Figure 4.32).

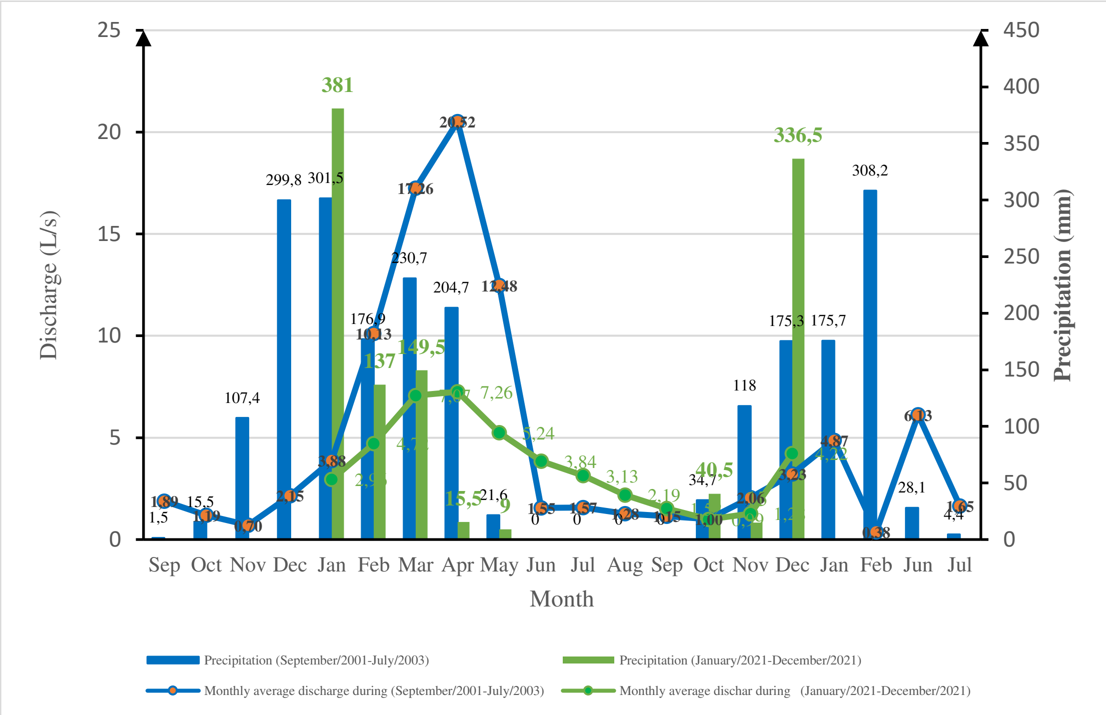

Figure 4.32. Average monthly discharge rates of Mergasur-1 spring between 2001 and 2003, and during 2021

According to the data collected from the previous years between 2001 and 2003, the discharges of the Haudian, Khardin, Megasur-1 springs were determined higher compare to the current year. The major reason for the decreasing and increasing in the discharges of these springs is the amount of precipitation. Because, the amount of precipitation was high in the previous years compare to the year 2021. The amount of precipitation during 2021 is low, so the discharges of the springs are low, too. However, the discharges of Kani Shakir Spring measured in the previous years are low compare to the other springs. The discharge measurement of this spring was only recorded in one outlet in the previous years. However, the current discharge measurements belong to 2021 were measured in three-outlets of Kani Shakir Spring. Therefore, the lower discharge rates of this spring measured in the previous years might be due to this reason.

5. CONCLUSIONS AND RECOMMENDATIONS

The study area is located in Diana – Mergasur Sub-Basin, contains five main formations; Lower Cretaceous Qamchuqa, Upper Cretaceous Bekhme, Late Campanian-Maastrichtian Shiranish, Campanian-Maastrichtian Tanjero, and Paleocene-Pliocene Red Bed Series formations. Tectonically it lies within the Imbrecated Zone which is part of the Unstable Shelf tectonic zone of Iraq.

The aquifer for Haudian, Kani Shakir and Mergasur-1 karstic springs is the fractured and karstificated limestones of Bekhme Formation, and aquifer for Khardin spring is the limestones of Govanda Formation. The marl, clay, marly limestone, red shales are the impermeable base of the fractured-karstic aquifers. The investigated karstic springs mostly discharge at the contant between impermeable layers and fractured and karstic limestones.

The investigated wells in the present study recharge from Bekhme and Shiranish Formation. According to the Jacob method, no meaningful difference is determined in the average hydraulic conductivity of marly limestone belonging to Shiranish Formation and average hydraulic conductivity of marly limestones and dolomitic limestones belonging to (Bekhme and Shiranish) Formation.

During 2021 the groundwater level in the study area significantly fluctuated. The main reasons for groundwater fluctuations are; (i) sharp changes in annual precipitation occurred during the period 2021-2022; its value was 485.4 mm this decrease was proportional with time, and (ii) higher water exploitation due to the growth population.

In the real regime, for Haudian spring, the first recession coefficient indicates turbulent flow in wide fissures and channels for 49 days, whereas the second recession coefficient shows laminar flow throw narrow fissures, fractures, and pores for 138 days in the karstic media. According to the Iraq standard, the average amount of domestic usage per person is 392 L/day. Around 1500 local residents utilize Haudian spring for drinking and domestic purposes. If just this spring alone is used for drinking and domestic purposes by a population of 1500, the period of this spring, in the real regime, was calculated as 785 days.

There are two flow regimes in Kani Shakir spring in the real regime. The first recession coefficient shows the turbulent flow during 78 days, whereas the second recession coefficient is the laminar flow during 99 days in the real regime of the Kani Shakir spring.

The recession coefficient for Khardin and Mergasur-1 springs in the real regimes reflect turbulent flow through channels in karstic aquifer.

The highest discharge rate is determined in Haudian spring, wheras the other karstic springs have the lower discharge rates. The discharge rate of the investigated karstic springs increase due to the large recharging areas. Conversely, as the recharge areas of the karstic springs narrow, their flow rates also decrease. In addition, fracture/crack width and the crack filling material are also effective on the flow rates of the springs.

Detailed hydrogeochemical investigation, including isotope analysis (^{18}O, ^{2}H, ^{3}H) are needed for karstic springs in the study area. Drilling of illegal wells must be stopped, and drilling of wells on the recharge areas of the karstic springs should be banned. The detailed hydrogeological studies also needed to determine hydraulic conductivity, specific yield and transmissivity of karstic limestones. In addition, some exploratory wells must be drilled in karstic limestones and the groundwater levels must be daily monitored.

The Balakian and Sedakan rivers converge near Zargali. It could be benefit for Soran district to transfer these surface waters by suitable pipes for suppling drinking and agricultural purposes in Soran. However, detailed scientifical searchers must be performed on these surface waters, before planning the transferring surface water to Soran district.

REFERENCES

Abdula, R. A. 2018. Geology Of Iraq (Kurdistan). *Bulletin Of The Geological Society Of Malaysia,* 65**,** 37-43.

Ali, S. S., Stevanovic, Z. & Jemcov, I. 2009. The Mechanism And Its Influence On Karstic Springs Flow Of Sarchinar Spring, A Case Example, Sulaimaniyah, Ne Iraq. *Iraqi Bulletin Of Geology And Mining,* 5**,** 87–100-87–100.

Al-Furaiji, M.H.O., Karim, U.F., Augustijn, D.C., Waisi, B.I.H. & Hulscher, S.J. 2016. Evaluation Of Water Demand And Supply In The south of Iraq. *Journal Of Water Reuse And Desalination*, 6, 1, 214-226.

Amit, H., Lyakhovsky, V., Katz, A., Starinsky, A. & Burg, A. 2002. Interpretation Of Spring Recession Curves. *Groundwater,* 40**,** 543-551.

Atkinson, T. 1977. Diffuse Flow And Conduit Flow In Limestone Terrain In The Mendip Hills, Somerset (Great Britain). *Journal Of Hydrology,* 35**,** 93-110.

Bakalowicz, M. 2005. Karst Groundwater: A Challenge For New Resources. *Hydrogeology Journal,* 13**,** 148-160.

Balaki, H. G. K. & Omar, A. A. 2019. Structural Assessment Of The Bradost And Berat Structures In Imbricate And High Folded Zones—Iraqi Kurdistan Zagros Belt. *Arabian Journal Of Geosciences,* 12**,** 1-21.

Bolton, C. 1958. The Geology Of Rania Area, Site Invest. *Co. Rep. Vol. Ixb***,** 117.

Buday, T. 1980. *The Regional Geology Of Iraq: Tectonism, Magmatism And Metamorphism*, State Organization For Minerals, Directorate General For Geological Survey.

Buday, T. & Jassim, S. 1987. The Regional Geology Of Iraq, Vol. 2: Tectonism, Magmatism And Metamorphism. *Geosurv, Baghdad, 352pp*.

Canik, B. 1998. *Hidrojeoloji*, Yeraltı Sularının Aranması, İşletilmesi, Kimyası. Ankara Üniversitesi Fen Fakültesi Jeoloji Mühendisliği Bölümü, Ankara.

Chnaray, M. 2003. *Hydrology And Hydrochemistry Of Kapran Basin Erbil North Of Iraq.* Ph. D. Thesis, Univ. Of Baghdad, Iraq.

Choi, B.-S. 2007. A Method For Storativity Compensation In Single Well Test Analysis. *Journal Of Soil And Groundwater Environment,* 12**,** 36-43.

Dara, R. N., Jirjees, S., Fatah, K. K. & Javadinejad, S. 2021. Climatic Parameters Analysis Of Koysinjaq Meteorological Station, Kurdistan Region, Northern Iraq. *The Iraqi Geological Journal***,** 99-109.

Deming, D. 2002. *Introduction To Hydrogeology*, Mcgraw-Hill Science, Engineering & Mathematics.

Ford And Williams 2007. Karst Hydrogeology And Geomorphology. Chichester,: John Wiley.

Fouad, S. F. 2010. Tectonic And Structural Evolution Of The Mesopotamia Foredeep, Iraq. *Iraqi Bulletin Of Geology And Mining,* 6**,** 41–53-41–53.

Hamed, M. H. 2013. Hydrogeology, Hydrochemistry And Groundwater Flow Modeling Of Shaqlawa-Hiran Basin In Erbil Governorate Iraqi Kurdistan Region. *Degree Of Doctor Of Philosophy In Geology. Salahaddin University*.

Hassan, I. 1998. Urban Hydrology Of Erbil City Region. *Degree Of Doctor Of Philosophy In Geology (Hydrogeology). University Of Baghdad*.

Jacob, C. E. 1947. Drawdown Test To Determine Effective Radius Of Artesian Well. *Transactions Of The American Society Of Civil Engineers,* 112**,** 1047-1064.

Jan, S. K., Al-Zubaidi, A. A. & Al-Dulaimi, S. I. 2012. Microfacies Analysis Of Shiranish Formation At Hijran Section-Ne Iraq. *Bulletin Of The Iraq Natural History Museum (P-Issn: 1017-8678, E-Issn: 2311-9799),* 12**,** 15-24.

Jassim, S. Z. & Goff, J. C. 2006. *Geology Of Iraq*, Dolin, Sro, Distributed By Geological Society Of London.

Karim, K. H., Ismail, K. M. & Ameen, B. M. 2008. Lithostratigraphic Study Of The Contact Between Kometan And Shiranish Formations (Cretaceous), In Sulaimaniyah Governorate, Kurdistan Region, Ne Iraq. *Iraqi Bulletin Of Geology And Mining,* 4**,** 15–27-15–27.

Karim, K. H. & Surdashy, A. M. 2005. Tectonic And Depositional History Of Upper Cretaceous Tanjero Formation In Sulaimaniya Area Ne-Iraq. *Journal Of Zankoy Sulaimani,* 8**,** 1-20.

Kruseman, G. P., De Ridder, N. A. & Verweij, J. M. 1970. *Analysis And Evaluation Of Pumping Test Data*, International Institute For Land Reclamation And Improvement Wageningen.

Maillet, E. 1905. Essais d'hydrolique Souterraine et Fluviale. Libreirie Scientifique, A. Hermann, 2018, Paris.

Mays, L. W. 2005. *Water Resource Engineering* (2005 Edition), New York, Usa, : John Wiley And Sons, .

Mouthereau, F., Lacombe, O. & Vergés, J. 2012. Building The Zagros Collisional Orogen: Timing, Strain Distribution And The Dynamics Of Arabia/Eurasia Plate Convergence. *Tectonophysics,* 532**,** 27-60.

Mustafa, O., Merkel, B. & Weise, S. M. 2015. Assessment Of Hydrogeochemistry And Environmental Isotopes In Karst Springs Of Makook Anticline, Kurdistan Region, Iraq. *Hydrology,* 2**,** 48-68.

Öztekin Okan Ö., Güven, A. & Çetindağ B. 2018. The hydrogeological investigation of Plajköy Spring (Elazığ). *Bulletin of the Mineral Research and Exploration*, 156, 221-236.

Shwani, S. 2008. Hydrogeology And Hydrochemistry Of Bashtapa Sub-Basin In Erbil Governorate Kurdistan Region-Iraq. *Degree Of Master Of Science In Geology. Salahaddin University*.

Sissakian, V. K. 2013. Geomorphology And Morphometry Of The Greater Zab River Basin, North Of Iraq. *Iraqi Bulletin Of Geology And Mining,* 9**,** 21-49.

Sissakian, V. K. & Al-Jiburi, B. S. 2014. Stratigraphy Of The High Folded Zone. *Iraqi Bulletin Of Geology And Mining***,** 73-161.

Stevanovic, Z. & Iurkiewicz, A. Geologic-Tectonic Factors Controlling Groundwater Flow Patterns And Discharge Of Karst Aquifers In Western Zagros (Northern Iraq). Proceedings Of 33rd Iah Congress & 7th Alhsud (Cd) Zacatecas, 2004.

Stevanovic, Z. & Markovic, M. 2003. Hydrogeology Of Northern Iraq, Climate, Hydrology, Geomorphology And Geology. *Spec. Edition Fao/Un***,** 1-122.

Stevanovic, Z. & Markovic, M. 2004. Hydrogeology Of Northern Iraq. Vol. 1. Climate, Hydrology, Geomorphology & Geology. Vol. 2. General Hydrogeology And Aquifer Systems.

Thornthwaite, C. 1944. Report Of The Committee On Transpiration And Evaporation 1943-44. *Transactions Of The American Geophysical Union,* 25**,** 683-693.

Thornthwaite, C. W. 1948. An Approach Toward A Rational Classification Of Climate. *Geographical Review,* 38**,** 55-94.

Tobia, F. & Kafy, R. 2016. Provenance Of Heavy Minerals From Recent Sediments Of Balakyan River, Kurdistan Region, Iraq. *Journal Of Zankoy Sulaimani,* 8**,** 147-168.

UN. 2013. Water in Iraq Factsheet. UN, Iraq.

Van Der Schaaf, S. 2004. A Single Well Pumping And Recovery Test To Measure In Situ Acrotelm Transmissivity In Raised Bogs. *Journal Of Hydrology,* 290**,** 152-160.

Weight, W. D. & Sonderegger, J. L. 2001. *Manual Of Applied Field Hydrogeology*, Mcgraw-Hill.

Wilson, E. M. 1990. *Engineering Hydrology*, Macmillan International Higher Education.

APPENDICES

APPENDIX- 1. THE MONTHLY AMOUNT OF PRECIPITATION AND SNOW IN SORAN STATION

Year	Months																		Total Rainfall	Total Snow
	Oct.		Nov.		Dec.		Jan.		Feb.		Mar.		Apr.	May.	Jun.	July	Aug.	Sep.		
	Rainfall	Snow	Rainfall	Snow	Rainfall	Snow	Rainfall	Snow	Rainfall	Snow	Rainfall	Snow	Rainfall	Rainfall	Rainfall	Rainfall	Rainfall	Rainfall		
2001	8.2		73.4	6	166		27.5	5	65.3	10	79.8		28.9	39.7				7.4	496.2	21
2002	47.6		54.2		189.4	26	179.1	33.5	47.9		116.6		169.6	21.6	4				830	59.5
2003	39		71.5		110		113	8	176.6	15	188.6		85.5	13.9	3.7				801.8	23
2004	3.3		199		27.1	5	210.2	3	108.2	44	31		177.1	44	0	2.3			802.2	52
2005	17.8		28.9		69.3		114	18	159	6	99.2		50.5	31.4					570.1	24
2006	222.4		51.3		31.9		149.3	54	295.5		56.6		131.1	38.5					976.6	54
2007			15.2		37.1		36.7	13.5	140.9	10	96.4		168.5	16.5	0.5				511.8	23.5
2008	52.9		40.3		71.3		52.7	5	116.6	5	83		3.4	2.5	1		1.6	23.9	449.2	10
2009	46.8		46.3		184.5		12.4		59.5		194.8		49	5.1				4.8	603.2	0
2010	12.9		0		58.9		76.3		94		55.4		99.2	36	0.8			0	433.5	0
2011	13.4		43.2		51.3		119.7	4	109.7	2	88.1		151.3	30.7				5.2	612.6	6
2012	56.9		46.1		174.7		89.4	6.5	81.5	9	108.3	23.5	51.2	17.1					625.2	39
2013			84.1		118	9	219.4	14	100.4		36.8		59.7	51.2					669.6	23
2014	192.8		174.6		76.5		74		9.5		144.3		32.5	5				3.9	713.1	0
2015	117.4		112.7		99.1		66.7	11	47.7		151.6		70	17.8				27.2	710.2	11
2016	11		51.6		180.5	12.5	151	13	55.7		217.7		110.5	11.8					789.8	25.5
2017	3.5		76		60.8		36		45.1	10.5	187.8		106	16.4					531.6	10.5
2018	110.6		112.9		268.9		85.1		236.6		58.7		52.5	144.2					1069.5	0
2019	16		87.4		94		149.9		134.7		194.1		166.8	48.6					891.5	0
2020	2.8		189.7		52		120.8	4	160.7	46	143.6		138	46.5					854.1	50
2021	24.5		13.5		145.6		127.1		81.1		70.6		7.8	15.2					485.4	0

APPENDIX- 2. THE MONTHLY AMOUNT OF PRECIPITATION AND SNOW IN MERGASUR STATION

Year	Months																		Total Rainfall	Total Snow
	Oct.		Nov.		Dec.		Jan.		Feb.		Mar.		Apr.	May.	Jun.	July	Aug.	Sep.		
	Rainfall	Snow	Rainfall	Snow	Rainfall	Snow	Rainfall	Snow	Rainfall	Snow	Rainfall	Snow	Rainfall	Rainfall	Rainfall	Rainfall	Rainfall	Rainfall		
2001	15.5		107.4	45	299.8	1	43	37	194.6	106.5	165.4		69	46.2				1.5	942.4	189.5
2002	34.7		118		175.3	98.5	301.5	254	176.9		230.7	5	204.7	21.6					1263.4	357.5
2003	174.1		139.3		259.8	23	175.7	18	308.2	148	436.5	3	112.4	28.1	4.4				1638.5	192
2004	5.2		376.8		18.2	28	304.1	61	235.9	122	32.8		226.5	98.9					1298.4	211
2005	26.3		81.7		143.9	37	242.9	163	211.1	73	194.5		78.6	49.3	2.2				1030.5	273
2006	343.3		130.8		28.8	83	279.1	154	544	40	103.2		312	65.2					1806.4	277
2007	3.7		84.5		74.9	2	107.1	111	160.4	44	167.1	12	250.1	47.2	2.3				897.3	169
2008	47.7		53.3		242	41	112.2	101	204.9	32	175.9		18	8.4				20.4	882.8	174
2009	306.3		115.3		438.8		33.7	5	149.6	18	322.7	42	119.7	8.3				12	1506.4	65
2010	13				178.9	8	302.3	15	145.1	7	112.2		150.7	60.9				3	966.1	30
2011	6.7		60.1		108.8	6	369.5	44	244.4	34	150.5		318.4	54	0.5			4	1316.9	84
2012	92.5		121.9		486.1	13	229.1	66	271.9	88	244.2	123	101.4	24				17	1588.1	290
2013	7		117		295.1	82	805.7	116	180.9	13	134.2	2	81.5	42.7					1664.1	213
2014	257.6		359.1		103.5	4	227.5		19.5		330.7	1	53.8	34.5				7.5	1393.7	5
2015	167.5		199.3		311.5	32	197.9	69	78	11	204.5	1	75	55.5				25	1314.2	113
2016	20.5		79.5	3	335.2	69	519.5	104	140		396.2		101.5	34					1626.4	176
2017	4		165.5		112	8	200.3	91	137	52	334.8	2	181	10.5					1145.1	153
2018	155		278		606	13	190.7	8	448.2	2	47.5		84	155.8					1965.2	23
2019	39.5		70		278.5		334.5	66	295	18	439.5		395	49					1901	84
2020	3.5		246.5		97.5	1	241.5	131	288.5	98	292.5		176	36					1382	230
2021	40.5		15		336.5	7	381	38	137	19	149.5		15.5	9					1084	64

APPENDIX- 3. MONTHLY AVERAGE TEMPERATURE (^{0}C) OF THE SORAN METEOROLOGICAL STATION.

Monthly average Tempreture. T.C in Soran												
Year	**Months**											
	Oct	**Nov**	**Dec**	**Jan**	**Feb**	**Mar**	**Aprl**	**May**	**Jun**	**July**	**Aug**	**Sep**
2002	18.1	13.3	3.5				14.4	22.0	29.0	33.3	31.9	28.0
2003	21.5	12.0	6.4	4.7	5.3	8.4	16.4	22.6	28.0	32.2	32.6	26.6
2004	22.1	11.5	4.2	5.0	6.0	13.6	14.9	20.5	27.5	32.0	30.9	27.6
2005	20.0	12.1	9.0	3.9	4.6	10.5	17.8	21.3	27.7	33.3	33.1	26.6
2006	20.6	10.5	5.5	3.3	6.1	13.2	16.7	22.2	30.5	32.2	34.2	27.7
2007	21.8	13.4	6.9	3.2	7.0	11.2	13.4	22.5	28.5	31.6	31.9	27.8
2008	19.7	12.7	6.4	2.8	6.0	14.9	19.9	22.0	28.1	31.7	32.8	27.3
2009	20.5	12.1	8.1	4.4	8.1	10.3	15.0	21.8	28.4	30.7	29.8	25.2
2010	21.1	14.2	8.9	8.3	9.0	13.0	15.5	20.8	28.5	31.7	32.1	28.6
2011	19.0	9.0	5.9	4.5	6.0	11.5	15.8	20.7	27.8	31.5	30.7	26.2
2012	20.6	13.3	7.0	3.5	5.5	7.4	17.4	22.7	28.9	31.3	31.1	27.4
2013	19.1	14.4	5.3	4.2	8.2	11.3	16.7	21.5	27.6	30.9	30.3	25.6
2014	18.7	11.0	7.0	6.8	8.8	12.5	17.2	23.1	28.0	31.7	31.8	26.4
2015	19.9	11.4	6.2	5.6	8.6	11.5	15.3	21.7	27.5	31.3	31.6	28.0
2016	20.5	12.0	4.8	3.7	9.8	11.3	16.8	21.7	27.8	31.8	32.4	25.9
2017	19.6	12.9	8.6	5.3	5.6	11.0	16.4	21.9	27.8	32.5	32.3	28.7
2018	21.5	11.8	7.0	6.7	9.4	15.8	17.4	20.9	27.6	32.2	31.3	27.9
2019	21.5	12.5	8.1	4.8	7.4	9.6	13.7	22.4	29.4	30.8	32.5	26.0
2020	21.9	13.1	7.3	5.1	4.3	11.9	15.9	21.9				
2021	20.7	14.0	7.3	6.3	9.1	12.5	18.8	24.8	28.9	32.7	32.2	26.5
Mean	**20.4**	**12.4**	**6.7**	**4.8**	**7.1**	**11.7**	**16.3**	**21.9**	**28.3**	**31.9**	**31.9**	**27.1**

APPENDIX- 4. MONTHLY AVERAGE TEMPEREAURE (^{0}C) OF THE MERGASUR METEOROLOGICAL STATION.

The amount of Air temp. oC Avg. in (Mergasur) station													
Year	Temp.	Months											
		Oct.	Nov.	Dec.	Jan.	Feb.	Mar.	Apr.	May.	Jun.	July.	Aug.	Sep.
2011	Avg.	20.5	5.2	4.0					17.0	25.0	32.3	32.4	26.6
2012	Avg.	20.5	12.2	5.7	2.8	3.6	4.9	12.4	20.8	26.0	29.4	27.8	25.8
2013	Avg.	18.7	12.3	3.3	2.7	7.3	9.9	11.6	14	22.5	29.7	26.2	25.2
2014	Avg.	16.1	11	8.1	3.1	2.2	12.2	15.1	21.2	23.1	29.8	27.4	25
2015	Avg.	15.5	13.7	3.4	2.8	5.7	9.4	12.8	17.2	24.4	29.4	28	18.5
2016	Avg.		11.8	6	0.6	9.4	10.3	14.9	19.8		29.1	25.3	21.2
2017	Avg.	17.1	13.3	3.1	3.3	6.3	10.3	13.6	20.4	26.8	30.4	26.8	20.6
2018	Avg.	15.8	10.5	5.2	5.5	7.3	11.5	12	14.3	24.6	30.4	26.8	20.6
2019	Avg.	15.5	12	8.7	2.2	7.1	9.6	12.3	17.629	24.6	30.4	26.8	20.6
2020	Avg.	17.1	10.8	10.4	-0.5	0.4	7.6	10.2	16.1	24.6	30.4	26.8	20.2
2021	Avg.	15.6	12.3	5.5	2.4	3.8	7	16.4	17.2	24.567	30.4	26.8	20.2
Mean		**17.2**	**11.4**	**5.8**	**2.5**	**5.3**	**9.3**	**13.1**	**17.8**	**24.6**	**30.2**	**27.4**	**22.2**

Appendix- 5. Pumping test and well test data of the wells (data are obtained from Directorate of Groundwater of Erbil)

1. Well name ; Prozhay Gashtyari Hasti

Well name	Prozhay Gashtyari Hasti	Test date	01/10/2020
Well location	Soran	Well test length (m)	135
Well depth(m)	205	Well test diameter(m)	2.5'=0.063
Static water level (m)	94	Well casing radius (m)	[8(5/8)']/2=0.11
Dynamic water level (m)	110	Effective well radius (m)	[12(1/4)']/2=0.16
Drawdown (m)	16	(UTM) X	458374
Well yield (Gpm)	72	(UTM) Y	4053948
Saturated thickness (m)	111	Elevation (m)	
Groundwater table (m)			
Time. (Minute)	Draw down(M)	Discharge(g\m)	
0	94	90	
0.5	100	83	
1	101	82	
1.5	102	81	
2	103	80	
3	104	79	
4	105	78	
5	106	77	
6	107	76	
7	108	75	
8	109	74	
9	109.5	73	
10	110	72	
15	110	72	
20	110	72	
25	110	72	
30	110	72	
40	110	72	
50	110	72	
60	110	72	
80	110	72	
100	110	72	
120	110	72	

2. Well name ; Kampi zankoy Soran

Well name	Kampi zankoy Soran	Test date	12/05/2019
Well location	soran	Well test length (m)	170
Well depth(m)	240	Well test diameter(m)	2.5'=0.063
Static water level (m)	114	Well casing radius (m)	[7(3/4)']/2=0.098
Dynamic water level (m)	130	Effective well radius (m)	[8(5/8)']/2=0.11
Drawdown (m)	16	(UTM) X	458611
Well yield (Gpm)	67	(UTM) Y	4055979
Saturated thickness (m)	126	Elevation (m)	
Time. (Minute)	Draw down(M)	Discharge(g\m)	
0	114	80	
0.5	121	78	
1	122	77	
1.5	123	76	
2	124	75	
3	125	74	
4	126	73	
5	127	72	
6	128	71	
7	129	70	
8	129.5	69	
9	129.8	68	
10	130	67	
15	130	67	
20	130	67	
25	130	67	
30	130	67	
40	130	67	
50	130	67	
60	130	67	
80	130	67	
100	130	67	
120	130	67	

3. Well name ; Saruchawa 8			
Well name	Saruchawa 8	Test date	12/08/2021
Well location	soran	Well test length (m)	76
Well depth(m)	229	Well test diameter(m)	2.5'=0.063
Static water level (m)	82	Well casing radius (m)	[8(5/8)']/2=0.11
Dynamic water level (m)	99	Effective well radius (m)	[10)']/2=0.127
Drawdown (m)	17	(UTM) X	460789
Well yield (Gpm)	77	(UTM) Y	405890
Saturated thickness (m)	105	Elevation (m)	765
Groundwater table (m)	683		
Time. (Minute)	Draw down(M)	Discharge(g\m)	
0	82	90	
0.5	88	89	
1	89	88	
1.5	90	87	
2	91	86	
3	92	85	
4	93	84	
5	94	83	
6	95	82	
7	96	81	
8	97	80	
9	98	79	
10	98.5	78	
15	99	77	
20	99	77	
25	99	77	
30	99	77	
40	99	77	
50	99	77	
60	99	77	
80	99	77	
100	99	77	
120	99	77	

4. Well name ; Sarychawa 9			
Well name	Sarychawa 9	Test date	08/08/2021
Well location	soran	Well test length (m)	76
Well depth(m)	107	Well test diameter(m)	2.5'=0.063
Static water level (m)	45	Well casing radius (m)	[10)']/2=0.127
Dynamic water level (m)	55	Effective well radius (m)	[10(5/8)']/2=0.13
Drawdown (m)	10	(UTM) X	460789
Well yield (Gpm)	90	(UTM) Y	405890
Saturated thickness (m)	54	Elevation (m)	715
Groundwater table (m)	670		
Time. (Minute)	Draw down(M)	Discharge(g\m)	
0	45	105	
0.5	46	102	
1	47	101	
1.5	48	100	
2	49	99	
3	50	98	
4	51	97	
5	52	96	
6	53	95	
7	53.5	94	
8	54	93	
9	54.5	92	
10	54.8	91	
15	55	90	
20	55	90	
25	55	90	
30	55	90	
40	55	90	
50	55	90	
60	55	90	
80	55	90	
100	55	90	
120	55	90	

5. Well name ; Shawrawa			
Well name	Shawrawa	Test date	26/07/2013
Well location	Shawrawa village	Well test length (m)	150
Well depth(m)	250	Well test diameter(m)	3'=0.076
Static water level (m)	56	Well casing radius (m)	[8(5/8)']/2=0.11
Dynamic water level (m)		Effective well radius (m)	[12(1/4)']/2=0.16
Drawdown (m)	34	(UTM) X	453070
Sell yield (Gpm)	70	(UTM) Y	4060789
Saturated thickness (m)	194	Elevation (m)	725
Time. (Minute)	Draw down(M)	Discharge(g\m)	
0	56	78	
0.5	56	78	
1	56	78	
1.5	58	78	
2	58	78	
3	60	78	
4	60	78	
5	65	78	
6	68	78	
7	70	78	
8	72	78	
9	75	77	
10	75	77	
15	79	77	
20	85	77	
25	88	70	
30	88	70	
40	90	70	
50	90	70	
60	90	70	
80	90	70	
100	90	70	
120	90	70	

6. Well name ; Mzgawti Majidawa			
Well name	Mzgawti Majidawa	Test date	29/11/2021
Well location	Majidawa village	Well test length (m)	148
Well depth(m)	200	Well test diameter(m)	2.5'=0.063
Static water level (m)	96	Pump Type	
Dynamic water level (m)	112	Well casing radius (m)	[8(5/8)']/2=0.11
Drawdown (m)	16	Effective well radius (m)	[12(1/4)']/2=0.16
Well yield (Gpm)	75	(UTM) X	453795
Saturated thickness (m)	104	(UTM) Y	4058325
Groundwater table (m)	559	Elevation (m)	655
Time. (Minute)	Draw down(M)	Discharge(g\m)	
0	96	90	
0.5	101	87	
1	102	86	
1.5	103	85	
2	104	84	
3	105	83	
4	106	82	
5	107	81	
6	108	80	
7	109	79	
8	110	78	
9	111	77	
10	111.5	76	
15	112	75	
20	112	75	
25	112	75	
30	112	75	
40	112	75	
50	112	75	
60	112	75	
80	112	75	
100	112	75	
120	112	75	

7. Well name ; Majidawa 4			
Well name	Majidawa 4	Test date	24/08/2020
Well location	Majidawa village	Well test length (m)	148
Well depth(m)	235	Well test diameter(m)	2.5'=0.063
Static water level (m)	101	Well casing radius (m)	[8(5/8)']/2=0.11
Dynamic water level (m)	118	Effective well radius (m)	[12(1/4)']/2=0.16
Drawdown (m)	17	(UTM) X	453643
Sell yield (Gpm)	70	(UTM) Y	4058304
Saturated thickness (m)	134	Elevation (m)	655
Groundwater table (m)	554		
Time. (Minute)	Draw down(M)	Discharge(g\m)	
0	101	85	
0.5	105	81	
1	108	80	
1.5	110	79	
2	111	78	
3	112	77	
4	113	76	
5	114	75	
6	115	74	
7	116	73	
8	117	72	
9	117.5	71	
10	118	70	
15	118	70	
20	118	70	
25	118	70	
30	118	70	
40	118	70	
50	118	70	
60	118	70	
80	118	70	
100	118	70	
120	118	70	

8. Well name ; Shivazyarat			
Well name	Shivazyarat	Test date	04/09/2006
Well location	Shivazyarat village	Well test length (m)	
Well depth(m)	157	Well test diameter(m)	3'=0.076
Static water level (m)	34	Well casing radius (m)	[8(5/8)']/2=0.11
Dynamic water level (m)	50	Effective well radius (m)	[12(1/4)']/2=0.16
Drawdown (m)	14.75	(UTM) X	453070
Well yield (Gpm)	75	(UTM) Y	4060440
Saturated thickness (m)	114	Elevation (m)	701
Time. (Minute)	Draw down(M)	Discharge(g\m)	
0	34	75	
0.5	37	75	
1	40.2	75	
1.5	41.1	75	
2	42.1	75	
3	43.75	75	
4	44.2	75	
5	45.2	75	
6	45.6	75	
7	46.2	75	
8	46.5	75	
9	46.6	75	
10	46.6	75	
15	47	75	
20	47.4	75	
25	47.6	75	
30	48.2	75	
40	48.6	75	
50	48.75	75	
60	48.75	75	

9. Well name ; Mazni-Garaki gulan			
Well name	Mazni-Garaki gulan	Test date	10/07/2018
Well location	Mazni	Well test length (m)	123
Well depth(m)	181	Well test diameter(m)	2.5'=0.063
Static water level (m)	81	Well casing radius (m)	[8(5/8)']/2=0.11
Dynamic water level (m)	95	Effective well radius (m)	[10(5/8)']/2=0.13
Drawdown (m)	14	(UTM) X	452095
Sell yield (Gpm)	75	(UTM) Y	4063570
Saturated thickness (m)	100	Elevation (m)	789
Groundwater table (m)	708		
Time. (Minute)	Draw down(M)	Discharge(g\m)	
0	81	90	
0.5	84	87	
1	85	86	
1.5	86	85	
2	87	84	
3	88	83	
4	89	82	
5	90	81	
6	91	80	
7	92	79	
8	93	78	
9	94	77	
10	94.5	76	
15	95	75	
20	95	75	
25	95	75	
30	95	75	
40	95	75	
50	95	75	
60	95	75	
80	95	75	
100	95	75	
120	95	75	

10. Well name ; Khardin			
Well name	Khardin	Test date	25/04/2007
Well location	khardin village	Well test length (m)	162
Well depth(m)	255	Well test diameter(m)	3'=0.076
Static water level (m)	43.7	Well casing radius (m)	[8(5/8)']/2=0.11
Dynamic water level (m)	157	Effective well radius (m)	[12(1/4)']/2=0.16
Drawdown (m)	113.3	(UTM) X	442467
Sell yield (Gpm)	20	(UTM) Y	4073711
Saturated thickness (m)	211.3	Elevation (m)	792
Groundwater table (m)	748.3		
Time. (Minute)	Draw down(M)	Discharge(g\m)	
0	43.7	80	
0.5	50	80	
1	53	80	
1.5	56.2	80	
2	56.2	80	
3	58.2	80	
4	58.2	80	
5	63	80	
6	70	80	
7	73.4	20	
8	75.4	20	
9	75.4	20	
10	77	20	
15	87	20	
20	97.2	20	
25	105	20	
30	110	20	
40	123	20	
50	141	20	
60	157	20	
80	157	20	
100	157	20	
120	157	20	

APPENDIX- 6. THE GROUNDWATER MEASUREMENT OF HAUDIAN-1 MONITORING WELL (DATA ARE OBTAINED FROM MINISTRY OF AGRICULTURE AND WATER RESOURCE/ DIRECTORATE OF ERBIL GROUNDWATER)

Date	G.W.L(m)	Date	G.W.L(m)	Date	G.W.L(m)	Date	G.W.L(m)
03/09/2000	32.63	05/03/2002	30.87	15/07/2003	37.67	26/10/2004	41.96
10/09/2000	32.83	12/03/2002	30.55	22/07/2003	37.7	04/11/2004	42.08
27/09/2000	33.45	19/03/2002	29.9	29/07/2003	37.74	11/11/2004	41.94
02/10/2000	33.45	26/03/2002	28.13	05/08/2003	40.75	25/11/2004	41.7
26/10/2000	34.18	02/04/2002	27.18	12/08/2003	42.28	07/12/2004	39.75
16/01/2001	35.5	09/04/2002	24.83	19/08/2003	44	14/12/2004	39.12
07/02/2001	35.43	16/04/2002	22.93	26/08/2003	45.02	21/12/2004	38.51
19/03/2001	30.6	23/04/2002	22.18	09/12/2003	36.81	04/01/2005	37.63
05/04/2001	30.35	30/04/2002	22.06	16/12/2003	33.87	11/01/2005	37.22
08/05/2001	35.2	07/05/2002	22	23/12/2003	31.12	18/01/2005	36.91
15/05/2001	35.38	14/05/2002	22.12	30/12/2003	30.2	25/01/2005	35.11
22/05/2001	35.78	21/05/2002	23.42	13/01/2004	29.63	01/02/2005	32.23
29/05/2001	36.55	28/05/2002	25.26	20/01/2004	29.28	08/02/2005	30.83
05/06/2001	36.75	04/06/2002	27.03	27/01/2004	28.83	15/02/2005	29.98
12/06/2001	36.78	11/06/2002	28.58	10/02/2004	28.63	22/02/2005	27.3
19/06/2001	36.82	18/06/2002	30.6	17/02/2004	24.91	01/03/2005	27.18
03/07/2001	37.15	25/06/2002	34.21	24/02/2004	22.32	08/03/2005	27.06
10/07/2001	37.19	02/07/2002	34.75	02/03/2004	22.2	15/03/2005	26.95
17/07/2001	37.25	09/07/2002	35.13	09/03/2004	22.11	22/03/2005	26.82
24/07/2001	37.68	16/07/2002	35.5	16/03/2004	22.05	24/03/2005	26.67
31/07/2001	37.75	23/07/2002	37	30/03/2004	22.26	05/04/2005	26.55
07/08/2001	37.78	30/07/2002	38.33	06/04/2004	23.08	12/04/2005	26.39
14/08/2001	37.8	13/08/2002	38.57	13/04/2004	24.59	19/04/2005	26.3
21/08/2001	37.89	20/08/2002	38.7	20/04/2004	25.68	26/04/2005	26.24
28/08/2001	38.45	27/08/2002	38.86	27/04/2004	25.8	03/05/2005	26.33
04/09/2001	38.58	10/09/2002	40.06	04/05/2004	25.98	10/05/2005	26.44
11/09/2001	38.63	17/09/2002	40.37	11/05/2004	26.05	17/05/2005	26.6
18/09/2001	38.67	24/09/2002	40.78	18/05/2004	26.3	24/05/2005	26.88
25/09/2001	38.71	01/10/2002	40.91	25/05/2004	26.52	31/05/2005	27.39
02/10/2001	38.76	08/10/2002	40.97	01/06/2004	28.86	07/06/2005	30.13
09/10/2001	38.8	15/10/2002	41.1	08/06/2004	30.68	14/06/2005	32.95
16/10/2001	38.83	22/10/2002	41.05	15/06/2004	32.21	21/06/2005	34.67
23/10/2001	38.85	29/10/2002	41.08	22/06/2004	36.62	28/06/2005	35.43
30/10/2001	38.86	05/11/2002	41.13	29/06/2004	37.27	05/07/2005	35.6
06/11/2001	38.9	12/11/2002	41.2	06/07/2004	37.38	12/07/2005	35.85
13/11/2001	38.75	26/11/2002	40	13/07/2004	37.55	19/07/2005	35.99
20/11/2001	38.56	03/12/2002	34.6	20/07/2004	37.71	26/07/2005	36.15
27/11/2001	38.35	10/12/2002	34.25	27/07/2004	37.92	02/08/2005	36.3
04/12/2001	38.17	17/12/2002	34.11	03/08/2004	38.08	09/08/2005	36.42
11/12/2001	38.1	24/12/2002	32.87	10/08/2004	38.6	16/08/2005	36.55
18/12/2001	37.98	31/12/2002	30.19	17/08/2004	38.7	23/08/2005	36.66
25/12/2001	37.88	07/01/2003	28.81	24/08/2004	38.78	30/08/2005	36.75
08/01/2002	36.95	14/01/2003	27.93	31/08/2004	38.88	06/09/2005	36.83
15/01/2002	35.85	21/01/2003	27.86	07/09/2004	40.02	13/09/2005	36.9
22/01/2002	34.01	28/01/2003	27.8	14/09/2004	41.35	20/09/2005	36.94
29/01/2002	33.4	04/02/2003	27.7	21/09/2004	41.5	27/09/2005	36.98
05/02/2002	33.05	10/06/2003	36.06	28/09/2004	41.6	04/10/2005	37.05
12/02/2002	32.2	17/06/2003	36.2	05/10/2004	41.71	11/10/2005	37.13
19/02/2002	31.2	24/06/2003	36.86	12/10/2004	41.82	18/10/2005	37.2
26/02/2002	31.02	01/07/2003	37.22	19/10/2004	41.9	25/10/2005	37.26
01/11/2005	37.32	28/11/2006	31.31	04/12/2007	35.3	08/12/2009	46.64
08/11/2005	37.39	12/05/2006	31.21	11/12/2007	35.38	22/12/2009	46
15/11/2005	37.44	12/12/2006	31.14	18/12/2007	35.44	05/01/2010	45.54
22/11/2005	37.46	19/12/2006	31.09	25/12/2007	35.5	19/01/2010	44.9
29/11/2005	37.5	26/12/2006	31	08/01/2008	35.54	02/02/2010	44.75
06/12/2005	37.03	01/02/2007	30.82	15/1/2008	35.72	16/02/2010	44.47
13/12/2005	36.5	01/09/2007	30.5	22/1/2008	35.86	02/03/2010	44.32
20/12/2005	35.89	16/1/2007	30.21	29/1/2008	35.99	15/03/2010	44.11
27/12/2005	35.07	23/1/2007	29.92	05/02/2008	35.76	27/04/2010	42.69
17/1/2006	32	30/1/2007	29.47	26/02/2008	35.35	11/05/2010	43
24/1/2006	30.83	02/06/2007	29.13	04/03/2008	35.47	25/05/2010	43.65
07/02/2006	29.2	13/2/2007	28.81	25/03/2008	35.91	08/06/2010	43.77
14/2/2006	28.46	20/2/2007	28.58	01/04/2008	36.37	22/06/2010	43.92
21/2/2006	27.68	27/2/2007	28.34	29/04/2008	37.89	06/07/2010	44.12
28/2/2006	27.11	03/06/2007	28.25	05/06/2008	37.98	20/07/2010	44.35
07/03/2006	27.3	13/3/2007	28.14	27/5/2008	38.46	03/08/2010	44.63
14/3/2006	27.08	20/3/2007	28.06	03/06/2008	38.58	24/08/2010	44.87
22/3/2006	26.59	27/3/2007	27.97	24/6/2008	39	14/09/2010	44.96
28/3/2006	26.25	04/03/2007	27.87	08/07/2008	39.2	28/09/2010	45.22
04/04/2006	26.11	04/10/2007	27.75	29/7/2008	39.96	12/10/2010	45.31
11/04/2006	25.9	17/4/2007	27.63	05/08/2008	40.1	26/10/2010	45.45
18/4/2006	25.73	24/4/2007	27.5	26/08/2008	40.81	09/11/2010	45.53
25/4/2006	25.65	05/08/2007	27.7	02/09/2008	41.02	23/11/2010	45.7
02/05/2006	25.78	15/5/2007	27.82	30/09/2008	41.77	07/12/2010	45.76
09/05/2006	25.89	22/5/2007	27.93	07/10/2008	41.9	21/12/2010	45.9
16/5/2006	26.09	29/5/2007	28.1	28/10/2008	42.22	25/01/2011	55.95
23/5/2006	26.25	06/05/2007	28.29	04/11/2008	42.3	02/04/2012	82
30/5/2006	26.48	12/06/2007	28.53	25/11/2008	42.55	05/05/2012	83.3
06/06/2006	26.7	19/6/2007	28.75	02/12/2008	42.72	06/10/2012	83
13/6/2006	26.87	26/6/2007	28.98	30/12/2008	43.43	07/08/2012	80
23/6/2006	27.18	03/07/2007	29.22	06/01/2009	43.6	11/08/2012	81.5
27/6/2006	27.45	10/07/2007	29.48	27/1/2009	43.92	15/9/2012	81
07/04/2006	27.8	17/7/2007	29.75	03/02/2009	44.05	12/11/2012	82.2
07/11/2006	28.83	24/7/2007	30.02	24/2/2009	44.2	11/12/2012	81.4
18/7/2006	28.8	31/7/2007	30.3	03/03/2009	44	31/01/2013	80.3
25/7/2006	29.93	08/07/2007	30.64	31/03/2009	43.25	25/02/2013	79.9
01/08/2006	29.7	14/8/2007	30.91	07/04/2009	43	25/03/2013	79.7
08/08/2006	30.18	21/8/2007	31.42	28/4/2009	42.83	24/04/2013	79.6
15/08/2006	30.66	28/8/2007	31.94	05/05/2009	42.98	20/05/2013	79.1
22/08/2006	30.98	04/09/2007	32.58	26/5/2009	43.39	19/06/2013	79
29/08/2006	31.51	11/09/2007	32.93	02/06/2009	43.55	03/07/2013	80.1
09/05/2006	31.86	18/9/2007	33.47	30/6/2009	43.96	28/08/2013	80.3
09/12/2006	32.17	25/9/2007	33.89	07/07/2009	44.07	25/09/2013	80.51
19/9/2006	32.43	02/10/2007	34.18	28/7/2009	44.47	22/10/2013	80.72
26/9/2006	32.74	09/10/2007	34.46	04/08/2009	44.6	22/11/2013	80.7
10/03/2006	32.6	16/10/2007	34.63	18/8/2009	44.88	19/12/2013	80.31
10/10/2006	32.48	23/10/2007	34.85	01/09/2009	45.07	29/01/2014	80.1
17/10/2006	32.31	30/10/2007	35.03	29/9/2009	45.64	26/02/2014	79.2
31/10/2006	31.94	6/112007	35.1	13/10/2009	45.8	22/05/2014	79
11/07/2006	31.81	1311/2007	35.16	27/10/2009	46.25	19/06/2014	79.2
14/11/2006	31.64	20/11/2007	35.21	03/11/2009	46.47		
21/11/2006	31.49	27/11/2007	35.26	17/11/2009	46.82		

CURRICULUM VITAE

Zana HUSSEIN OMAR OMAR

[redacted]

[redacted]

[redacted]

[redacted]

[redacted]